Enzymological Studies of Cysteine Desulfurase and Selenocysteine Lyase

Hisaaki Mihara

1999

Enzymological Studies of Cysteine Desulfurase and Selenocysteine Lyase

Hisaaki Mihara

1999

CONTENTS

LIST OF FIGURES

LIST OF TABLES

ABBREVIATIONS

AAT	aspartate aminotransferase (EC 2.6.1.1)
AspDC	aspartate β-decarboxylase (EC 4.1.1.12)
BSA	bovine serum albumin
CBL	cystathionine β-lyase (EC 4.4.1.8)
DTT	dithiothreitol
DIG	digoxigenin
EDTA	ethylenediamine tetraacetate dihydrate
EST	expressed sequence tag
IPTG	isopropyl-β-D-thiogalactopyranoside
KPB	potassium phosphate buffer
MIR	multiple isomorphous replacement
ORF	open reading frame
PAGE	polyacrylamide gel electrophoresis
PCR	polymerase chain reaction
PEG	polyethylene glycol
PLP	pyridoxal 5'-phosphate
PMA	phenyl mercury acetate
PMP	pyridoxamine 5'-phosphate
PMSF	phenylmethanesulfonyl fluoride
PSAT	phosphoserine aminotransferase (EC 2.6.1.52)
PVDF	poly(vinylidene fluoride)
RACE	rapid amplification of cDNA end
rms	root mean square
SCL	selenocysteine lyase (EC 4.4.1.16)
SDS	sodium dodecyl sulfate
SPS	selenophosphate synthetase
TFA	trifluoroacetate

GENERAL INTRODUCTION

Both inorganic and organic forms of selenium cause selenosis to man and animals (1). For example, a cattle ailment known as "alkali disease" is caused by intake of such selenoamino acids as *Se*-methyl-selenocysteine and selenocystathionine, which are the two most prominent selenium compounds found in selenium accumulator plants *Astragalus pectinatus* (2). Selenocysteine, selenocystine, and selenomethionine are also toxic for animals, and hydrogen selenide is the most toxic selenium compounds so far studied (3). Although the mechanism of selenium toxicity is not yet clarified, it is probably concerned with sulfur-selenium antagonism because of the resemblance in chemical and physical properties between sulfur and selenium atoms. The toxicity of organoselenium compounds apparently depends on whether their sulfur analogs are intermediates in sulfur metabolism (4): L-selenocystine is shown to be several times as toxic as its D-isomer to rats (5).

Selenium, at the same time, is an essential micronutrient for several vertebrates and bacteria (1). This unexpected nutritional role of selenium emerged in 1957 with the discovery by Schwarz and Foltz that the element was required for prevention of dietary liver necrosis in vitamin E-deficient rats (6). A number of serious diseases occur in various species of livestock and poultry due to selenium deficiency. The physiological functions of selenium as an essential micronutrient have partly been explained by the anti-oxidative nature of selenocompounds and the action of several selenoproteins that contain catalytically essential selenocysteine residue in the polypeptide chain (7).

Because of both toxicity and essentiality of selenium, enzymes that are specific to selenium compounds are expected to have important functions in selenium metabolism. It was pointed out that several enzymes that normally catalyze the transformation of sulfur compounds also react with the corresponding selenium analogs (8). Some enzymes are known to be equally reactive with the selenium analog and with the normal substrate when the two are compared at the same concentrations, but such enzymes are not capable of producing appreciable amounts of the selenium metabolites *in vivo* unless high and toxic levels of selenium are present. At normal ratio of sulfur to selenium, the number of selenium substrate molecules transformed would be very small. Hence, although the lack of specificity of enzymes involved in sulfur metabolism may play a key role in selenium toxicity, different enzymes that selectively react with selenium compounds at low concentrations must serve as the catalysts in normal essential selenium metabolism. In so far as selenium toxicity is concerned, neither the biological effects of the selenium compounds produced by a nonspecific enzyme nor the combined effects of several such sidereactions are known in detail. However, it is reasonable to suppose that indiscriminate substitution of selenium for sulfur in proteins, nucleic acids, and derivatives of complex carbohydrates has marked deleterious effects. Examples of enzymes that catalyze reactions in which a selenium compound can substitute for the normal substrate to some degree are ATP sulfurylase (9), cysteinyl-tRNA synthetase (10), tRNA sulfur transferase (11), methionyl-tRNA synthetase (12), *S*-adenosylmethionine synthetase (13), *S*-adenosylmethionine methyl transferase, mammalian cystathionine γ-lyase (14),

and bacterial methionine γ-lyase (14). On the other hand, selenocysteine lyase (SCL) (EC 4.4.1.16) (15), selenophosphate synthetase (16), selenocysteine synthase (17), and selenocysteine methyltransferase (18) are known to act specifically on selenium compounds.

Esaki *et al.* found SCL in mammals (14) and bacteria (19), and purified the enzyme from pig liver (14) and *Citrobacter freundii* (20). The enzyme specifically decomposes L-selenocysteine into L-alanine and elemental selenium; L-cysteine is inert as a substrate. Zheng *et al.* (21) demonstrated the function of NifS protein, which is required for the efficient construction of the Fe-S clusters of nitrogenase in a diazotrophic bacterium *Azotobacter vinelandii*. NifS catalyzes the same type of reaction as SCL, but acts on both L-cysteine and L-selenocysteine indiscriminately. The enzyme was named cysteine desulfurase, based on its inherent physiological role (21).

Clarifying a mechanism of the discrimination between selenium and sulfur in analogous substrates is important to reveal the role of selenium as an essential trace element in mammals and other organisms. The author carried out enzymological studies of cysteine desulfurase and SCL to elucidate mechanistic differences between the selenium-specific reaction and the non-selenium-specific reaction.

Biosynthesis of Selenoproteins

Selenocysteine is recognized as the 21st amino acid in ribosome-mediated protein synthesis, and its specific incorporation is directed by the UGA codon, which conventionally serves as one of the three translation termination signals

(22, 23). The translation of the selenocysteine UGA codon in the bacterial formate dehydrogenase mRNA requires a specific stem-loop in the coding region immediately downstream of the UGA codon (23, 24). In addition, four genes, *selA*, *selB*, *selC*, and *selD*, are required for selenocysteine codon recognition and translation (25-28). The *selC* gene product is a unique selenocysteine-specific tRNA (29) that becomes charged with L-serine by seryl-tRNA synthetase (29, 30). The product of the *selA* gene, selenocysteine synthase, converts seryl-tRNA^{Sec} to selenocysteyl-tRNA^{Sec} via an aminoacrylyl intermediate (17, 31). The active selenium donor species in this reaction is monoselenophosphate (32), which is synthesized from selenide and ATP by the *selD* gene product, selenophosphate synthetase (16). In the final step of bacterial selenoprotein synthesis, selenocysteyl-tRNA^{Sec} is bound to a specific translation factor, SELB, which also binds the stem-loop structure, and decodes the UGA specifying selenocysteine (33-35).

Several eukaryotic selenoproteins have also been identified, including glutathione peroxidases (36), selenoprotein P (37, 38), the type I iodothyronine 5'-deiodinase (39), and thioredoxin reductase (40). However, the mechanisms of recognition and translation of selenocysteine codons differ between prokaryotes and eukaryotes. Although stable stem-loop structures are required for eukaryotic selenoprotein synthesis, these elements are situated within the 3'-untranslated region of the mRNAs (41). In addition, the sequences of the prokaryotic and eukaryotic stem-loop structures are not conserved (23, 41).

Selenocysteine Lyase

L-Selenocysteine was shown to be synthesized by the coupled reactions with cystathionine β-synthase (EC 4.2.1.22) and cystathionine γ-lyase (EC 4.4.1.1) purified from rat liver, and also by the reaction system with a rat liver homogenate (14). During the course of this study, selenocysteine lyase has been discovered as the first enzyme which specifically acts on selenium compounds. SCL exclusively catalyzes the removal of elemental selenium from L-selenocysteine to form L-alanine: cysteine is not a substrate of the enzyme (42, 43). The enzyme is distributed widely in mammalian tissues and various bacteria such as *C. freundii*, *Alcaligenes viscolactis*, and *Pseudomonas alkanolytica* (19). The enzyme activities in the liver and kidney are higher than those in other tissues in several animals. SCL has been purified from pig liver and *C. freundii* and characterized. Although the bacterial enzyme is different from the mammalian enzyme in its physicochemical properties and amino acid composition, both the enzymes contain pyridoxal 5'-phosphate (PLP) as a coenzyme and they are very similar to each other in their enzymological properties.

Mechanism of the reactions catalyzed by SCL from the pig and *C. freundii* has been proposed (42, 43). It is pointed out that the difference of selenol and thiol in their enzymatic reactivities is not derived from that in their dissociation states because cysteine competitively inhibits the enzyme reaction even at pH 7.0-9.0, and a thiol group of cysteine is ionized at least partially in this pH range. In addition, a two-base mechanism is proposed for the enzyme reaction from the studies of the reaction in deuterium oxide: the α protonation and

deprotonation is performed by one base, and the other base mediates the β protonation. The enzyme is inactivated through transamination between selenocysteine and the PLP to produce pyridoxamine 5'-phosphate and a keto analog of selenocysteine or pyruvate. Despite those extensive studies on SCL, no gene encoding SCL has been identified yet, and physiological functions of the enzyme remain unknown.

NifS (Cysteine Desulfurase)

NifS protein from nitrogen-fixing bacteria *A. vinelandii* has been identified as cysteine desulfurase, which catalyzes the removal of elemental sulfur from L-cysteine to form L-alanine (21). In contrast to SCL, NifS acts on both L-cysteine and L-selenocysteine (21).

The *nifS* gene is located on the *nif* gene cluster, which is responsible for the nitrogen-fixing function of *A. vinelandii*. NifS protein is thought to mobilize sulfur for incorporation into the metallocluster of nitrogenase (21, 44). NifS catalyzes *de novo* assembly of iron-sulfur clusters *in vitro* (45-47). NifS homologs have been identified in numerous prokaryotes, including non-nitrogen-fixing bacteria, and in eukaryotes. It has been reported that the *nifS*-like genes of *Bacillus subtilis* and *Saccharomyces cerevisiae* are involved in NAD^+ biosynthesis (48) and tRNA processing (49), respectively. Although a specific function of these NifS-like proteins is unknown, it is assumed that they play a general role in providing sulfur atoms for iron-sulfur clusters.

The present study was aimed at the enzymological properties and structure-function relationships of cysteine desulfurase and SCL. In Chapter I, cloning of a mouse liver cDNA encoding SCL is described. The recombinant enzyme was produced in *Escherichia coli*, purified, and characterized. Chapter II deals with the characterization of an *E. coli* NifS homolog encoded by *csdA* mapped at 63.4 min. The enzyme (CSD) was characterized as cysteine sulfinate desulfinase with SCL and cysteine desulfurase activities. Chapter III describes characterization of another *E. coli* NifS homolog encoded by *csdB* mapped at 37.9 min. The gene product CsdB possesses SCL activity with a high specificity. Crystallization and preliminary X-ray studies of CsdB are also described. Chapter IV deals with the extensive characterization of the reaction catalyzed by three NifS homologs of *E. coli*, *i.e.*, CSD, CsdB, and IscS. Site-directed mutagenesis and steady-state kinetic studies revealed that cysteine desulfurase reaction and SCL reaction are mechanistically different from each other in those enzymes. In Chapter V, the three-dimensional structure of CsdB determined by X-ray crystallographic analyses is presented. The results provides the first detailed insight into the NifS/SCL family protein at a molecular level. In Chapter VI, I describe the three-dimensional structures of CsdB complexed with substrates and substrate analogs, L-aspartate, L-cysteine sulfinate, L-β-chloroalanine, and L-propargylglycine. Based on the structural and kinetic data obtained, a possible reaction mechanism of the enzyme is proposed.

CHAPTER I

cDNA Cloning, Purification and Characterization of Mouse Liver Selenocysteine Lyase: a Candidate for the Selenium Delivery Protein in the Selenoprotein Synthesis

INTRODUCTION

Selenocysteine is contained in several bacterial and mammalian selenoproteins as a crucial catalytic residue (1, 7, 8, 23, 28, 50, 51). Selenocysteine is cotranslationally incorporated into a nascent polypeptide as encoded by UGA-stop codon (22, 23). The *selD* gene product from *Escherichia coli*, selenophosphate synthetase (SPS), plays a role in the initial step of the biosynthesis of selenoproteins. SPS catalyzes the formation of monoselenophosphate from selenide and ATP (16). One of the substrate of SPS, selenide, is proposed to be supplied by selenocysteine-specific selenocysteine lyase (SCL) *in vivo* (52), based on the evidence that the level of selenide concentration in cells is generally lower than K_m for SPS (16), and Se derived from L-selenocysteine is preferentially incorporated into selenocysteine residue of selenoproteins (52). SCL is a pyridoxal 5'-phosphate (PLP) enzyme which catalyzes elimination of elemental selenium from L-selenocysteine to form L-alanine. The enzyme was identified previously as the first enzyme that can specifically act on a selenium-containing compound. The enzymes from the pig liver (15) and *Citrobacter freundii* (43)

are well characterized and exhibit high specificity to L-selenocysteine: no activity is detected with L-cysteine. The mammalian enzyme is a homodimer with a subunit M_r of 48,000, whereas the enzyme from *C. freundii* is monomeric with a M_r of 64,000. Although SCL is distributed widely in several mammals (15) and aerobic bacteria (19), no gene encoding SCL has been identified to date.

The specificity of SCL to selenocysteine suggests that it is involved in selenium-specific events such as selenocysteine biosynthesis and detoxification of L-selenocysteine. To investigate the physiological function as well as the catalytic mechanism of SCL in detail, I performed cDNA cloning and characterization of mouse SCL (m-SCL).

In this Chapter, I describe the determination of partial amino acid sequences of pig SCL. The peptide sequences enabled me to identify mouse EST clones which apparently encode a protein showing significant sequence identity to pig SCL. Entire coding sequence of the m-SCL cDNA, termed m-*Scl*, was determined, and the subsequent production of the recombinant mouse protein and characterization of its catalytic activity and kinetic properties confirmed that this cDNA encodes functional mouse liver SCL. The tissue distribution and subcellular localization of the enzyme are also reported. This is the first report of the cloning of mammalian SCL.

EXPERIMENTAL PROCEDURES

Materials—L-Selenocystine was synthesized as described previously (53). Oligonucleotides were provided by Espec Oligo Service (Tsukuba, Japan).

Restriction and DNA modification enzymes were purchased from New England Biolabs (Beverly, MA) and Takara Shuzo (Kyoto, Japan). All chemicals were of analytical grade.

Purification of Pig Liver SCL—All steps were carried out at 4 °C unless otherwise stated. Potassium phosphate buffer (KPB) (pH 7.4) containing 20 μM PLP and 0.01% 2-mercaptoethanol was used as a standard buffer. Pig liver (1.5 kg) was minced with an ice-cooled meat mincer and homogenized with a Waring Blender in 7.5 liter of 50 mM standard buffer. The homogenate was centrifuged and the supernatant was passed through a nylon mesh. The crude extract was fractionated with ammonium sulfate (25-45% saturation) and dialyzed with 10 mM standard buffer. The enzyme solution was applied to a DEAE-Toyopearl column (10 × 16 cm) equilibrated with 10 mM standard buffer and eluted with a 10-liter linear gradient (0-0.2 M) of KCl in the same buffer. The fractions containing the enzyme were concentrated by ammonium sulfate precipitation (50% saturation). The enzyme was applied to a Phenyl-Toyopearl column (5 × 15 cm) equilibrated with 10 mM standard buffer containing 0.6 M ammonium sulfate and eluted with 1.5 liters of the same buffer. The enzyme fractions were concentrated by ultrafiltration with a UP-20 membrane (Advantec, Naha, Japan) The enzyme was dialyzed against 10 mM standard buffer containing 0.7 M ammonium sulfate, applied to a second Phenyl-Toyopearl column (5 × 14 cm) equilibrated with the same buffer and eluted with 10 mM standard buffer containing 0.6 M ammonium sulfate. The active fractions were pooled, concentrated by ultrafiltration as above and dialyzed against 20 mM standard buffer. The enzyme was loaded onto a

hydroxyapatite column (2.5 × 10 cm) equilibrated with 20 mM standard butter, and eluted stepwise with 40 mM and 80 mM standard buffers. The enzyme fractions were pooled, concentrated by ultrafiltration and dialyzed against 20 mM standard buffer. The enzyme was applied to a Superdex 200 column (1 × 30 cm) and fractionated with the same buffer at a flow rate of 0.25 ml/min with FPLC pump system. The enzyme fractions were collected and dialyzed against 10 mM standard buffer.

Sequencing of Pig Liver SCL—For N-terminal peptide sequencing, the enzyme separated by SDS-PAGE was electroblotted to a polyvinylidene difluoride (PVDF) membrane, stained with 0.1% Ponceau S, excised with a razor blade, and subjected to sequence analysis with an automated protein sequencer PPSQ-10 (Shimadzu, Kyoto, Japan). In order to determine the internal sequences of pig liver SCL, in-gel digestion was performed as follows. The enzyme separated by SDS-PAGE was stained with Coomassie Brilliant Blue, and the stained band corresponding to the enzyme was cut with a razor blade. The gel band was washed twice with 150 μl of 50% acetonitrile in 0.1 M Tris-HCl, pH 9.0, at 30 °C for 20 min, left in the air for 10 min at room temperature to make it to semidry, and then partially rehydrated with 70 μl of 0.02% Tween 20 in 0.1 M Tris-HCl, pH 9.0. Lysyl endopeptidase (0.5 μg) was added to the sample, and the mixture was incubated for 16 h at 37 °C. The peptides generated in the gel were recovered with 500 μl of 60% acetonitrile containing 0.1% TFA at 37 °C for 20 min with a gentle vortex. The gel was crushed, and a second extraction was performed with the same solution by shaking for 1 h. The crushed gel was removed with a Ultrafree C3GV filter (Millipore). The extracts were combined and concentrated to 20 μl

with a vacuum evaporator. The peptides were separated with an Asahipak ODP-50 column (6 × 150 mm) connected to an HPLC system (Tosho, Japan) with a 50-ml linear gradient (24-64%) of acetonitrile in 0.05% (v/v) TFA at a flow rate of 0.5 ml/min. The separated peptides were subjected to the sequence analysis.

Isolation of Mouse SCL cDNA—Based on the sequences of two mouse EST clones W64820 and MUS94C09, the following primers were designed: Mp1 (5'-CCGACAGTGCGCTCCCTTCAA-3') and Mp2 (5'-GTGAACCAT GTATCCCTTCAG-3') are flanking the apparent coding region of W64820, and Mp3 (5'-CAGGATCGGTGCTCTGTATGT-3') and Mp4 (5'-GGCTGTT CAAATGGATTCT CT-3') are flanking that of MUS94C09. DNA fragments corresponding to parts of W64820 and MUS94C09 were obtained by PCR with the above primers and a mouse liver cDNA as a template. The PCR products were gel-purified, labeled with digoxigenin (DIG), and used as probes to obtain a longer m-*Scl* gene from a mouse liver λZAP cDNA library. Immunodetection was performed with anti-DIG Fab fragment alkaline phosphatase conjugate (Roche Diagnostics), nitrobluetetrazolium, and 5-bromo-4-chloro-3-indolylphosphate-*p*-toluidine salt. Positive clones were isolated, and its cDNA inserts were excised in the form of pBluescript plasmid and analyzed by sequencing. The cDNA clone, termed m-*Scl-1*, thus isolated from the cDNA library lacked several nucleotides including the initiation ATG codon. To complete the 5' end and missing region of the transcript, 5'-RACE and CapFinder Techniques were performed with total RNA isolated from a liver of BALB/c mouse (6 weeks, male). DNA sequencing was performed

with an Applied Biosystems Prism Sequencing kit and an ABI 370A automated sequencer.

Expression of the m-SCL-2 Protein in E. coli and Production of the Antisera—Initiation codon, ATG, and four bases, TAGG, were introduced into the incomplete cDNA clone m-*Scl-1* by two-step PCR using overlap-extension procedure (Higuchi, R., 1990). Primers, Mp5 (5'-GGGGAATT*C ATATG* GACGCGGCGCGAAATGGCGCG-3') and Mp6 (5'-CACCTTGG CCTTCCTACCTGACACATAGGAGC-3'), were used for amplification of the DNA fragment encoding the N-terminal part of m-SCL. Another set of primers, Mp7 (5'-CAGGTAGGAAGGCCAAGGACATTATAAATG-3') and Mp8 (5'-CCCC*AAGCTT*CTAGAGCCGCCCTTCCAGTTGGGCC-3'), were used to amplify the DNA coding for the C-terminal fragment of m-SCL. The initiation codon to be introduced is double-underlined, and underlined nucleotides indicate the 4 bases to be inserted. The restriction enzyme sites, *Nde*I and *Hin*dIII are shown in italics. After 2nd round of PCR, the final 1.3-kbp product was purified, digested with *Nde*I and *Hin*dIII, and subcloned into the same sites of pET21a to form a construct pSCL-2.

The construct pSCL-2 provides a fusion protein (m-SCL-2) with a C-terminal His6 tag. The fusion protein was produced in *E. coli* BL21(DE3) as an inclusion body, purified with a His•Bind column (Novagen, Madison, WI), and used for the generation of polyclonal antibodies against m-SCL-2 in rabbits.

Preparation of Cell Extracts and Subfractions from Mouse Tissues—Eight tissues (brain, heart, lung, liver, stomach, spleen, kidney, and testis) from

mouse were homogenized in ice-cooled 0.25 M sucrose solution containing 3 mM Tris-HCl, pH 7.4, and 0.1 mM EDTA, and were centrifuged for 10 min at 700 × *g*. The supernatant was centrifuged for 10 min at 7,000 × *g* to obtain crude mitochondrial pellets. The supernatant was centrifuged again for 60 min at 105,000 × *g* to obtain microsomal fraction and cytosolic fraction. The pure nuclear fraction was obtained using the method of Blobel and Potter (54).

Western Blot Analysis with Anti-m-SCL-2 Antibody—Proteins in various cell homogenates and subcellular fractions were separated by SDS-PAGE and transferred to PVDF membranes. Western analysis was performed with anti-m-SCL-2 antibodies, and the proteins were detected by chemiluminescence using CDP-Star (Roche Diagnostics)

RT-PCR Analysis—Eight tissues (brain, heart, lung, liver, stomach, spleen, kidney, and testis) from mouse were excised from BALB/c mouse (6 weeks, male), and total RNA was isolated with Sepasol-RNA I (Nacalai Tesque, Kyoto, Japan). RT-PCR was performed with primers which are specific to the m-*Scl* transcript: Mp9, 5'-TGGGCAGTGTGGAGAG-3' and Mp10, 5'-GTGCCCCCAGAAGTGAAGATGATGT-3'.

Enzyme Assays—The enzyme was assayed in 0.12 M Tricine-NaOH buffer at pH 9.0. The enzymatic activity toward L-selenocysteine was measured with lead acetate as described previously (15). Sulfite produced from L-cysteine sulfinic acid was determined with fuchsin (55). Production of alanine from substrates was determined with a Beckman high performance amino acid analyzer 7300 (Beckman Coulter, Fullerton, CA). Specific activity was expressed as units/mg of protein, with one unit of enzyme defined as the

amount that catalyzed the formation of 1 μmol of the product in one minute.

Expression and Purification of Functional m-SCL—The entire coding sequence of m-*Scl* was obtained by PCR with the primers Mp5 and Mp8 and with a total RNA as a template. The product was subcloned by PCR into the *Nde*I and *Hin*dIII sites of pET21a to yield pESL. This construct provides a functional non-fusion m-SCL (Fig. 2).

Purification of m-SCL was performed at 0-4 °C, and KPB (pH 7.4) was used as the buffer. *E. coli* BL21(DE3) harboring pESL was grown in 500 ml of LB medium containing 100 μg/ml ampicillin at 28 °C for 18 h with induction of the gene expression by 1 mM IPTG. The cells were harvested by centrifugation, suspended in 50 mM KPB containing 2 mM PMSF, 5 mM EDTA, and 2 μg/ml pepstatin A, and then disrupted by sonication. The cell debris was removed by centrifugation, and the supernatant solution was fractionated by ammonium sulfate precipitation (1.0-3.0 M). The enzyme was dissolved in 10 mM KPB containing 1.0 M ammonium sulfate and applied to a Butyl-Toyopearl column (3 × 9.5 cm) equilibrated with the same buffer. After the column was washed with the same buffer, the enzyme was eluted with a 0.8-liter linear gradient of 1.0-0 M ammonium sulfate in the buffer. The active fractions were pooled and concentrated by 3.0 M ammonium sulfate. The enzyme was collected by centrifugation, resuspended in 10 mM KPB containing 1 mM DTT, 0.5 mM PMSF, 1 mM EDTA, and 1 μg/ml of pepstatin A, and then desalted with a Sephadex G-25 column (2 × 24 cm) equilibrated with 50 mM KPB. The active fractions were collected and applied to a Q-Sepharose column (3 × 10 cm) equilibrated with the same buffer. After the column was washed with the same buffer, the enzyme was eluted with a 0.8-

liter linear gradient of 0-0.2 M NaCl in the buffer, and the active fractions were pooled and concentrated with ammonium sulfate as above. The enzyme collected by centrifugation was resuspended in 10 mM KPB containing 1 mM DTT, 0.5 mM EDTA, and 20 μM PLP and then dialyzed against the same buffer. The final preparation was stored at -80 °C until use.

Analytical Methods—Protein was quantified by the Bradford method (56) using Protein Assay CBB Solution (Nacalai Tesque, Kyoto, Japan) with bovine serum albumin as a standard. The concentration of the purified enzyme was determined with the value $\varepsilon_M = 1.7 \times 10^4\ M^{-1} \cdot cm^{-1}$ at 280 nm, which was calculated from the content of tyrosine, tryptophan and cysteine (57). The subunit and the native M_r of m-SCL were determined by SDS-PAGE (58) and gel filtration with Superose 12 (Amersham Pharmacia Biotech, Uppsala, Sweden), respectively.

RESULTS

Determination of Amino Acid Sequence of Pig Liver SCL—Pig liver SCL (p-SCL) was purified 1,600-fold to about 60% homogeneity with specific activity of 21 units/mg (Table I). The preparation provided two bands at 37 kDa and 43 kDa on SDS-PAGE. The 43-kDa band corresponding to p-SCL was further purified with SDS-PAGE and digested in gel matrix with lysyl endopeptidase. The peptides were separated by reverse-phase C_{18} column chromatography and subjected to sequence analysis. Amino acid sequences were obtained for five peptides, comprising 104 amino acid residues in total (Table II).

TABLE I
Purification of pig liver selenocysteine lyase

Step	Total Protein	Total Activity[a]	Specific activity	Purity	Yield
	mg	*units*	*units/mg*	*fold*	*%*
Crude extract	260,000	3,400	0.013	1	100
Ammonium sulfate	56,000	2,500	0.045	3.5	74
DEAE-Toyopearl	4,200	1,100	0.26	20	32
1st Phenyl-Toyopearl	500	560	1.1	85	16
2nd Phenyl-Toyopearl	170	450	2.6	200	13
Hydroxyapatite	24	170	7.1	550	5.0
Superdex 200 FPLC	4.6	95	21	1600	2.8

[a] measured with 5 mM L-selenocysteine.

TABLE II
Amino acid sequences of peptides derived from pig selenocysteine lyase digested with lysyl endopeptidase

Peptide 1	KSLLDRKVYMDYNATTPLEPEV
Peptide 2	VTILAARESLARMVGGRPQDVIF
Peptide 3	RRVDVWDLGVDFLTIVGHK
Peptide 4	FYGPRIGALYVRGLGELTVA
Peptide 5	AAELVAENCEAYEAHMETVR

Isolation of m-SCL-1 cDNA from cDNA Library and Expression of m-Scl-2 in E. coli—BLAST analysis of expressed sequence tag (EST) databases using the sequences in Table II resulted in the identification of highly homologous mouse and human cDNA sequences (Fig. 1). Two cDNA fragments corresponding to parts of mouse EST clones, W64820 and MUS94C09, were amplified by PCR from mouse liver cDNA using two sets of primers (Mp1 plus Mp2 and Mp3 plus Mp4), and used as probes to screen the mouse liver cDNA library. In total, 25 positive phage clones were isolated by screening of 1×10^6 plaques and sequenced, and all appeared to have the

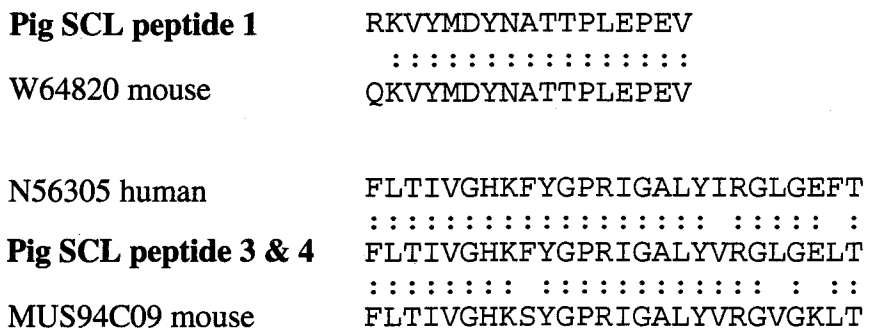

FIG. 1. **Comparison of the amino acid sequences derived from EST clones in database with those of pig liver SCL.** The nucleotide sequences of EST clones, W64820, MUS94C09, and N56305, were found in the database by homology search using BLAST program with the pig SCL sequences.

identical sequence. Sequencing of an isolated clone, m-*Scl-1*, revealed that it is comprised of 2,173 bp including a poly(A)$^+$ tail in the 3' end region. However, the clone lacked 4 bp, TAGG, at the position 165, which corresponds to the position 132-135 of the EST clone W64820, and no in-frame ATG codon was apparent near the 5' end of this sequence (Fig. 2). The 4-bp deletion should cause a frameshift at the position, resulting in failure to encode the polypeptide that is similar to p-SCL. Therefore I performed 5'-RACE and CapFinder using total RNA or poly(A)$^+$ RNA freshly prepared from BALB/c mouse liver in order to obtain an additional 5' sequence and the missing 4 bp to assemble a complete cDNA (Fig. 2). The 4 bases, 5'-TAGG-3', were shown to be present in the PCR products from both the fresh preparation of a transcript and a genomic DNA. A possible initiation ATG codon was found by 5'-RACE and with CapFinder in a position just adjacent to the 5' end of m-*Scl-1* (Fig. 2). Therefore, it is probable to assume that an

in vivo transcript contains the 4 bases together with the initiation AUG codon adjacent to the 5'-end of the m-*Scl-1* sequence in order to encode a functional SCL.

The initiation ATG and the 4 bases, TAGG, were introduced into m-*Scl-1* by PCR, and the cDNA thus obtained, m-*Scl-2*, containing the expected entire ORF was inserted into pET21a to form pSCL-2. However, the recombinant m-SCL-2 protein, whose calculated molecular mass is 46,532 Da, accumulated as an inclusion body in the host *E. coli* cells and was detected as a 46-kDa band by SDS-PAGE. No SCL activity was detected in the soluble extract nor in the solubilized pellet.

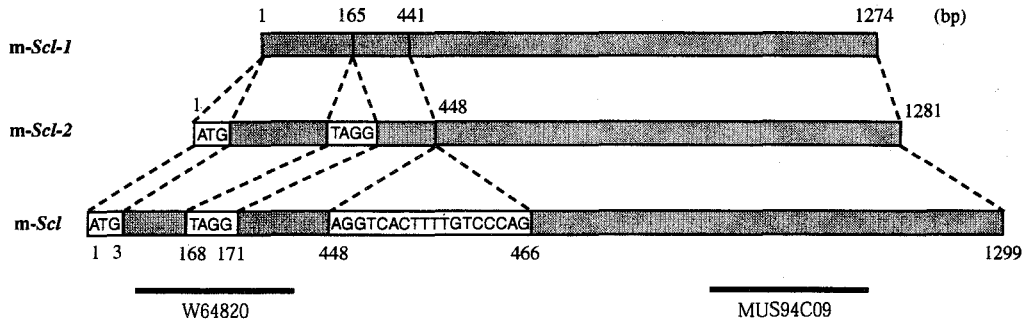

FIG. 2. **Schematic drawing of the DNA encoding m-SCL.** Differences in the coding region are shown. *Numbers* represent the positions in the nucleotide sequence of each cDNA. *m-Scl-1* was isolated by screening of the mouse cDNA library. The ATG codon and missing TAGG were introduced to construct *m-Scl-2*. *m-Scl* encodes the functional m-SCL and thus represents the entire coding sequence of m-SCL cDNA. The *horizontal lines* indicate the positions of the sequences of the mouse EST clones, W64820 and MUS94C09.

Isolation of a cDNA, m-Scl, Encoding Functional m-SCL—I isolated total

RNA from a BALB/c mouse liver, synthesized first strand cDNA, and carried out RT-PCR by using a set of primers, Mp5 and Mp8, which anneal the sequences flanking the entire ORF of m-*Scl-2*. A single 1.3-kbp cDNA fragment was obtained and directly sequenced. As a consequence of the direct sequence analysis of the cDNA fragment, an additional 18-bp insertion, 5'-AGGTCACTTTTGTCCCAG-3', was found in the region corresponding to that between the positions 448 and 449 in the ORF of m-*Scl-2* (Fig. 2). The deduced amino acid sequence of the region including 18-bp insertion, EVTFVPV, was highly conserved among the human SCL and the NifS proteins from various organisms (Fig. 9). Therefore, m-*Scl-1* lacks not only the 5' end region and the 4-bp fragment but also the 18-bp fragment.

The full-length m-SCL cDNA sequence thus obtained was termed m-*Scl*, and its nucleotide sequence and the deduced amino acid sequence are shown in Fig. 3. The total length of the assembled m-*Scl* cDNA was 2,172 bp, containing an open reading frame encoding a polypeptide chain of 432 amino acids. The 3' untranslated region contains poly(A)$^+$ tail and two potential overlapping polyadenylation signals, AATTAA and ATTAAA, located 33 and 32 bp, respectively, upstream from the poly(A)$^+$ tail.

An expression vector for m-*Scl* were constructed by introducing the entire coding region of the cDNA into pET21a to form pESL. The crude extract of the *E. coli* BL21(DE3) cells carrying pESL exhibited an SCL activity (5.9 units/mg) at pH 9.

Functional Analysis of Recombinant m-SCL—The functional enzyme, m-SCL, was produced, and the product amounted to about 20% of the total

```
                                                                GATCAGGGGG   10
ATGGACGCGGCGCGAAATGGCGCGCTGGGCAGTGTGGAGAGCCTACCCGACAGGAAGGTCTATATGGACTATAAT   85
 M  D  A  A  R  N  G  A  L  G  S  V  E  S  L  P  D  R  K  V  Y  M  D  Y  N    25
GCCACCACACCTCTAGAGCCCGAAGTCATCCAGGCTGTGACAGAGGCCATGAAGGAAGCCTGGGGAAACCCCAGC  160
 A  T  T  P  L  E  P  E  V  I  Q  A  V  T  E  A  M  K  E  A  W  G  N  P  S    50
AGCTCCTATGTGTCAGGTAGGAAGGCCAAGGACATTATAAATGCAGCTCGAGCGAGCCTGGCCAAGATGATAGGT  235
 S  S  Y  V  S  G  R  K  A  K  D  I  I  N  A  A  R  A  S  L  A  K  M  I  G    75
GGAAAGCCCCAGGACATCATCTTCACTTCTGGGGGCACCGAGTCAAATAATTTAGTAATCCACTCTATGGTAAGA  310
 G  K  P  Q  D  I  I  F  T  S  G  G  T  E  S  N  N  L  V  I  H  S  M  V  R   100
TGCTTCCATGAACAGCAGACCCTGAAGGGGAACATGGTTGACCAGCACAGCCCAGAAGAGGGGACCAGGCCCCAT  385
 C  F  H  E  Q  Q  T  L  K  G  N  M  V  D  Q  H  S  P  E  E  G  T  R  P  H   125
TTTATCACTTGCACAGTGGAACACGACTCCATCCGGCTGCCCCTGGAGCACCTGGTGGAAAATCAAATGGCAGAG  460
 F  I  T  C  T  V  E  H  D  S  I  R  L  P  L  E  H  L  V  E  N  Q  M  A  E   150
GTCACTTTTGTCCCAGTGTCGAAGGTGAATGGGCAGGCAGAGGTCGAGGATATCCTGGCGGCTGTCCGTCCCACC  535
 V  T  F  V  P  V  S  K  V  N  G  Q  A  E  V  E  D  I  L  A  A  V  R  P  T   175
ACATGCCTTGTGACCATCATGCTGGCCAATAATGAGACCGGCGTCATCATGCCTGTCTCCGAGATCAGTAGGCGA  610
 T  C  L  V  T  I  M  L  A  N  N  E  T  G  V  I  M  P  V  S  E  I  S  R  R   200
ATTAAAGCCCTGAACCAGATCCGGGCTGCCTCGGGGCTGCCCCGAGTCCTGGTGCACACAGACGCTGCTCAGGCA  685
 I  K  A  L  N  Q  I  R  A  A  S  G  L  P  R  V  L  V  H  T  D  A  A  Q  A   225
CTGGGGAAGAGGCGAGTGGATGTCGAAGACCTGGGCGTGGACTTCCTGACCATCGTGGGACATAAGTTCTACGGC  760
 L  G  K  R  R  V  D  V  E  D  L  G  V  D  F  L  T  I  V  G  H  K  F  Y  G   250
CCCAGGATCGGTGCTCTGTATGTACGAGGGGTCGGTAAACTTACCCCCCTGTACCCCATGCTGTTTGGAGGTGGA  835
 P  R  I  G  A  L  Y  V  R  G  V  G  K  L  T  P  L  Y  P  M  L  F  G  G  G   275
CAAGAGCGGAATTTCAGGCCAGGGACCGAGAACACGCCCATGATTGCTGGCCTTGGGAAGGCTGCTGATCTGGTG  910
 Q  E  R  N  F  R  P  G  T  E  N  T  P  M  I  A  G  L  G  K  A  A  D  L  V   300
AGCGAGAACTGCGAGACTTATGAGGCCCACATGAGAGACATCCGAGATTACCTGGAGGAGAGGCTGGAGGCTGAG  985
 S  E  N  C  E  T  Y  E  A  H  M  R  D  I  R  D  Y  L  E  E  R  L  E  A  E   325
TTTGGTAAGAGAATCCATTTGAACAGCCGGTTTCCAGGAGTGGAGAGGCTTCCAAACACCTGCAACTTTTCCATC 1060
 F  G  K  R  I  H  L  N  S  R  F  P  G  V  E  R  L  P  N  T  C  N  F  S  I   350
CAGGGGTCCCAGCTTCAAGGGTACACGGTCCTTGCACAGTGCCGGACACTGCTGGCCAGTGTGGGAGCATCATGC 1135
 Q  G  S  Q  L  Q  G  Y  T  V  L  A  Q  C  R  T  L  L  A  S  V  G  A  S  C   375
CACTCAAATCACGAGGACCGGCCATCCCCAGTGCTGCTGAGCTGCGGCATTCCTGTGGACGTGGCCCGGAATGCG 1210
 H  S  N  H  E  D  R  P  S  P  V  L  L  S  C  G  I  P  V  D  V  A  R  N  A   400
GTCCGGCTCAGCGTGGGCCGCGGTACCACCAGGGCTGATGTGGATCTCATCGTACAGGACCTGAAGCAGGCCGTG 1285
 V  R  L  S  V  G  R  G  T  T  R  A  D  V  D  L  I  V  Q  D  L  K  Q  A  V   425
GCCCAACTGGAAGGGCGGCTCTAGAACTAGCAGCCGCTCTCTGTAGCCAGCTGGACTTTTACCACTCGATCCATA 1360
 A  Q  L  E  G  R  L                                                        432
GGAAACCGCTTGCAAAAGCCCTTGGTCCCTAAGCTGCCCCATCTCAAGAGCTGCGTTGAGGTGACTTGTCCTACT 1435
GTGGGGTGCAGAGTGACGAGGGGCTGCCCACCGCACAGAATCCCACCCCAGCACCCATCCTTACAAGCTCAGGAC 1510
AGCCATGTCACATAGGACTTCTCCCTGTCACCTTCTGACAAAGGCCACAGGGGAATAGGAATATTCCAGTTATCG 1585
GGCAGCCTGCCAGGACCGCCTGACCCCAGAAGGCACCTTGGTCAGAAGACAAAACCCAAGTCTTGGTCCGGTGTC 1660
ACTTAGCTGCTAGTGTGAGAATAGGAAAGTTGATTTTGACTCCCCCTCCTACCCCCAACCCCCCACCCCCGTGCT 1735
TCCCCTGTGCACCTACAGACACACCCTTCTCCAGTGCAGCCCTGCCTCTGCCCTCAGCCAGCCACTGCCCACCTG 1810
CCTCCCTGGCCTGATGGTCCGCAGATGTCCCATGCCTTGTCCCCGGAAGTCGAAGCTTACCCTGCCCCCCACTCA 1885
GGGACACAACCCCAGCGTGGTACCGGGAGGCTGGTGCCTGAGCTCAGTCTTTGCCAAAGTGGGAAATCTGATCAT 1960
TTCTCGCTCACATTCCATTTTAATTTTATTTTGCAAAAGGCTGTGCCACCTTAAAGGATGTTGTGGCACACATCG 2035
CACCCAAGGTTTATATAAGAATGTTCTCCCCTGGAAGGCTGCCTTTTTGGGTTCTGTGGACCAAAGGATGACCCA 2110
ACCCCGTGAAAACAGTTGTCAGAAAATTAAATTGAACTAATGAAAAAAAAAAAAAAAAAAA               2172
```

FIG. 3. **Nucleotide and deduced amino acid sequences of the full-length m-*Scl*.** Two possible overlapping polyadenylation signals are *underlined*. Numbers of nucleotides and amino acid residues are shown.

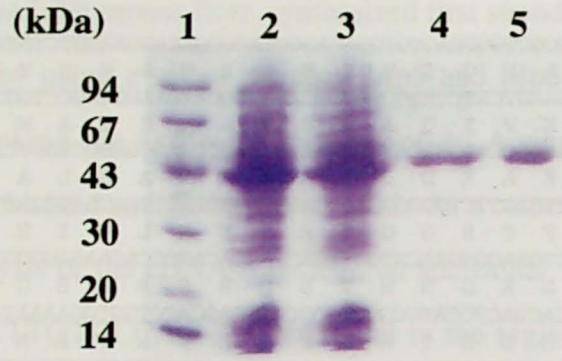

FIG. 4. **Purification of recombinant m-SCL.** SDS-PAGE was performed with the different preparations obtained during purification of m-SCL. *Lane 1*, marker proteins, the molecular masses are shown in kDa; *lane 2*, crude extracts; *lane 3*, ammonium sulfate precipitation; *lane 4*, Butyl-Toyopearl; *lane 5*, Q-Sepharose. The proteins were stained with Coomassie Brilliant Blue R-250.

protein in the crude extract of *E. coli* BL21(DE3) harboring pESL. Purified m-SCL provided a 47-kDa single band on SDS-PAGE (Fig. 4). The N-terminal sequence of the purified enzyme, MDAARNGALG, agreed with that deduced from the nucleotide sequence of cDNA, m-*Scl*. The M_r of the native enzyme was determined to be 105,000 by gel filtration. Therefore, the enzyme is a dimer composed of two identical subunits. The enzyme was yellow and exhibited an absorption maximum at 420 nm, which is a characteristic of PLP enzymes. The requirement of PLP as a cofactor of the enzyme was examined as follows. Reduction with sodium borohydride resulted in an irreversible inactivation of the enzyme and a disappearance of the absorption band at 420 nm with a concomitant increase in the absorbance at 330 nm. When the enzyme was incubated with 1 mM hydroxylamine, the activity decreased to 25% of the original activity. Addition of 0.2 mM of PLP to the dialyzed

enzyme restored 90% of the original activity. Thus, PLP serves as a cofactor of the enzyme and probably binds to the ε-amino group of a lysine residue at the active site of the enzyme through an aldimine linkage as in other PLP enzyme studied so far.

The specific activity of the purified enzyme (29 units/mg) with L-selenocysteine was comparable to that of pig liver SCL (37 units/mg) (15) (Table III). The enzyme showed the maximum reactivity at about pH 9 when measured in Tricine-NaOH (pH 7.0-9.5) and glycine-NaOH (pH 8.5-11) buffers. Therefore, the optimum pH of the m-SCL activity is similar to that of p-SCL (pH 9.0) (15). The production of elemental selenium from L-selenocysteine was examined in the same manner as described previously (42). When a molar ratio of DTT/L-selenocystine was 1 or below it, the formation of red elemental selenium was observed and selenide was not detected. When the molar ratio was higher than 1, selenide was produced. These results show that the product by m-SCL from L-selenocysteine is elemental selenium, and that the formation of selenide is due to a nonenzymatic reaction of selenium with DTT.

TABLE III
Purification of mouse liver selenocysteine lyase

Step	Total Protein	Total Activity[a]	Specific activity	Purity	Yield
	mg	*units*	*units mg*	*fold*	*%*
Crude extract	440	2600	5.9	1	100
Ammonium sulfate	550	3600	6.5	1.1	130
Butyl-Toyopearl	120	1600	13	2.2	62
Q-Sepharose	56	1600	29	4.9	62

[a] measured with 5 mM L-selenocysteine.

TABLE IV

Substrate specificity and kinetic parameters of m-SCL

Substrate	K_m	V_{max}	k_{cat}	k_{cat}/K_m
	mM	*μmol·min $^{-1}$ ·mg $^{-1}$*	*s^{-1}*	*mM^{-1} ·s^{-1}*
L-Selenocysteine	9.9	58	46	4.6
L-Cysteine sulfinate	8.6	0.45	0.35	0.041
L-Cysteine	ND[a]	0.0029	0.0023	ND[a]

[a] ND, not determined.

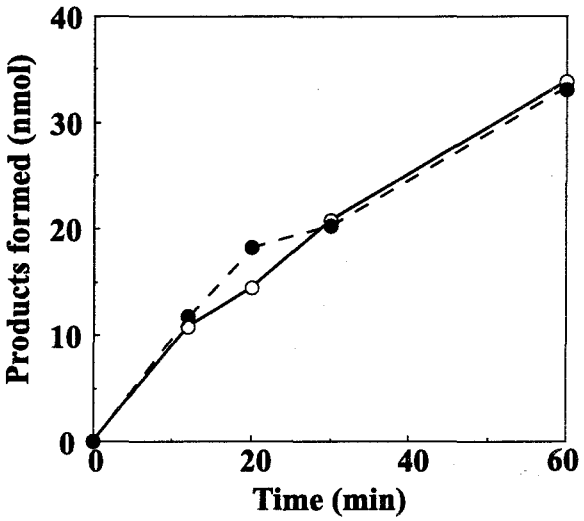

FIG. 5. **Determination of products of the SCL reaction.** Selenide (●) and alanine (○) are formed from L-selenocysteine in approximately equal amounts.

The ability of the enzyme to catalyze cleavage of several amino acids was investigated. When L-cysteine sulfinate and L-cysteine were used as substrates, a small amount of alanine was formed. The amount of the enzyme used for the reaction with these amino acids was 100 times greater than that used for the reaction with L-selenocysteine. The substrate specificity and kinetic parameters for m-SCL with L-selenocysteine, L-cysteine sulfinate, and L-cysteine are summarized in Table IV. The enzyme exhibits an extremely

high, though not absolute, specificity to L-selenocysteine. The k_{cat}/K_m value for L-selenocysteine is about 100 times higher than that for L-cysteine sulfinate, and the V_{max} value for L-selenocysteine is 2×10^4 times higher than that for L-cysteine, confirming that this enzyme is the mouse counterpart of pig SCL. The production of alanine was not detected under the reaction condition where L-aspartate, DL-kynurenine, L-selenocystine, L-cystine, D-selenocysteine, and D-selenocystine were used as substrates.

Experiments were performed to establish the stoichiometry of the enzymatic decomposition of L-selenocysteine. In order to investigate the ratio of the amount of alanine and selenium formed, alanine was analyzed by amino acid analyzer, and selenide derived from selenium in the presence of DTT was determined with lead acetate. As shown in Fig. 5, these two products formed in a 1:1 stoichiometry.

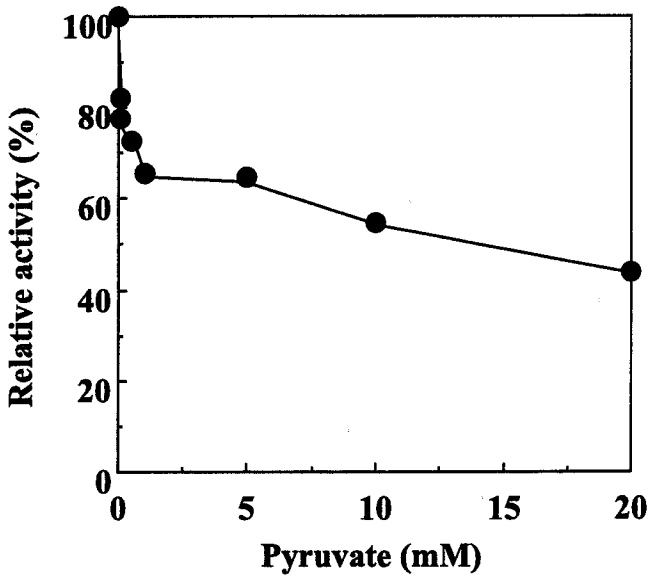

FIG. 6. **Effect of pyruvate concentration on the m-SCL reaction.** The enzyme activity was determined with 12 mM L-selenocysteine as a substrate in the presence of various concentrations of pyruvate.

Effect of Pyruvate—To investigate the effect of pyruvate, selenocysteine lyase was incubated with various concentrations of pyruvate (0-20 mM). The activity was measured with L-selenocysteine as a substrate. Significant inactivation of the enzyme was observed and the extent of inactivation depends on the concentration of pyruvate as shown in Fig. 6.

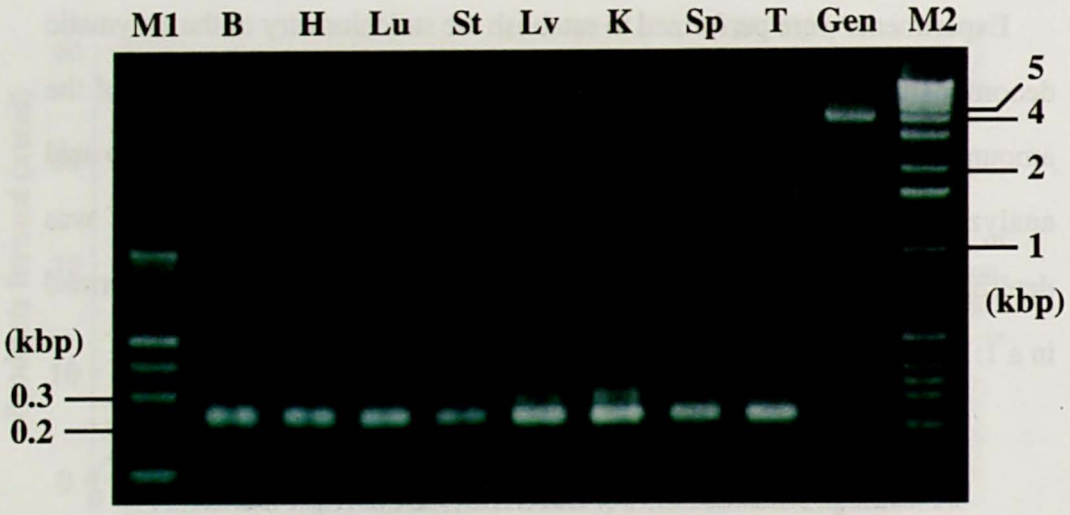

FIG. 7. **RT-PCR analysis of tissue distribution of mSCL mRNA.** RT-PCR products obtained were subjected to agarose gel electrophoresis. Lanes: *M1*, 100-bp DNA ladder marker; *B*, brain; *H*, heart; *Lu*, lung; *St*, stomach; *Lv*, liver; *K*, kidney; *Sp*, spleen; *T*, testis; *M2*, 1-kbp DNA ladder marker; *Gen*, a negative control reaction was performed with the same primers using the genomic DNA as a template.

Tissue Distribution and Intracellular Localization of m-SCL—In order to determine the tissue distribution of the m-*Scl* transcript, RT-PCR was performed using a set of primers (Mp9 and Mp10), which are specific to m-*Scl*, and total RNAs prepared from various mouse tissues (brain, heart, lung, stomach, liver, kidney, spleen, and testis) as a template. As a control, PCR

was performed using the same set of primers with the mouse genomic DNA as a template. As shown in Fig. 7, a single 270-bp fragment was amplified in all examined tissues, indicating that *m-SCL* is expressed ubiquitously. In the control reaction using the genomic DNA, a single fragment (> 4 kbp) was amplified (Fig. 7). The results indicate that this region of the genomic DNA contains at least one intron, and the 270-bp fragments were specifically derived from RNA.

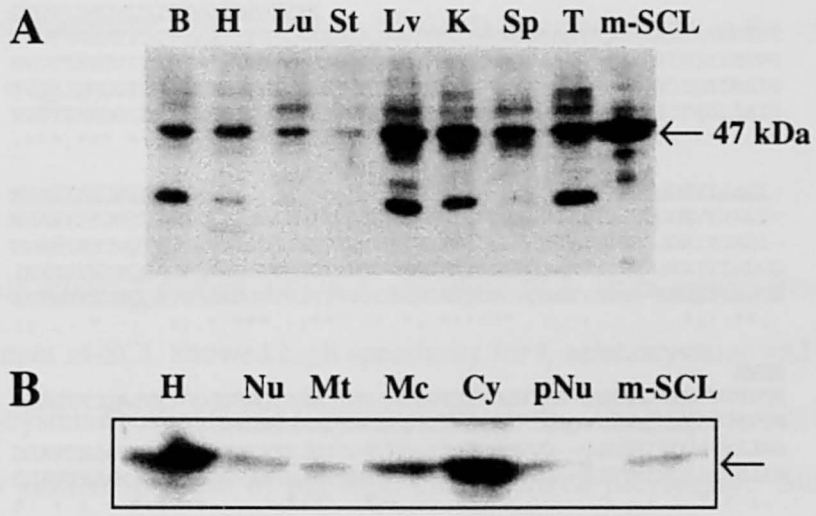

FIG. 8. **Western blot analysis of m-SCL in mouse tissues and intracellular localization of the enzyme.** (A) Each 30 μg of cell extracts from 8 tissues of mouse (*B*, brain; *H*, heart; *Lu*, lung; *St*, stomach; *Lv*, liver; *K*, kidney; *Sp*, spleen; *T*, tests; *m-SCL*, purified m-SCL as a control) were separated with 12.5% SDS-PAGE, blotted onto a PVDF membrane, and analyzed with polyclonal anti-m-SCL-1 antibody. An arrow indicates the position of the m-SCL. (B) The immunoblot of m-SCL in each subcellular fraction of mouse liver cells is shown: *H*, cell homogenate; *Nu*, the nuclear fraction by low-spin centrifugation of the cell homogenates; *Mt*, the mitochondrial fraction; *Mc*, the microsomal fractions; *Cy*, the cytosolic fraction; *pNu*, the pure nuclear fraction prepared by the method of Blobel and Potter (Ref. 54). The position of the m-SCL is indicated by an arrow.

```
m-SCL                                                        MDAARNGALGSVE 15
h-SCL1                                                    MEAAVAPGRDAPAPAASQPSGCGKH 27
m-Nfs1     MVGSVAGNMLLRAAWRRASLAATSLALGRSSVPTRGLRLRVVDHGPHSPVHS------EA 54
h-NifS             MLLRVAWRRAAVAVTAAPGPKPAAPTRGLRLRVGDRAPQSAVPADTTAAPEV 52
                                                          .  . .

Pig SCL   KSLLDRKVYMDYNATTPLEPEV                                VTILAARESLAR
m-SCL      SLPDRKVYMDYNATTPLEPEVIQAVTEAMKEAWGNPSS-SYVSGRKAKDIINAARASLAK 72
h-SCL1     NSPERKVYMDYNATTPVEPEVIQAMTKAMWEAWGNPSS-PYSAGRKAKDIINAARESLAK 84
m-Nfs1     EAVLRPLYMDVQATTPLDPRVLDAMLPYLVNYYGNPHSRTHAYGWESEAAMERARQQVAS 114
h-NifS     GPVLRPLYMDVQATTPLDPRVLDAMLPYLINYYGNPHSRTHAYGWESEAAMERARQQVAS 112
                 :*** :****::*.*::*:   : : :*** * .:  * :::  :: ** .:*.

Pig SCL   MVGGRPQDVIF
m-SCL      MIGGKPQDIIFTSGGTESNNLVIHSMVRCFHEQQTLKGNMVDQHSPEEGTRPHFITCTVE 132
h-SCL1     MIGGKPQDIIFTSGGTESNNLVIHSVVKHFHANQTSKGHTGGHHSPVKGAKPHFITSSVE 144
m-Nfs1     LIGADPREIIFTSGATESNNIAIKGVARFYRS----------------RKKHLVTTQTE 157
h-NifS     LIGADPREIIFTSGATESNNIAIKGVARFYRS----------------RKKHLITTQTE 155
           :**..*::******.*****:.*:.:.: ::                    : *::*  .*

m-SCL      HDSIRLPLEHLVENQMAEVTFVPVSKVNGQAEVEDILAAVRPTTCLVTIMLANNETGVIM 192
h-SCL1     HDSIRLPLEHLVEEQVAAVTFVPVSKVSGQAEVDDILAAVRPTTRLVTIMLANNETGIVM 204
m-Nfs1     HKCV-LDSCRSLEAEGFRVTYLPVQKS-GIIDLKELEAAIQPDTSLVSVMTVNNEIGVKQ 215
h-NifS     HKCV-LDSCRSLEAEGFQVTYLPVQKS-GIIDLKELEAAIQPDTSLVSVMTVNNEIGVKQ 213
           *..: *   : :* :   **::**.*  *  ::.:: **::* * **::* .*** *:

Pig SCL                                                  RRVDVWDLGVDFLTIVGHKFYGPR
m-SCL      PVSEISRRIKALNQIRAASGLPRVLVHTDAAQALGKRRVDVEDLGVDFLTIVGHKFYGPR 252
h-SCL1     PVPEISQRIKALNQERVAAGLPPILVHTDAAQALGKQRVDVEDLGVDFLTIVGHKFYGPR 264
m-Nfs1     PIAEIRQICSSR----------KVYFHTDAAQAVGKIPLDVNDMKIDLMSISGHKLYGPK 265
h-NifS     PIAEIGRICSSR----------KVYFHTDAAQAVGKIPLDVNDMKIDLMSISGHKIYGPK 263
           *:.** :  .:             : .*******:**  :**:*: :*:::* ***:***:

Pig SCL   -IGALYVRGLGELTVA                                  AAELVAENCEAYEAHM
m-SCL      -IGALYVRGVGKLTPLYPMLFGGGQERNFRPGTENTPMIAGLGKAADLVSENCETYEAHM 311
h-SCL1     -IGALYIRGLGEFTPLYPMLFGGGQERNFRPGTENTPMIAGLGKAAELVTQNCEAYEAHM 323
m-Nfs1     GVGAIYIRRR-PRVRVEALQSGGGQERGMRSGTVPTPLVVGLGAACELAQQEMEYDHKRI 324
h-NifS     GVGAIYIRRR-PRVRVEALQSGGGQERGMRSGTVPTPLVVGLGAACEVAQQEMEYDHKRI 322
            :**:*:*     . : .:  ******.:*.**  **::.*** *.::. :: *  . ::

Pig SCL   ETVR
m-SCL      RDIRDYLEERLEAEFG-KRIHLNSRFPGVERLPNTCNFSIQGSQLQGYTVLAQCRTLLAS 370
h-SCL1     RDVRDYLEERLEAEFGQKRIHLNSQFPGTQRLPNTCNFSIRGPR...               367
m-Nfs1     SKLAERLVQKIMKNLP--DVVMNGDPK--QHYPGCINLSFAYVEGE--SLLMALKDVALS 378
h-NifS     SKLSERLIQNIMKSLP--DVVMNGDPK--HHYPGCINLSFAYVEGE--SLLMALKDVALS 376
            .: : * :.:  .:    : :*.     .: *.  *:*:   . :  ::*   : :  *

m-SCL      VGASCHSNHEDRPSPVLLNCGIPVDVARNAVRLSVGRGTTRADVDLIVQDLKQAVAQLEG 430
m-Nfs1     SGSACT-SASLEPSYVFRAIGIDEDLAHSSIRFGIGRFTTEEEVDYTAEKCIHHVKRLRE 437
h-NifS     SGSSCS-LHPWSPLMCLEQLALMRIYSHSSIRFGIGAFTTEEEVDYTVEKCIQHVNRLRE 435
            *::*       *   :   .:    ::.::*:.:*  **. :**  .:.  : * :*.

m-SCL      RL                      432
m-Nfs1     MSPLWEMVQDGIDLKSIKWTQH 459
h-NifS     MSPLWEMVQDGIDLKSIKWTQH 457
```

FIG. 9. **Comparison of amino acid sequences of mammalian SCLs and NifSs.** The amino acid sequences of the mammalian *Scl* gene products from mouse (m-SCL) and human (h-SCL1), and those of the mammalian *nifS*-like gene products from mouse (m-Nfs1) and human (h-NifS) are shown. Amino acid identities are indicated by *asterisks*; similarities are marked by *colon* or *dot* in the order of the extent of a similarity. The sequences of pig SCL are also shown with *underlines*.

The tissue distribution of the m-SCL protein was also examined by Western blotting. Polyclonal antibodies raised against m-SCL-2 were used to detect m-SCL in various tissue homogenates of the mouse. An immunoreactive protein of 47 kDa was detected in all cell homogenate examined (Fig. 8). On the basis of a comparison of the intensity of the stained protein bands, liver, kidney, and testis appeared to contain the highest enzyme levels.

I determined the intracellular localization of m-SCL by Western blot analysis with anti-m-SCL antibodies. Mouse liver was homogenized and fractionated into nucleus, mitochondrial, microsomal, and cytosolic fractions. The immunoreactive 47-kDa protein band was detected mainly in the cytosolic fraction (Fig. 8).

DISCUSSION

In this study, I cloned a cDNA encoding SCL from mouse liver. The recombinant m-SCL showed high specificity for L-selenocysteine and did not act on L-cysteine sulfinate and L-cysteine efficiently. The properties of m-SCL are very similar to those of pig SCL characterized previously. Similarity searches using the BLAST program against the nonredundant database revealed that several dbEST sequences from human showed strong homology with m-SCL. The amino acid sequence of the human protein was deduced by assembling 11 independent partial cDNA sequences in dbEST and a putative human SCL cDNA clone, h-*Scl1*, isolated by the author (Fig. 9), although the 3'-end of h-*Scl1* has not yet been obtained, and the presented sequence

lacks the C-terminal region. The peptide sequences of pig SCL also showed striking similarity with m-SCL and human SCL (h-SCL1) (Fig. 9). Although the overall similarity is found between mammalian NifS and mammalian SCL, they are clearly classified into two distinct groups, NifS and SCL. These observations suggest that SCL establishes a different class of eukaryotic enzymes, which should not be called a "NifS-like protein" in those mammals (Fig. 10).

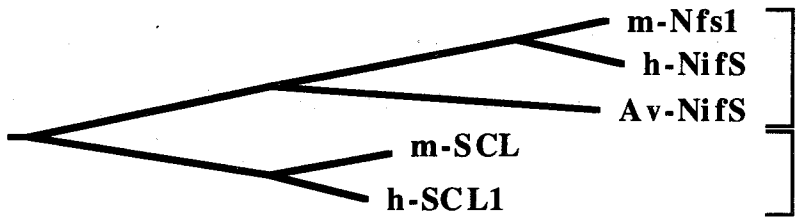

FIG. 10. **Phylogenetic tree showing the divergence of SCL and NifS.** The protein sequences were aligned, and phylogenetic relations were analyzed with MegAlign proglam of the DNASTAR package (DNASTAR, Inc.). Av-NifS represents NifS from *A. vinelandii*. It is clearly shown that m-SCL and h-SCL1 establish two different classes of enzymes.

RT-PCR and immunoblotting analysis showed that mRNA of m-SCL is widely distributed and expressed in significant levels, suggesting that the enzyme plays a house-keeping function in mouse cells. This result is consistent with the wide distribution of the enzyme activity in various mammalian tissues described previously (15). m-SCL was preferentially expressed in the crude enzyme preparation of liver, kidney, and testis. Interestingly, mouse homolog of selenophosphate synthetase is also highly

expressed in liver, kidney, and testis, where selenoproteins are produced (59). This implies that m-SCL would cooperate with selenophosphate synthetase in production of selenophosphate as a selenium donor for selenoprotein biosynthesis in eukaryotes.

Recent studies on eukaryotic NifS-like proteins from human (60), mouse (61), and yeast (61, 62) showed that they have mitochondrial sorting signals at their N-terminal regions. Mouse Nfs1 preferentially exists in mitochondrial matrix (61). Yeast Nfs1 is sorted mainly to mitochondrial matrix and to the nucleus in a small amount (61). Furthermore, different form of human NifS, which are derived from a single transcript through initiation at alternative in-frame ATGs, are shown to localize either to mitochondria or to the cytosol and nucleus (60). Several iron-sulfur proteins such as components of TCA cycle proteins and respiratory chain proteins are present in eukaryotic mitochondria.. The subcellular localization of NifS is consistent with the hypothesis that eukaryotic NifS is involved in the *de novo* formation of iron-sulfur clusters.

On the other hand, m-SCL exists mainly in cytosolic fraction. Because enzymes involved in selenoprotein biosynthesis are known to exist in cytosol, the result consistent with the hypothesis that m-SCL would deliver an active-form of selenium to selenophosphate synthetase reaction *in vivo*. Recently, Lacourciere and Stadtman (52) found that the replacement of selenide by NifS and L-selenocysteine in an *in vitro* selenophosphate synthetase assay system resulted in an increased rate of formation of selenophosphate, indicating that selenium derived from L-selenocysteine by the action of NifS serves as a better substrate than selenide for selenophosphate synthetase. Therefore, it is

reasonable to assume that enzymes which are specific toward L-selenocysteine such as m-SCL function in a physiological selenide delivery system in organisms.

Selenocysteine is usually found in the polypeptide chains of selenoproteins. Free selenocysteine is probably formed by degrading those selenoproteins. Another possible pathway which yields free selenocysteine in mammalian cells is the enzymatic biosynthesis of selenocysteine from selenomethionine by cystathionine β–synthase and cystathionine γ-lyase (14). Free selenocysteine itself is known as a toxic compound, and accumulation of selenocysteine is lethal (63). Therefore, excess selenocysteine probably has to be decomposed in order to decrease its concentration in the cell. SCL decomposes selenocysteine into alanine and elemental selenium. Elemental selenium is known to be chemically inactive and safe in cells (64). Under a reductive condition, elemental selenium is reduced to selenide, which subsequently could be detoxified through methylation to form dimethyl selenide (3). Thus, SCL could function as an enzyme to detoxify selenocysteine. The result obtained in the present study that the SCL gene is expressed in various tissues is compatible with the detoxification hypothesis. It is also possible that the formation of selenium (or selenide) by SCL could be an effective mechanism to maintain the level of selenium concentration in the cells (52). Selenium is known to be essential at lower concentrations (0.05-0.3 ppm) and toxic at higher concentration (> 2 ppm) (65). These values differ only by an order of magnitude. A regulation of SCL level or its activity may facilitate a control of a selenium level, which regulates the subsequent physiological processes. Further experiments are necessary to clarify the physiological role of the

enzyme.

SUMMARY

Selenocysteine lyase (SCL) (EC 4.4.1.16) is a pyridoxal 5'-phosphate-dependent enzyme which specifically catalyzes decomposition of L-selenocysteine to L-alanine and elemental selenium. Its ability to discriminate L-selenocysteine from the sulfur analog, L-cysteine, suggests that the enzyme may function as a selenide delivery protein to selenophosphate synthetase in selenoprotein biosynthesis. I presented here the first cloning, sequencing, and functional expression in *Escherichia coli* of cDNA encoding mouse liver SCL. The sequences of mouse EST clones whose deduced amino acid sequences show significant identity to the sequences of pig SCL peptides were used as probes to isolate a mouse liver cDNA clone. The mouse cDNA, termed m-*Scl*, was determined to be 2,172 bp in length, containing an open reading frame encoding a polypeptide chain of 432 amino acids. Two potential overlapping polyadenylation signals, AATTAA and ATTAAA, located 13 and 12 bp, respectively, upstream from the poly(A)$^+$ tail. The deduced sequence of the cDNA suggests a distant relationship of the enzyme with NifS, a cysteine desulfurase, that is proposed to provide sulfur in iron-sulfur clusters. The recombinant m-SCL overproduced in *E. coli* was a pyridoxal phosphate-dependent homodimer with the subunit M_r of 46,000 and highly, though not exclusively, specific toward L-selenocysteine (about 10^4 times of activity to L-cysteine). RT-PCR and Western blot analyses revealed that mouse SCL mRNA preferably exists in liver, kidney, and testis, where mouse selenophosphate synthetase is also highly present, implying that m-SCL may function in cooperation with selenophosphate synthetase in the the

selenoprotein synthesis.

CHAPTER II

CSD, a NifS-like Protein of *Escherichia coli* with Selenocysteine Lyase and Cysteine Desulfurase Activities: Gene Cloning, Purification, and Characterization of a Novel Pyridoxal Enzyme

INTRODUCTION

The nucleotide sequence of the whole *Escherichia coli* genome has been determined (66), and the bacterium appears to contain three *nifS*-like genes (67, 68). One of the genes (*iscS*) located at 57.3 min (67) in the chromosome presumably encodes the NifS-like protein purified by Flint (69). Not only the amino acid sequence but also the catalytic properties of the enzyme resemble those of *A. vinelandii* NifS. I have showed that the amino acid sequence of mouse liver selenocysteine lyase is similar to that of NifS (Chapter I). If *E. coli* contains selenocysteine lyase and the enzyme resembles NifS, one or both of the other two *nifS*-like genes may encode selenocysteine lyase(s). Alternatively, the genes may encode new enzymes participating in an unknown metabolism of sulfur or selenium amino acids.

I have cloned the *nifS*-like gene mapped at 63.4 min (*csdA*), and found that the gene product (CSD) is a novel PLP-dependent enzyme decomposing L-selenocysteine, L-selenocystine, L-cysteine, and L-cystine. L-Cysteine sulfinic acid is also decomposed to L-alanine as the best substrate of the enzyme. I describe here the characteristics of the enzyme and compare it with

other related enzymes such as selenocysteine lyase and NifS.

EXPERIMENTAL PROCEDURES

Materials—Molecular weight markers for SDS-PAGE and gel filtration were purchased from Amersham Pharmacia Biotech (Uppsala, Sweden) and Oriental Yeast (Tokyo, Japan), respectively; restriction enzymes and other DNA modifying enzymes from Takara Shuzo (Kyoto, Japan); synthetic oligonucleotides from Japan Bio Service (Saitama, Japan) and Biologica (Nagoya, Japan). L-Selenocystine was synthesized from L-β-chloroalanine, which was kindly provided by Showa Denko, and from disodium diselenide, as described previously (53). L-Selenocysteine was prepared from L-selenocystine according to the previous method (15). All other chemicals were of analytical grade.

Cloning of csdA—The DNA fragment containing the ORF for CSD was amplified with a Perkin Elmer Thermal Cycler 480. The reaction mixture (50 μl) contained: 10 mM Tris-HCl (pH 8.3), 50 mM KCl, 1.5 mM $MgCl_2$, 10% DMSO, 400 μM each dNTP, 0.2 μM each primer (5'-GGAATTCATCAAGC CG**AGGA**GTAC-CATGAACG-3' and 5'-AACTGCAGCGGCGAATTGCG GGTTTGTCATTAA-3'; underlines indicate *Eco*RI and *Pst*I sites; boldface letters, a putative ribosome binding sequence), 2.5 units of Ex Taq DNA polymerase (Takara Shuzo), and 100 ng of template DNA from *E. coli* JM109 isolated by the method reported (70). The conditions were: the first cycle, 2 min (94°C), 5 min (55°C), and 10 min (72°C); the following 24 cycles, 1 min (94°C), 1 min (58°C), then 3 min (72°C); the last cycle, 1 min (94°C), 1 min

(58°C), 15 min (72°C). The *Eco*RI-*Pst*I fragment was ligated into pUC118 to give a plasmid pCSD1.

Assays and Definition of Units—CSD was assayed by determination of H_2Se formed from L-selenocysteine with lead acetate as described previously (15). A standard reaction mixture containing 5 mM L-selenocysteine, 50 mM DTT, 0.02 mM PLP, 120 mM Tricine-NaOH buffer (pH 7.5), and enzyme (0.006-0.032 units) in a final volume of 0.1 ml was incubated at 37°C. A molar turbidity coefficient of PbSe at 400 nm, 1.18×10^4 $M^{-1} \cdot cm^{-1}$, was used. One unit of enzyme was defined as the amount of enzyme that catalyzes the formation of 1 μmol of the product (alanine or elemental selenium) per min. Specific activity was expressed as units per mg of protein.

Cysteine desulfurase activity was measured by the determination of H_2S formed from L-cysteine with lead acetate in the manner described above. An apparent molar turbidity coefficient of colloidal PbS at 360 nm, 1.31×10^4 $M^{-1} \cdot cm^{-1}$, was used (71). Pyruvate was determined with lactate dehydrogenase (Sigma) at 37°C in a reaction mixture (1 ml) containing 5 mM L-β-chloroalanine, lactate dehydrogenase (22 units), 0.02 mM PLP, 0.15 mM NADH, 120 mM Tricine-NaOH buffer (pH 8.5), and enzyme. Sulfite produced from L-cysteine sulfinic acid was determined with fuchsin (55). Protein was determined with a Bio-Rad protein assay kit with BSA as a standard.

Purification of CSD—The buffer used throughout the purification was 10 mM potassium phosphate (pH 7.4), and was supplemented with salts when required for chromatographies. All operations (Table V) were done at 4°C.

Elution patterns of protein were estimated by absorption at 280 nm. *E. coli* XL1-Blue (Stratagene) carrying pCSD1 was cultured aerobically in LB broth (3 L) supplemented with ampicillin (200 μg/ml) at 37°C for 11 h, and then IPTG was added to the culture at a final concentration of 1 mM. The cells were cultured for another 2 h, and harvested by centrifugation. The final preparation of the enzyme was stored frozen at -30°C in the buffer supplemented with 0.02 mM PLP until use.

Mass Spectrometry—The molecular mass of the enzyme was determined with a Vision 2000 reflector-type time-of-flight mass spectrometer (Thermoquest, Tokyo) equipped with a nitrogen laser (337 nm, pulse length 10 ns). The enzyme solution (1.0×10^{-5} - 2.5×10^{-6} M) was mixed with the same volume of 1% (w/v) 2,5-dihydroxybenzoic acid solution in 10% acetonitrile containing 0.1% (v/v) TFA. Spectral measurements were repeated one hundred times, and the average of their sum was recorded. BSA was used as a standard protein.

Site-directed Mutagenesis—The mutants enzymes were prepared by the Kunkel method (72). ssDNA was obtained with another plasmid named pCSL2, which was constructed in the same manner as pCSL1 except that the following primer was used for the upstream region: 5'-GGGAATTCCATATG AACGTTTTTAATCCCGCGCAGTTTCG-3' (the *Eco*RI site is underlined). The ssDNA was prepared from *E. coli* BW313 carrying pCSL2, by infection with helper phage VCSM13 (Stratagene). The following mutagenic primers were used: 5'-ACGCGCATAGGCTTGTGCC-AC-3' (Cys100), 5'-CAGATC CGGGGCACCGCCAGT-3' (Cys176), 5'-GG-AATCCTGGGCGCGGAAT

GA-3' (Cys323), and 5'-GGCTGAGCGGCATGCTG-CCC-3' (Cys358) (mutagenized nucleotides are underlined). The nucleotide sequences were confirmed with a Dye Terminator sequencing kit and an Applied Biosystem 370A DNA sequencer. Mutant enzymes were prepared with *E. coli* JM109 as a host.

RESULTS

Cloning and Expression of csdA—I cloned the cDNA encoding mouse selenocysteine lyase (m-SCL) and found that its amino acid sequence is similar to that of NifS protein (Chapter I). Thus, selenocysteine lyase, if it occurs in *E. coli*, probably has a primary structure similar to that of NifS or m-SCL. The amino acid sequence deduced from ORF o401 located at 63.4 min in the *E. coli* K-12 genome was found to have about 20% homology with that of *A. vinelandii* NifS. I cloned the gene by PCR, with the *E. coli* JM109 chromosomal DNA as a template and the synthetic primers shown above. The DNA sequence of the gene thus cloned agreed completely with that registered in GenBank, accession number U295810.

The molecular weight of the homogeneous preparation of the gene product estimated by SDS-PAGE (58) (about 43,000) agreed with the value calculated from the deduced amino acid sequence (43,238). The N-terminal amino acid sequence of the purified protein agreed with that deduced from the nucleotide sequence (Fig. 11). Although I did not determine the C-terminal amino acid sequence of the protein, the molecular mass of the protein determined by mass spectrometry was essentially identical with the predicted value: *m/z* 43279.6 corresponding to $(M+H)^{1+}$. The molecular weight of the purified protein in the

```
                                SD
CACGATCGGTGCATCAAGCCGAGGAGTACCATGAACGTTTTTAATCCCGCGCAGTTTCGCGCCCAGTTTCCCGCA   75
                                M  N  V  F  N  P  A  Q  F  R  A  Q  F  P  A    15

CTACAGGATGCGGGCGTCTATCTCGACAGCGCCGCGACCGCGCTTAAACCTGAAGCCGTGGTTGAAGCCACCCAA  150
L  Q  D  A  G  V  Y  L  D  S  A  A  T  A  L  K  P  E  A  V  V  E  A  T  Q    40

CAGTTTTACAGTCTGAGCGCCGGAAACGTCCATCGCAGCCAGTTTGCCGAAGCCCAACGCCTGACCGCGCGTTAT  225
Q  F  Y  S  L  S  A  G  N  V  H  R  S  Q  F  A  E  A  Q  R  L  T  A  R  Y    65

GAAGCTGCACGAGAGAAAGTGGCGCAATTACTGAATGCACCGGATGATAAAACTATCGTCTGGACGCGCGGCACC  300
E  A  A  R  E  K  V  A  Q  L  L  N  A  P  D  D  K  T  I  V  W  T  R  G  T    90

ACTGAATCCATCAACATGGTGGCACAATGCTATGCGCGTCCGCGTCTGCAACCGGGCGATGAGATTATTGTCAGC  375
T  E  S  I  N  M  V  A  Q  C  Y  A  R  P  R  L  Q  P  G  D  E  I  I  V  S    115

GTGGCAGAACACCACGCCAACCTCGTCCCCTGGCTGATGGTCGCCCAACAAACTGGAGCCAAAGTGGTGAAATTG  450
V  A  E  H  H  A  N  L  V  P  W  L  M  V  A  Q  Q  T  G  A  K  V  V  K  L    140

CCGCTTAATGCGCAGCGACTGCCGGATGTCGATTTGTTGCCAGAACTGATTACTCCCCGTAGTCGGATTCTGGCG  525
P  L  N  A  Q  R  L  P  D  V  D  L  L  P  E  L  I  T  P  R  S  R  I  L  A    165

TTGGGTCAGATGTCGAACGTTACTGGCGGTTGCCCGGATCTGGCGCGAGCGATTACCTTTGCTCATTCAGCCGGG  600
L  G  Q  M  S  N  V  T  G  G  C  P  D  L  A  R  A  I  T  F  A  H  S  A  G    190

ATGGTGGTGATGGTTGATGGTGCTCAGGGGGCAGTGCATTTCCCCGCGGATGTTCAGCAACTGGATATTGATTTC  675
M  V  V  M  V  D  G  A  Q  G  A  V  H  F  P  A  D  V  Q  Q  L  D  I  D  F    215

TATGCTTTTTCAGGTCACAAACTGTATGGCCCGACAGGTATCGGCGTGCTGTATGGTAAATCAGAACTGCTGGAG  750
Y  A  F  S  G  H  K  L  Y  G  P  T  G  I  G  V  L  Y  G  K  S  E  L  L  E    240

GCGATGTCGCCCTGGCTGGGCGGCGGCAAAATGGTTCACGAAGTGAGTTTTGACGGCTTCACGACTCAATCTGCG  825
A  M  S  P  W  L  G  G  G  K  M  V  H  E  V  S  F  D  G  F  T  T  Q  S  A    265

CCGTGGAAACTGGAAGCTGGAACGCCAAATGTCGCTGGTGTCATAGGATTAAGCGCGGCGCTGGAATGGCTGGCA  900
P  W  K  L  E  A  G  T  P  N  V  A  G  V  I  G  L  S  A  A  L  E  W  L  A    290

GATTACGATATCAACCAGGCCGAAAGCTGGAGCCGTAGCTTAGCAACGCTGGCGGAAGATGCGCTGGCGAAACGT  975
D  Y  D  I  N  Q  A  E  S  W  S  R  S  L  A  T  L  A  E  D  A  L  A  K  R    315

CCCGGCTTTCGTTCATTCCGCTGCCAGGATTCCAGCCTGCTGGCCTTTGATTTTGCTGGCGTTCATCATAGCGAT 1050
P  G  F  R  S  F  R  C  Q  D  S  S  L  L  A  F  D  F  A  G  V  H  H  S  D    340

ATGGTGACGCTGCTGGCGGAGTACGGTATTGCCCTGCGGGCCGGGCAGCATTGCGCTCAGCCGCTACTGGCAGAA 1125
M  V  T  L  L  A  E  Y  G  I  A  L  R  A  G  Q  H  C  A  Q  P  L  L  A  E    365

TTAGGCGTAACCGGCACACTGCGCGCCTCTTTTGCGCCATATAATACAAAGAGTGATGTGGATGCGCTGGTGAAT 1200
L  G  V  T  G  T  L  R  A  S  F  A  P  Y  N  T  K  S  D  V  D  A  L  V  N    390

GCCGTTGACCGCGCGCTGGAATTATTGGTGGATTAATGACAAACCCGCAATTCGCCGGACATCCGTTCGGCACAA 1275
A  V  D  R  A  L  E  L  L  V  D                                              401
```

FIG. 11. **Nucleotide and the deduced amino acid sequences of the gene encoding CSD.** The possible Shine-Dalgarno sequence is double-underlined; the N-terminal amino acid sequence determined with a protein sequencer is underlined. The nucleotide sequence is available from the GenBank/EMBL databases with the accession number U29581 (ORF o401). The nucleotide sequence in the region from base number 13 to 1256 was also confirmed in the present study.

native form was estimated to be about 97,000 by gel filtration with a Superose 12 (1 × 30 cm) column.

Catalytic Activity of CSD—An extract of the cloned cells showed both selenocysteine lyase and cysteine desulfurase activity. Because the selenocysteine lyase activity was higher than that of cysteine desulfurase, I routinely used L-selenocysteine as a substrate of the enzyme throughout the purification (Table V).

TABLE V
Purification of CSD

Step	Total protein	Total activity[a]	Specific activity	Yield
	mg	*units*	*units/mg*	%
Crude extract[b]	1900	1100	0.58	100
Ammonium sulfate[c]	720	920	1.3	84
1st DEAE-Toyopearl[d]	420	790	1.9	72
2nd DEAE-Toyopearl[e]	90	360	4.0	33
1st Phenyl-Toyopearl[f]	29	190	6.6	17
2nd Phenyl-Toyopearl[g]	28	230	8.2	21

[a] Determined with L-selenocysteine as a substrate.

[b] Cells (13.8 g) suspended in 50 ml buffer were sonicated.

[c] The fraction between 25 and 50% saturation was collected and dialyzed.

[d] Column size, 3.0 × 18 cm; elution, with 0.15 M NaCl. The active fractions were concentrated with 55% saturation of ammonium sulfate and dialyzed.

[e] Column size, 3.0 × 18 cm; elution, with 1000-ml linear gradient of 0-0.2 M NaCl. The active fractions were concentrated with UP-20 membrane (Advantec) and dialyzed against 0.4 M ammonium sulfate.

[f] Column size, 0.7 × 6 cm; equilibration, with 0.4 M ammonium sulfate; elution, with 0.4 M ammonium sulfate. The active fractions were concentrated with UP-20 membrane and dialyzed against 0.65 M ammonium sulfate.

[g] Column size, 0.7 × 6 cm; equilibration, with 0.65 M ammonium sulfate; elution, with 100-ml linear gradient of 0.65-0.3 M ammonium sulfate. The active fractions were concentrated with a UP-20 membrane and dialyzed against the buffer containing 0.02 mM PLP.

The specific activity of the homogeneous preparation of the enzyme toward L-selenocysteine (8.2 units/mg) was comparable to that of selenocysteine lyase from *C. freundii* (6.47 units/mg) (20). However, these values were about five-times lower than that of selenocysteine lyase from pig liver (37 units/mg) (15).

The cysteine desulfurase activity of the new enzyme (3.4 units/mg) was also much higher than that of *A. vinelandii* NifS (73) and the *E. coli* NifS-like enzyme (69). However, the concentration of L-cysteine used (80 mM) was much higher than that used for the other enzymes (*A. vinelandii* NifS, 0.5 mM; the *E. coli* NifS-like protein, 2.5 mM). The specific activity of my enzyme decreased at lower L-cysteine concentrations (0.050 unit/mg at 0.5 mM; 0.23 unit/mg at 2.5 mM). These values were comparable to those reported for *A. vinelandii* NifS (0.089 unit/mg at 0.5 mM) (21) and the *E. coli* NifS-like protein (0.078 unit/mg at 2.5 mM) (69).

The optimal pH values for the removal of selenium and sulfur atoms from L-selenocysteine and L-cysteine were around pH 7.0 and 7.5, respectively, in Tricine-NaOH. The enzyme kept essentially the same activity at 4°C for at least 2 weeks, and also at -30°C for more than 6 months.

Cofactor—The enzyme showed at pH 7.4 an absorption maximum at 420 nm (Fig. 12, *curve a*), which is characteristic of bound PLP. Reduction with sodium borohydride resulted in the disappearance of the absorption band at 420 nm with a concomitant increase in the absorbance at 335 nm (Fig. 12, *curve b*). The reduced enzyme was catalytically inactive and the addition of PLP did not reverse the inactivation. These results show that the enzyme

requires PLP as a cofactor.

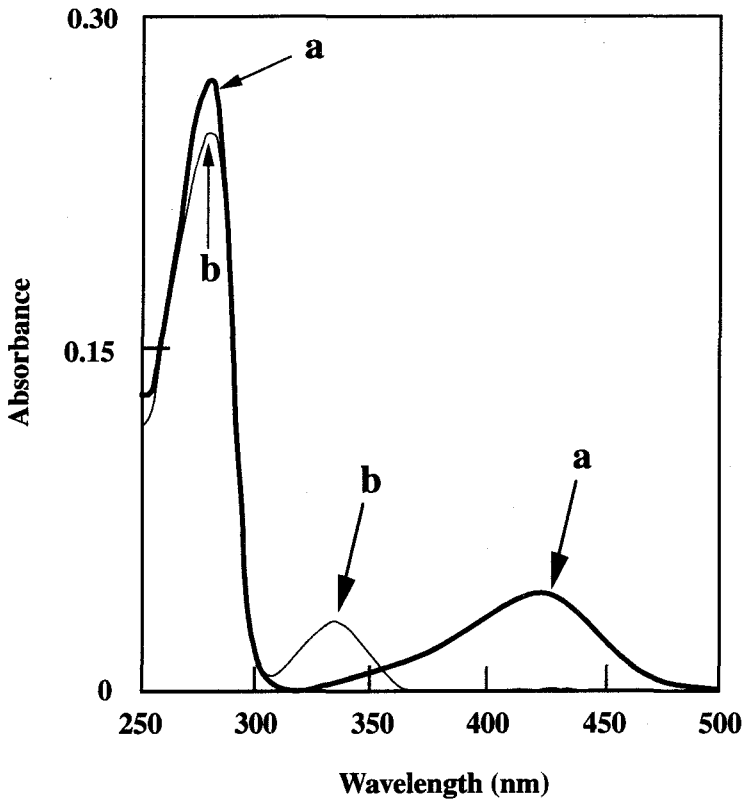

FIG. 12. **Absorption spectra of CSD.** Absorption spectra were taken in 10 mM potassium phosphate buffer (pH 7.4) at an enzyme concentration of 0.4 mg/ml. *Curve a*, native enzyme; *curve b*, 1 min after addition of sodium borohydride (1 mM) to the enzyme solution.

Substrate Specificity—The enzyme resembles selenocysteine lyase and NifS in that it removes elemental sulfur or selenium from L-cysteine or L-selenocysteine, respectively, in the reaction. L-Cysteine sulfinic acid served as the best substrate of the enzyme, and essentially the same amounts of L-alanine and sulfite were produced in the reaction (data not shown). Maximum activity for the desulfination was found at around pH 8.2 in Tricine-NaOH. I named

the new enzyme CSD, because the enzyme showed the lowest K_m value and the highest k_{cat} and k_{cat}/K_m values for L-cysteine sulfinic acid (Table VI).

The enzyme resembles aspartate β-decarboxylase (EC 4.1.1.12) and kynureninase (EC 3.7.1.3) in that alanine is produced from the substrate. However, both L-aspartate and L-kynurenine were inert as the substrates (Table VI). L-Aspartate was not converted to alanine even at pH 5.0 in an acetate buffer, which is the optimum condition for the aspartate β-decarboxylase reaction (74).

TABLE VI

Substrate specificity of CSD and kinetic constants of the enzyme reactions

The following amino acids and derivatives were inert as the substrates, when production of alanine or consumption of the substrates were examined with a Beckman high performance amino acid analyzer 7300: D-cysteine, D-cystine, DL-cysteic acid, DL-serine, *S*-methyl-L-cysteine, *S*-benzyl-L-cysteine, DL-homocysteine, DL-homocystine, DL-methionine, DL-homoserine, L-homocysteic acid, cysteamine, cystamine, selenocystamine, L-asparagine, L-aspartic acid, L-kynurenine, DL-lanthionine, L-cystathionine, L-allo-cystathionine, and DL-djenkolic acid.

	K_m	V_{max}	k_{cat}	k_{cat}/K_m
	mM	$\mu mol \cdot min^{-1} \cdot mg^{-1}$	s^{-1}	$mM^{-1} \cdot s^{-1}$
L-Cysteine sulfinic acid[a]	0.24	20	15	63
L-Selenocysteine[b]	1.0	7.4	5.3	5.3
L-Cysteine[b]	35	3.4	2.4	0.070
L-Cystine[a]	3.3	0.017	0.012	0.0036

[a] Alanine formed, in the reaction system with Tricine-NaOH (pH 8.5), was determined with alanine dehydrogenase with a mixture (1.0 ml) containing 5 mM substrate, 0.02 mM PLP, 2.5 mM NAD^+, 0.3 unit of L-alanine dehydrogenase (Unitika), 120 mM Tricine-NaOH buffer (pH 8.5), and enzyme at 37 °C.

[b] The reactions were carried out in Tricine-NaOH (pH 7.5), and H_2Se and H_2S formed were determined with lead acetate.

CSD is distinct from selenocysteine lyase and NifS in that it acts also on L-

cystine and L-selenocystine. L-Alanine as well as elemental sulfur or selenium were produced from either substrate . The amount of L-alanine produced was only 1.5 times larger than that of L-cystine consumed in the reaction. I expected that double amounts of alanine would be produced from cystine in the reaction, because *S*-sulfocysteine is presumably produced from cystine and then converted with the release of elemental sulfur to reproduce cysteine, which would give another molecule of alanine in the second reaction. Therefore, some part of the *S*-sulfocysteine is probably converted to another unknown compound which is inert as a substrate.

Action on β -Chloroalanine —β-Chloroalanine is a mechanism-based inactivator for several PLP-dependent enzymes (75). CSD was incubated with various concentrations of L-β-chloroalanine (0.5-8.0 mM) for various periods up to 4.5 h, and the remaining activity was determined with L-selenocysteine as a substrate. No inactivation of the enzyme was observed. The enzyme catalyzed only α,β-elimination of β-chloroalanine to form pyruvate without formation of alanine.

Role of Cysteinyl Residues of CSD—Both *A. vinelandii* NifS and the *E. coli* NifS-like protein contain cysteinyl residues which are catalytically essential (73, 69). Selenocysteine lyase from *C. freundii* was completely inactivated by thiol reagents (20). Cysteinyl residues corresponding to Cys325 of *A. vinelandii* NifS, which was shown to be catalytically essential (73), are fully conserved among all NifS family proteins (Fig. 13). I examined the roles of all cysteinyl residues of CSD including Cys358, which corresponds to the conserved Cys325 of *A. vinelandii* NifS, by site-directed mutagenesis. All

the alanine mutants for Cys100, Cys176, Cys323 and Cys358 were fully active toward L-selenocysteine. Thus, CSD has no essential cysteine residues, and differs markedly from *A. vinelandii* NifS and the NifS-like protein of *E. coli*.

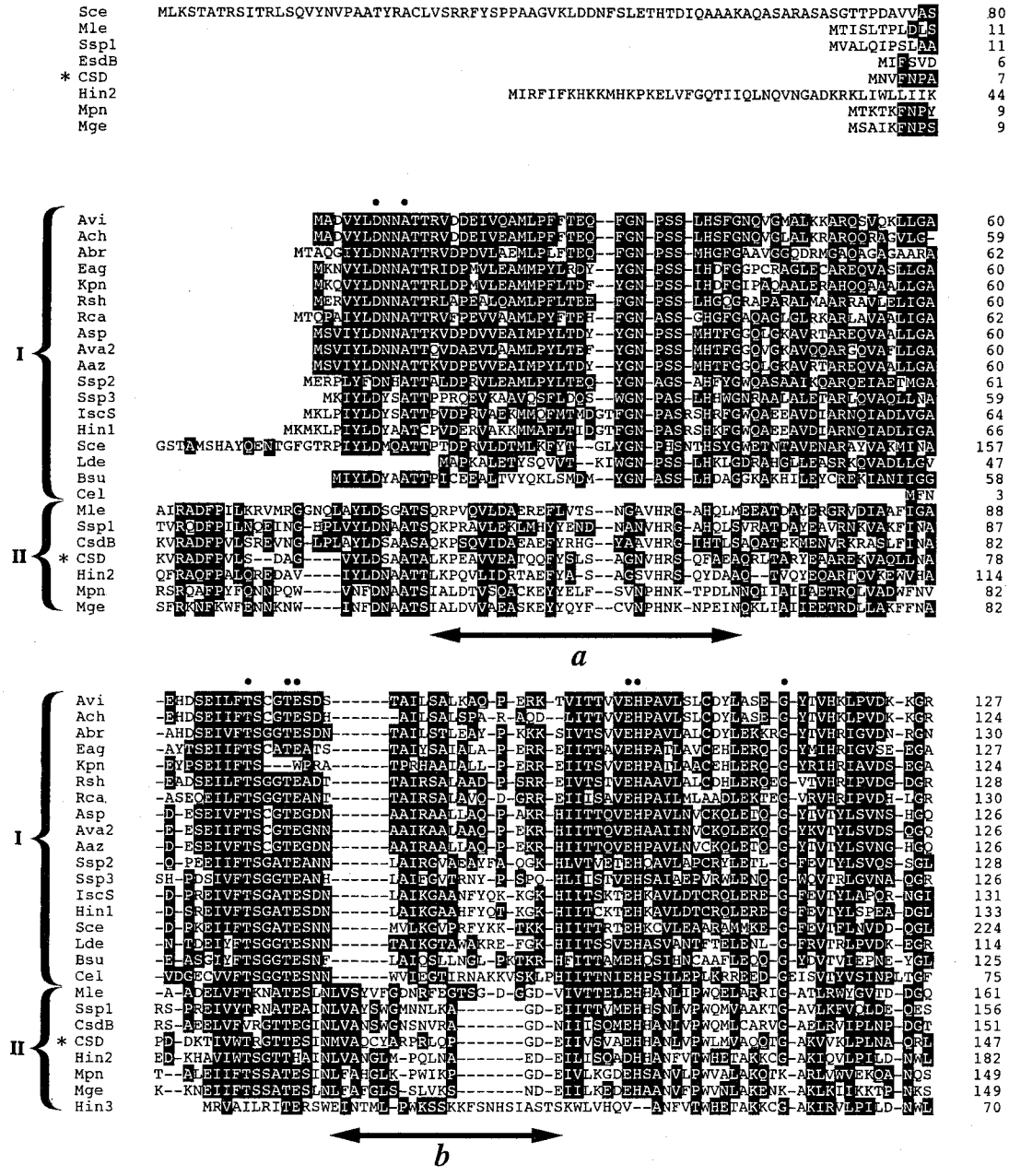

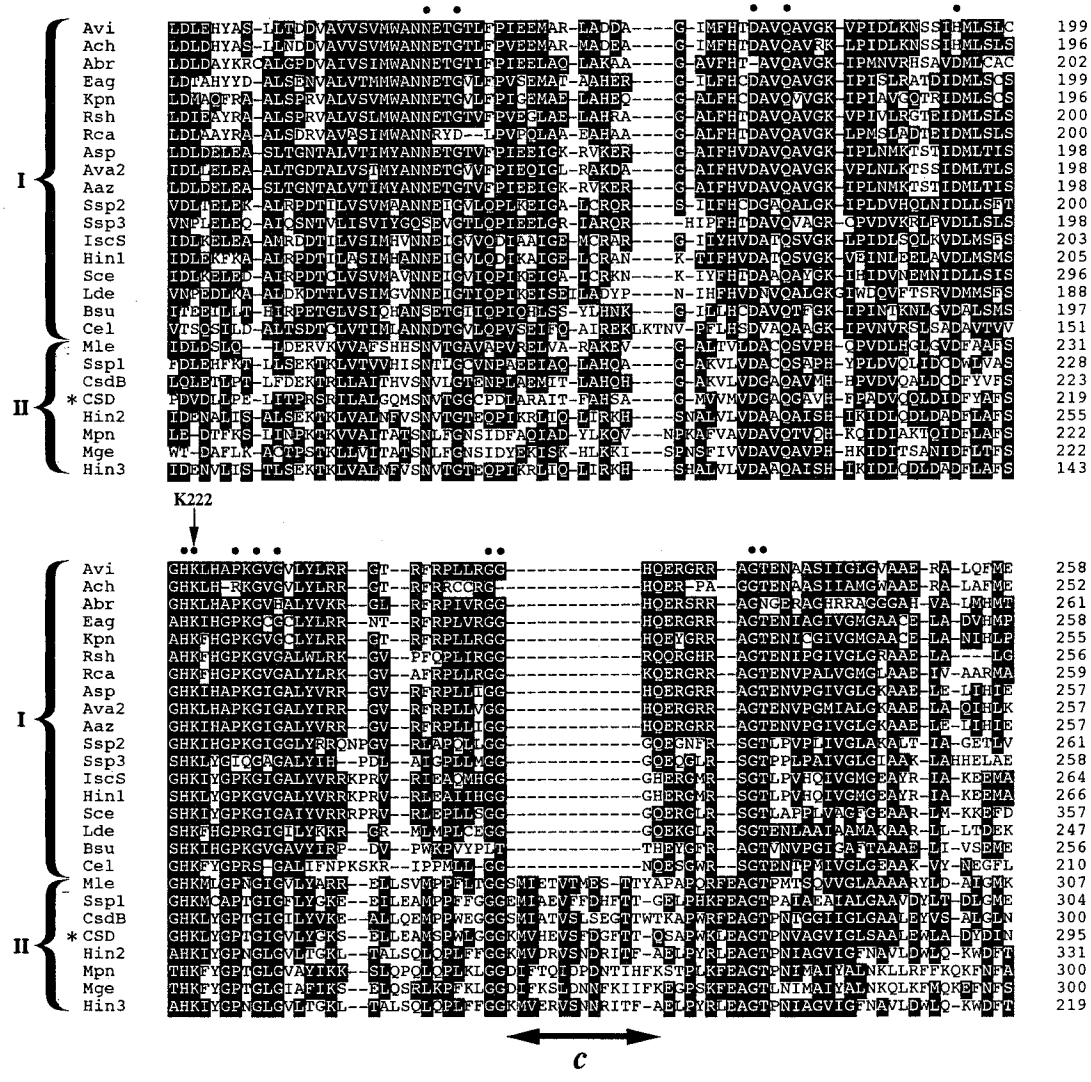
Avi
Ach
Abr
Eag
Kpn
Rsh
Rca
Asp
Ava2
Aaz
Ssp2
Ssp3
IscS
Hin1
Sce
Lde
Bsu
Cel
Mle
Ssp1
CsdB
CSD
Hin2
Mpn
Mge
Hin3
I
II
K222

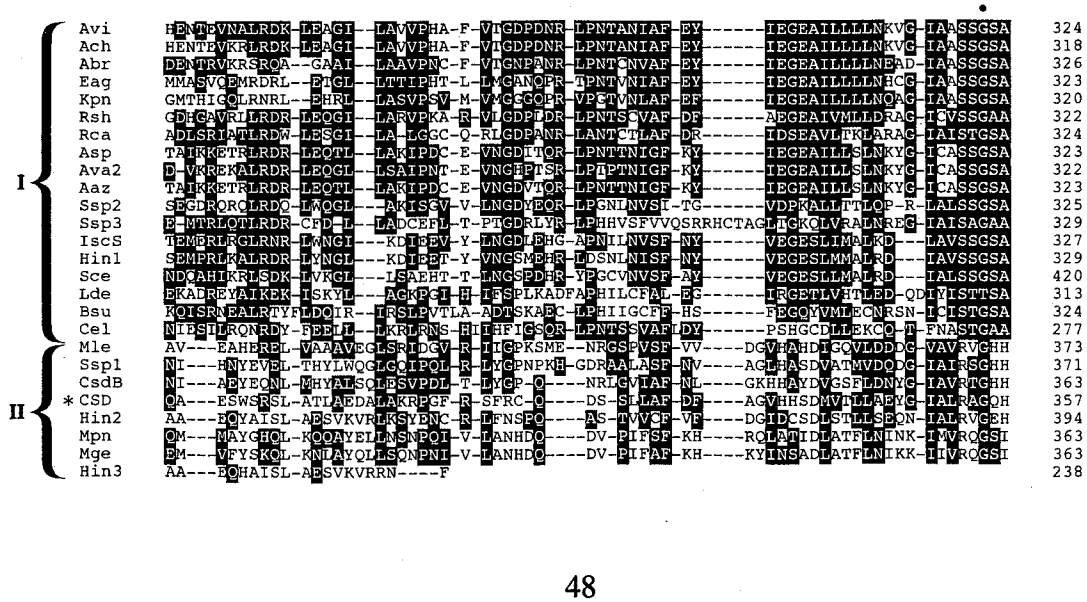
Avi
Ach
Abr
Eag
Kpn
Rsh
Rca
Asp
Ava2
Aaz
Ssp2
Ssp3
IscS
Hin1
Sce
Lde
Bsu
Cel
Mle
Ssp1
CsdB
CSD
Hin2
Mpn
Mge
Hin3
I
II
c

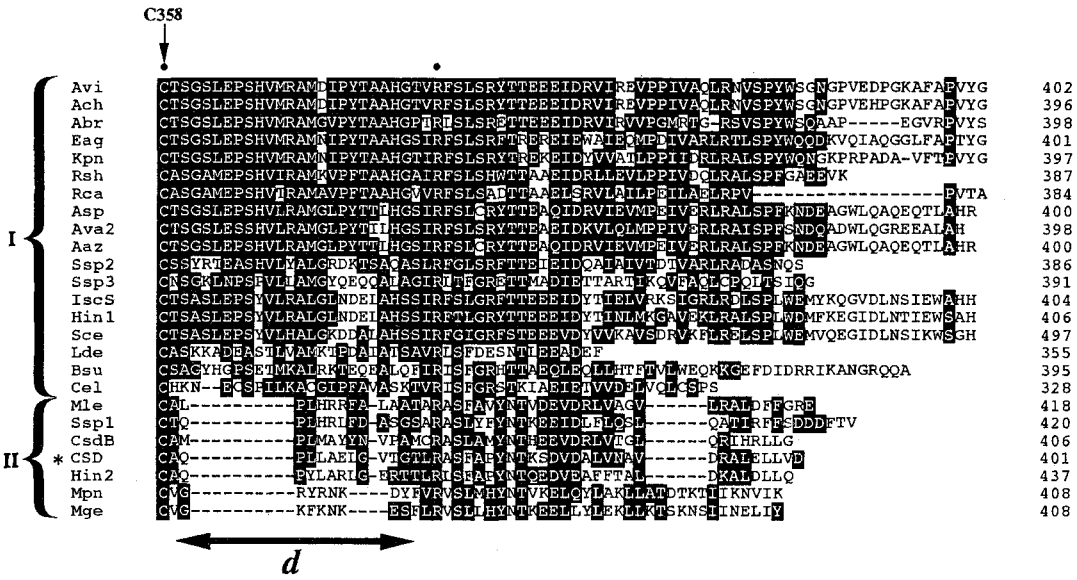

FIG. 13. **Sequence alignment of CSD, NifSs, and NifS-like proteins.** NifS-like proteins with sequence similarity to that of *A. vinelandii* NifS were searched with BLAST (105) and FASTA (106) programs, and aligned with Clastal V program of a DNASTAR software (DNASTAR, Inc.). Gaps (shown with *dashes*) are introduced in the sequences where necessary to give better alignment. The *black boxes* show the residues that are identical or similar (classified into the groups PAGST, QNED, ILVM, HKR, YFW, and C) to one another in the sequences. The residues conserved among more than 23 of total 26 sequences are indicated by *filled circles*. Conserved Cys is indicated by an *arrow*. *Numbers* refer to amino acid residues. The regions *a-d* show the parts in which the sequences of two groups differ markedly from each other. The group are shown by *braces*, and *I* and *II* indicate Group I and II, respectively. Lys, indecated by an *arrow*, is conserved among all sequences and suggested to be the PLP-binding residue (21). Abbreviations of protein names are given in Table VII. CSD is *asterisked*.

DISCUSSION

NifS of *A. vinelandii* participates in construction of the Fe-S clusters of not only nitrogenase (45), but also other iron-sulfur proteins such as SoxR (47) and FNR (46). The NifS-like enzyme of *E. coli* found by Flint (69) also provides apo dihydroxy-acid dehydratase with a [4Fe-4S] cluster to reconstitute the enzyme *in vitro*. The N-terminal amino acid sequence of the enzyme was identical with that deduced from another *nifS*-like gene of *E. coli*

(*iscS* in Table VII). This gene, together with a *nifU*-like gene, forms a unique gene cluster, which is similar to that found for *nifS* of *Anabaena* sp. (76-78). Three *nifS*-like genes have been demonstrated also in the genome of *Haemophilus influenzae*, and a similar gene cluster occurs around the Hin1 gene (Table VII) of the genome. Therefore, *iscS* and Hin1 probably participate in construction of the Fe-S clusters of iron-sulfur proteins, in the same manner as NifS of *A. vinelandii*. *Synechocystis* sp. PCC6803 also contains three *nifS*-like genes. However, I found no such gene organization around them. Similarly, neither of *csdA* and the third *nifS*-like gene (*csdB* in Table VII) of *E. coli* form such gene clusters. The same is true for the other *nifS*-like genes of *H. influenzae* (Hin2 and Hin3). Therefore, these NifS-like proteins probably have biochemical functions different from those of *iscS*, Hin1 and *A. vinelandii* NifS.

NifS has been classified into the same group as aminotransferases of class V (79) and subgroup IV (80), which include serine-pyruvate aminotransferase (EC 2.6.1.51) and phosphoserine aminotransferase (EC 2.6.1.52), on the basis of sequence homology analysis. Isopenicillin N epimerase belongs to the same group as various PLP-dependent enzymes, other than aminotransferases (79, 80). It has therefore been suggested that NifS and isopenicillin N epimerase evolved from the common ancestral protein for the aminotransferases of these classes.

Chocat *et al.* have found that NifS family proteins are classified into two groups, I and II, according to their sequence similarities. The two groups are clearly distinct from each other in the regions named *a*, *b*, *c* and *d* (Fig. 13).

TABLE VII
NifSs and NifS-like proteins

Source	Abbreviation	Accession	Length	Reference
Azotobacter vinelandii	Avi	P05341[a]	402	(90)
Azotobacter chroococcum	Ach	P23120[a]	396	(91)
Azospirillum brasilense	Abr	U26427[b]	398	(92)
Enterobacter agglomerans	Eag	X99694[b]	401	(93)
Klebsiella pneumoniae	Kpn	P05344[a]	397	(90)
Rhodobacter sphaeroides	Rsh	Q01179[a]	387	(94)
Rhodobacter capsulatus	Rca	Q07177[a]	384	(95)
Anabaena sp. PCC7120	Asp	P12623[a]	400	(77)
Anabaena variabilis	Ava2	U49859[b]	398	(96)
Anabaena azollae	Aaz	L34879[b]	400	(78)
Synechocystis sp. PCC6803	Ssp1	D64004[b,d]	420	(97)
Synechocystis sp. PCC6803	Ssp2	D63999[b,e]	386	(97)
Synechocystis sp. PCC6803	Ssp3	D90899[b,f]	391	(98)
Haemophilus influenzae Rd	Hin1	HI0378[c]	406	(99)
Haemophilus influenzae Rd	Hin2	HI1295[c]	437	(99)
Haemophilus influenzae Rd	Hin3	HI1343[c]	238	(99)
Escherichia coli K-12	IscS	D90883[b, g]	404	(67)
Escherichia coli K-12	CsdB	D90811[b, h]	406	(68)
Escherichia coli K-12	CSD	U295810[b, i]	401	(67)
Saccharomyces cerevisiae	Sce	P25374[a]	497	(49)
Lactobacillus delbrueckii	Lde	P31672[a]	355	(100)
Bacillus subtilis	Bsu	P38033[a]	395	(48)
Caenorhabditis elegans	Cel	U23139[b, j]	328	(101)
Mycobacterium leprae	Mle	U00013[b]	418	(102)
Mycoplasma pneumoniae	Mpn	AE000034[b]	408	(103)
Mycoplasma genitalium	Mge	U39716[b]	408	(104)

[a] SWISS-PROT.
[b] GenBank/EMBL.
[c] TIGR Microbial data base.
[d] slr0077.
[e] slr0387.
[f] sll0704.
[g] yzz0.
[h] 0320#17.
[i] o401.
[j] F13H8.9.

Average sequence similarities of CSD to Group I and II members were 23 and 37%, respectively. The similarity relationship among NifS family proteins is shown in a phylogenetic tree (Fig. 14), which also indicates that the proteins are classified into two major groups. The proteins Cel, Lde, Bsu and Ssp3 are far from the others, but are close to the members of Group I than to the Group II proteins.

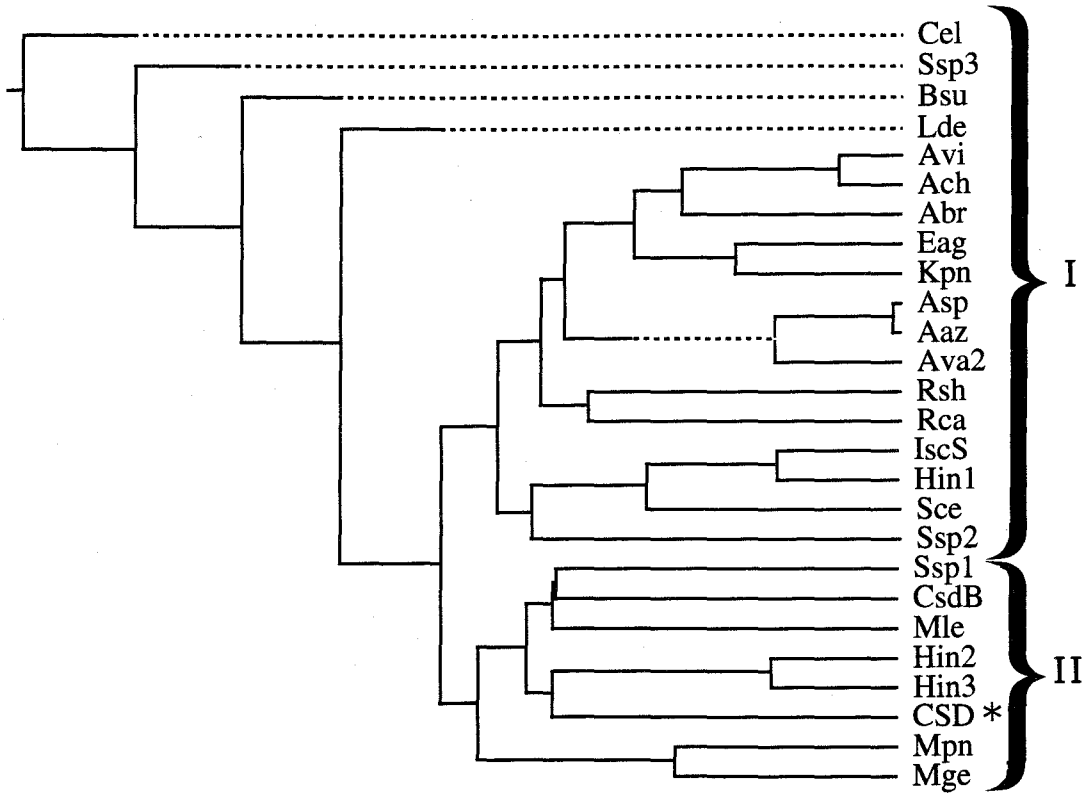

Fig. 14. **Phylogenetic relations of NifS family proteins.** The protein sequences were aligned as shown in Fig. 3, and their similarity relationships were calculated with the MegAlign program of the DNASTAR package. Abbreviations of protein names are shown in Table VII. CSD is *asterisked*. The proteins are classified into two groups as shown by *braces*, and *I* and *II* indicate Group I and II, respectively.

I have shown that selenocysteine lyase from *C. freundii* is quite different from the pig liver enzyme in various physicochemical properties (20). The amino acid compositions of pig liver selenocysteine lyase (Pig), CSD, *A. vinelandii* NifS (Avi), and *E. coli* NifS-like protein (IscS) resemble each other, but are distinct from that of selenocysteine lyase from *C. freundii* (CFR) (Fig. 15). Therefore, the latter enzyme probably belongs to a different family of proteins.

The NifS-like protein from *E. coli* and NifS from *A. vinelandii* have common characteristics: both contain essential cysteinyl residues at the active sites. The thiol group presumably attacks as a nucleophile the sulfur atom of the substrate, cysteine, to form the intermediate, enzyme-bound cysteinyl persulfide (45, 69). By contrast, no cysteinyl residue of CSD is essential for catalysis. The CSD-reaction is assumed to proceed through direct release of elemental selenium or sulfur atom from the substrate, selenocysteine or cysteine. It has been assumed that formation of the enzyme-bound cysteinyl persulfide is crucial to deliver sulfur atoms efficiently to iron-sulfur proteins. If this is the case, CSD will not be related metabolically to the formation of Fe-S clusters, although sulfur atoms produced from cysteine by the enzyme are probably incorporated into iron-sulfur proteins with low efficiency in the same manner as observed for *O*-acetylserine sulfhydrylase A (EC 4.2.99.8), *O*-acetylserine sulfhydrylase B (EC 4.2.99.8), and β-cystathionase (EC 4.4.1.8) (81). The fact that the K_m value of CSD for cysteine is high also suggests that cysteine is not the physiological substrate of the enzyme.

The irreversible inactivation of PLP enzymes by β-chloroalanine has been

shown to proceed through modification of the enzyme-bound PLP with nascent α-aminoacrylate formed from β-chloroalanine (82-84). CSD catalyzes the same type of reaction as selenocysteine lyase, aspartate β-decarboxylase, and kynureninase. All these enzymes except CSD are inactivated by β-chloroalanine (15, 85, 86). Nascent α-aminoacrylate is probably released from the active site of CSD much more quickly than from those of the other enzymes. Alternatively, α-aminoacrylate may be hydrolyzed quickly to pyruvate and ammonia, and the enzyme can escape from modification with α-aminoacrylate.

In mammals, cysteine is oxidized by cysteine dioxygenase (EC 1.13.11.20) to form cysteine sulfinic acid, which is decarboxylated to form hypotaurine by cysteine sulfinate decarboxylase (EC 4.1.1.29). cDNAs for cysteine dioxygenase (87) and cysteine sulfinate decarboxylase (88) were cloned and sequenced. I found no sequences similar to those of the cDNAs in the whole-genomic sequence of *E. coli* K-12. If *E. coli* has a cysteine dioxygenase, it will have little sequence similarity to the mammalian enzyme. Alternatively, if no cysteine dioxygenase occurs in *E. coli*, the cysteine desulfination may be a side function of the enzyme with no metabolic relevance. Aspartate β-decarboxylase and aspartate aminotransferase also use cysteine sulfinate as a good substrate and desulfinate it (74, 85, 89). Whatever the physiological function of CSD is, this is the first enzyme in Group II whose catalytic function has been clarified (Fig. 14). Other proteins of this group probably have a similar catalytic function to CSD. Cloning and expression of the *csdB* gene, the last *nifS*-like gene of *E. coli* mapped at

37.9 min (68) in the chromosome, and characterization of the gene product, are described in the next chapter (Chapter III).

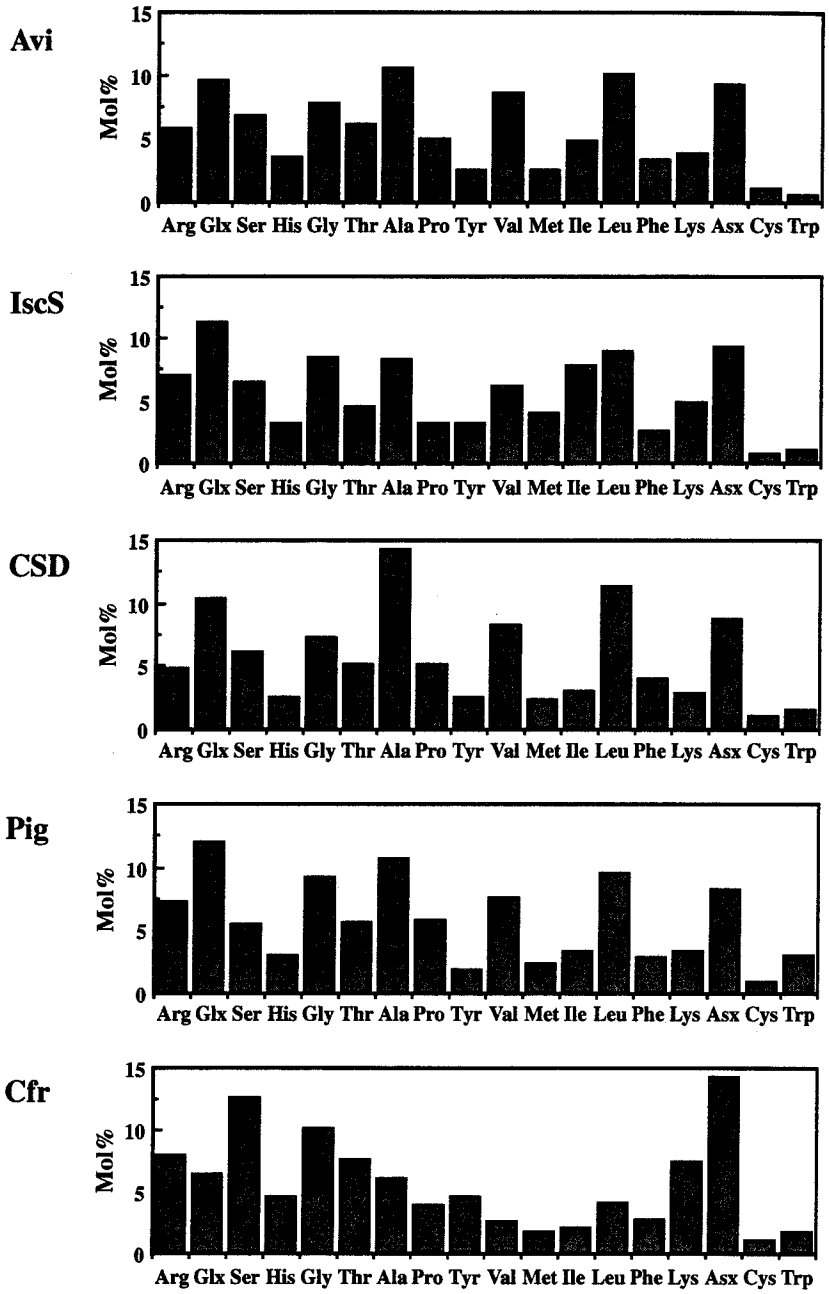

FIG. 15. **Comparison of the amino acid compositions of selenocysteine lyase and NifS family proteins.** The amino acid compositions of selenocysteine lyase were obtained from the previous report (20). Those of NifS family proteins were calculated from the amino acid sequences deduced from the nucleotide sequences of the genes. Histograms show the amino acid compositions: *Avi, A. vinelandii* NifS; *IscS, E. coli* NifS-like protein; *CSD*, CSD; *PIG*, pig liver selenocysteine lyase; *CFR, C. freundii* selenocysteine lyase.

SUMMARY

Selenocysteine lyase (EC 4.4.1.16) exclusively decomposes selenocysteine to alanine and elemental selenium, whereas cysteine desulfurase (NifS protein) of *Azotobacter vinelandii* acts indiscriminately on both cysteine and selenocysteine to produce elemental sulfur and selenium, respectively, and alanine. These proteins exhibit some sequence homology. The *Escherichia coli* genome contains three genes with sequence homology to *nifS*. I have cloned and expressed the gene mapped at 63.4 min (*csdA*) in the chromosome, and have purified to homogeneity and characterized the gene product (CSD). The enzyme comprises two identical subunits with 401 amino acid residues (M_r 43,238) and contains pyridoxal 5'-phosphate as a coenzyme. The enzyme catalyzes the removal of elemental sulfur and selenium atoms from L-cysteine, L-cystine, L-selenocysteine and L-selenocystine to produce L-alanine. L-Cysteine sulfinic acid was desulfinated to form L-alanine as the preferred substrate. Mutant enzymes having alanine substituted for each of the four cysteinyl residues (Cys100, Cys176, Cys323 and Cys358) were all active for L-selenocysteine. Cys358 corresponding to Cys325 of *A. vinelandii* NifS, which is conserved among all NifS-like proteins and catalytically essential (Zheng, L., White, R. H., Cash, V. L., and Dean, D. R. (1994) *Biochemistry* **33,** 4714-4720), is not required for CSD. Thus, the enzyme is distinct from *A. vinelandii* NifS in this respect.

CHAPTER III

A *nifS*-like Gene, *csdB*, Encodes an *Escherichia coli* Counterpart of Mammalian Selenocysteine Lyase: Gene Cloning, Purification, Characterization and Preliminary X-Ray Crystallographic Studies

INTRODUCTION

The *E. coli* genome contains three genes with sequence homology to both of *nifS* and m-*Scl* (Fig. 16). Two enzymes, IscS (69) and CSD (107) (Chapter II), among the three NifS homologs have been isolated and characterized. *E. coli* IscS, which shows significant sequence identity (40%) to *A. vinelandii* NifS, can deliver the sulfur from L-cysteine for the *in vitro* synthesis of the Fe-S cluster of dihydroxy-acid dehydratase from *E. coli* (69). CSD exhibits both selenocysteine lyase and cysteine desulfurase activities in addition to cysteine sulfinate desulfinase activity, and the enzyme is distinct from *A. vinelandii* NifS in its amino acid sequence, absorption spectrum and lack of cysteine residues catalytically essential for the decomposition of L-selenocysteine (107, Chapter II). Neither enzyme shows strict specificity for L-selenocysteine, and both act on L-cysteine. Thus, I have explored the possibility that the last *nifS* homolog (*csdB*) mapped at 37.9 min (108) in the chromosome encodes selenocysteine lyase (SCL), which may play a crucial role in selenophosphate synthesis. I have isolated the gene product (CsdB), studied its enzymatic properties, and carried out preliminary X-ray

crystallographic studies.

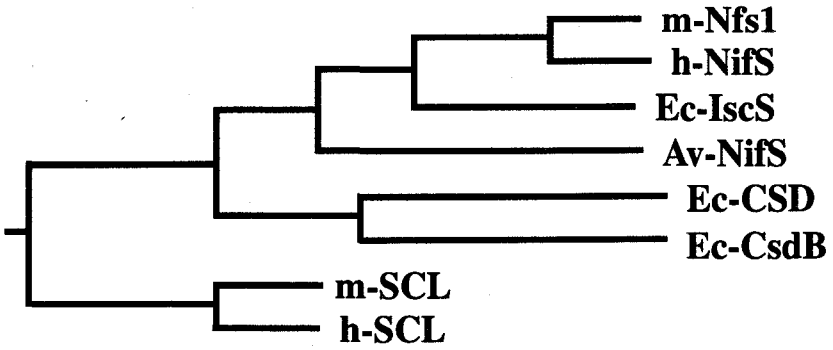

FIG. 16. **Phylogenetic relations of SCL, NifS, and three *E. coli* homologs.** *m-SCL*, mouse selenocysteine lyase; *h-SCL*, human selenocysteine lyase homolog; *m-Nfs1*, mouse NifS-like protein; *h-NifS*, human NifS; *Av-NifS*, *A. vinelandii* NifS; *Ec-IscS*, *E. coli iscS* gene product; *Ec-CSD*, *E. coli* CSD; *Ec-CsdB*, *E. coli csdB* gene product.

EXPERIMENTAL PROCEDURES

Materials—Restriction enzymes and other DNA modifying enzymes were purchased from New England Biolabs (Beverly, MA) and Takara Shuzo (Kyoto, Japan); molecular weight markers for SDS-PAGE and gel filtration from Amersham Pharmacia Biotech (Uppsala, Sweden) and Oriental Yeast (Tokyo, Japan); oligonucleotides from Biologica (Nagoya, Japan); Gigapite from Seikagaku Corporation (Tokyo, Japan); DEAE-Toyopearl, Phenyl-Toyopearl and Butyl-Toyopearl from Tosoh (Tokyo, Japan). L-Selenocystine was synthesized as described previously (109). L-Selenocysteine was prepared from L-selenocystine according to the previous method (15). The Kohara/Isono miniset clone No. 430 (110) was a kind gift from Dr. Yuji

Kohara, National Institute of Genetics, Japan. All other chemicals were of analytical grade.

Cloning of the csdB gene—The DNA fragment containing *csdB* was cloned from the chromosomal DNA of *E. coli* K-12 ICR130 by PCR in a manner identical to that used for cloning of *csdA* (107, Chapter II). Oligonucleotide primers used were 5'-GGAATTC**AGGA**GGTGCCATATGA TTTTTTCCGTCGAC-3' (upstream) and 5'-CCCAAGCTTATCCCAGCAAA CGGTG-3' (downstream); underlining indicates *Eco*RI and *Hin*dIII sites, respectively, and bold face indicates a putative ribosome binding sequence. The PCR product was ligated into pUC118 and then the resultant expression plasmid, pCSDB, was introduced into *E. coli* JM109 competent cells.

Enzyme Assays—The enzyme was assayed in 0.12 M Tricine-NaOH buffer at pH 7.5. The enzymatic activities toward L-selenocysteine and L-cysteine were measured with lead acetate as described previously (107, Chapter II). The previously reported value (15) for a molar turbidity coefficient of PbSe at 400 nm was corrected as 1.18×10^4 $M^{-1} \cdot cm^{-1}$, and this value was used in this study. Sulfite produced from L-cysteine sulfinic acid was determined with fuchsin (55). Production of alanine from substrates was determined with a Beckman high performance amino acid analyzer 7300 (Beckman Coulter, Fullerton, CA). Specific activity was expressed as units/mg of protein, with one unit of enzyme defined as the amount that catalyzed the formation of 1 μmol of the product in one minute.

Purification of the csdB gene product (CsdB)—Purification was carried out at 0-4 °C, and potassium phosphate buffer (KPB) (pH 7.4) was used as

the buffer throughout the purification. *E. coli* JM109 cells harboring pCSDB were grown in 9 liters of LB medium containing 200 μg/ml ampicillin and 1 mM isopropyl-1-thio-β-D-galactopyranoside at 37°C for 16 h. The cells were harvested by centrifugation, suspended in 10 mM KPB and disrupted by sonication. The cell debris was removed by centrifugation, and the supernatant solution was fractionated by ammonium sulfate precipitation (25-50% saturation). The enzyme was dissolved in 10 mM KPB and dialyzed against the same buffer. The enzyme was applied to a DEAE-Toyopearl column (3 × 15 cm) equilibrated with the same buffer. After the column was washed with the same buffer, the enzyme was eluted with a 0.8-liter linear gradient of 0-0.25 M NaCl in the buffer. The active fractions were pooled (110 ml) and concentrated by ultrafiltration through an Advantec UP-20 membrane (Advantec, Naha, Japan). The enzyme was dialyzed against 10 mM buffer containing 0.65 M ammonium sulfate and applied to a Phenyl-Toyopearl column (3 × 15 cm) equilibrated with the same buffer. The enzyme was eluted with a 0.7-liter linear gradient of 0.65-0.3 M ammonium sulfate in the buffer, and the active fractions were pooled and concentrated as above. The enzyme was dialyzed against 10 mM buffer and applied to a Gigapite column (3 × 10 cm) equilibrated with the same buffer. The enzyme was eluted with a one-liter linear gradient of 10-150 mM KPB, and the active fractions were collected and concentrated. The final preparation was further concentrated with Centriprep-10 (Millipore, Bedford, MA) to a volume of 2.7 ml.

Purification of CSD and IscS—Purification of CSD from *E. coli* JM109 transformed with a plasmid pCSD1 containing the *csdA* gene was performed as described in Chapter II (107). Expression and purification of recombinant

IscS will be described in Chapter IV. Briefly, the *iscS* gene was amplified by PCR with the Kohara miniset clone No. 430 (110) as a template and inserted into the *Nde*I and *Hin*dIII sites in pET21a (Novagen, Madison, WI) to yield pEF1. IscS was isolated from BL21(DE3) pLysS cells harboring pEF1 by sonication, ammonium sulfate fractionation and chromatography with Phenyl-Toyopearl, DEAE-Toyopearl, Butyl-Toyopearl, Gigapite and Superose 12 (Amersham Pharmacia Biotech, Uppsala, Sweden) columns.

Analytical Methods—Protein was quantified by the Bradford method (56) using Protein Assay CBB Solution (Nacalai Tesque, Kyoto, Japan) with BSA as a standard. The concentration of the purified enzyme was determined with the value $\varepsilon_M = 4.8 \times 10^4\ M^{-1} \cdot cm^{-1}$ at 280 nm, which was calculated from the content of tyrosine, tryptophan and cysteine (111). The subunit and the native M_r of CsdB were determined by SDS-PAGE (58) and gel filtration with Superdex 200 (Amersham Pharmacia Biotech, Uppsala, Sweden), respectively. The PLP content of the enzyme was determined fluorometrically with KCN according to the method of Adams (112).

Crystallography—Crystals of CsdB were grown by the hanging drop vapor diffusion method. Each droplet was prepared by mixing 5 μl of 20 mg/ml enzyme in 10 mM KPB (pH 7.4) with an equal volume of each reservoir solution of the Crystal Screen™ (Hampton Research, CA) initially, and of a modified reservoir solution subsequently. The yellow crystals of CsdB were mounted in glass capillaries with the crystallographic c^*-axis along the rotation axis of the spindle and subjected to X-ray experiments. Native data for structure determination were collected at 20 °C with a Rigaku

R-AXIS IIC imaging plate detector using double focusing mirror-monochromated CuK_α radiation which was generated with a 0.3 mm focal cup of an X-ray generator RU300 (Rigaku, Tokyo, Japan) operated at 40 kV and 100 mA. The crystal-to-detector distance was set to 130.0 mm. Data reduction was carried out using the R-AXIS IIC software package.

RESULTS

Cloning and Expression of the csdB Gene and Purification of the Product—For the production of a large amount of CsdB, expression plasmids were constructed as described in 'Experimental Procedures' with chromosomal DNA isolated from *E. coli* K-12. The nucleotide sequence of *csdB* in the expression vector (pCSDB) was confirmed to be identical with that registered in GenBank™, accession number D90811 (open reading frame o320#17). The clone provided overexpression of the cloned gene: about 10% of the total protein in the extract of *E. coli* JM109 recombinant cells. In the representative purification (Table V), about 8 mg of homogeneous preparation of CsdB was obtained per liter of culture.

Physical Characterization—CsdB provided a single band corresponding to the M_r of 43,000 on SDS-PAGE (Fig. 17). The N-terminal sequence of the purified enzyme, MIFSVDKVRA, agreed with that deduced from the nucleotide sequence of *csdB*. The M_r of the native enzyme was determined to be 88,000 by gel filtration. Consequently, the enzyme is a dimer composed of two identical subunits. The spectrophotometric properties of the enzyme were very similar to those of CSD with an absorption maximum at 420 nm

(Fig. 18) at pH 7.4. No significant changes in the absorption spectrum were observed in the range of pH 6-8. This absorption peak is characteristic of PLP enzymes, which contain the cofactor bound to the ε-amino group of a lysine residue at the active site. However, CsdB is distinct from either of two *A. vinelandii* proteins, NifS and IscS, and also from IscS of *E. coli*, all of which have an absorption maximum around 390 nm (21, 69, 113). Reduction with sodium borohydride resulted in a decrease in the absorption peak at 420 nm with a concomitant increase in the absorbance at 335 nm (Fig. 18). This result is consistent with that this is a PLP enzyme. The PLP content of CsdB was determined to be 1.0 mol per mol of subunit by the fluorometric method (112).

TABLE VIII
Purification of CsdB

Step	Total protein	Total activity[a]	Specific activity	Purification	Yield
	mg	*units*	*units/mg*	*fold*	*%*
Crude extract	3100	1600	0.52	1	100
Ammonium sulfate	1000	920	0.92	1.8	58
DEAE-Toyopearl	370	890	2.4	4.6	56
Phenyl-Toyopearl	85	430	5.1	9.8	27
Gigapite	70	390	5.6	11	24

[a] Determined with L-selenocysteine as a substrate.

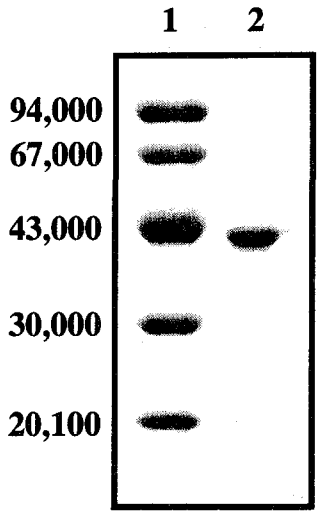

FIG. 17. **SDS-PAGE analysis of the purified CsdB.** *Lanes: 1*, M_r standards that include phosphorylase *b*, bovine serum albumin, ovalbumin, carbonic anhydrase, and soybean trypsin inhibitor; *2*, purified CsdB (4 μg). Coomassie Brilliant Blue R-250 was used for staining. *Numbers* represent M_r of marker proteins.

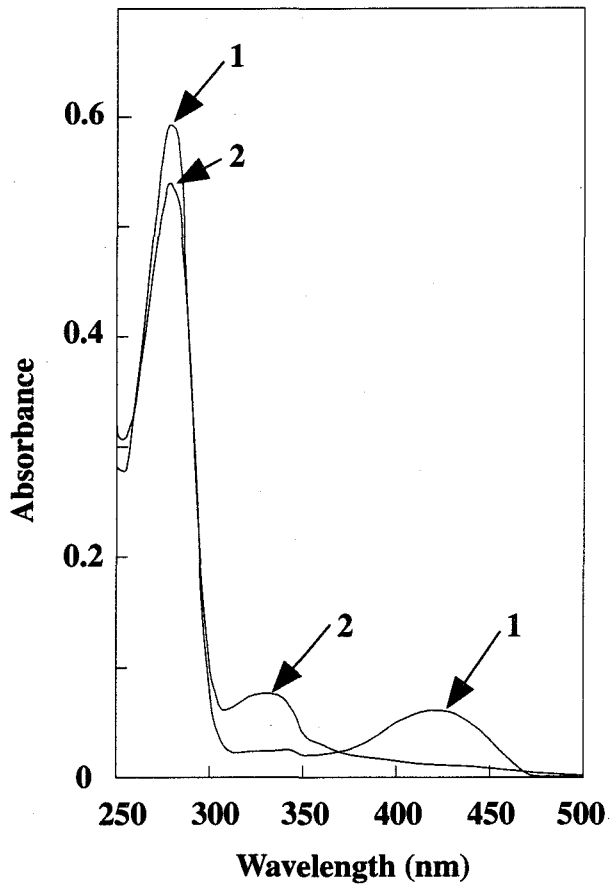

FIG. 18. **Absorption spectra of CsdB.** Conditions: 10 mM KPB, pH 7.4, 25 °C, 0.64 mg/ml of the enzyme. *Curve 1*, native enzyme; *curve 2*, 1 min after addition of sodium borohydride (1 mM) to the enzyme solution.

TABLE IX

Substrate specificity of CsdB

The following amino acids were inert as the substrates when production of alanine was examined in the reaction mixture containing 10 mM substrate at 37 °C for 12 h: D-selenocysteine, D-cysteine, D-selenocystine, D-cystine, D-kynurenine, D-djenkolic acid, DL-selenocysteamine, *S*-benzyl-L-cysteine.

Substrate	Specific activity[a]	Relative activity
	units/mg	%
L-Selenocysteine	5.5	100
L-Cysteine sulfinic acid	0.82	15
L-Cysteine	0.019	0.35
L-Selenocystine	0.0044	0.080
L-Cystine	0.0031	0.056
L-Aspartic acid	0.0044	0.080

[a] Activity was measured in the reaction buffer containing one of the following substrates: L-selenocysteine, 12 mM; L-cysteine sulfinic acid, 12 mM; L-cysteine; 12 mM; L-selenocystine, 20 mM; L-cystine, 20 mM; L-aspartic acid, 20 mM.

Catalytic Activity and Substrate Specificity—CsdB catalyzed the removal of a substituent at the β-carbon of L-selenocysteine, L-cysteine and L-cysteine sulfinic acid to yield L-alanine. The production of elemental selenium and elemental sulfur from L-selenocysteine and L-cysteine, respectively, in the reaction was confirmed in the same manner as reported previously (42). The optimal pH value for the removal of selenium from L-selenocysteine was between 6.5 and 7.5 in Tricine-NaOH or 2-(*N*-morpholino)ethanesulfonic acid buffer. The substrate specificity of the enzyme is summarized in Table IX; L-selenocysteine was the best substrate followed by L-cysteine sulfinic acid and L-cysteine, in that order. The specific activity of CsdB on L-selenocysteine (5.5 units/mg) was comparable to that of CSD and IscS (Table X), but was about 5 and 7 times lower than that of m-SCL (29 units/mg)

(Chapter I) and p-SCL (37 units/mg) (15), respectively. The cysteine desulfurase activity of CsdB was about 2% and 5% of that of CSD and IscS, respectively, at a substrate concentration of 12 mM (Table X). The specific activity of CsdB for L-cysteine was about 1/290 of the activity with L-selenocysteine (Table X). This value is much lower than those of CSD and IscS (Table X). In contrast with CsdB, *A. vinelandii* NifS favors L-cysteine as a substrate over its selenium analog (52). CsdB acted on L-cystine, L-selenocystine and L-aspartic acid, although at extremely low rates (<0.08% of the rate for L-selenocysteine) (Table IX).

TABLE X

Discrimination of L -selenocysteine from L -cysteine in the reaction catalyzed by CsdB, CSD and IscS

Enzyme[a]	Map position	Specific activity		Discrimination factor[b]
		L-Selenocysteine	L-Cysteine	
	min	*units/mg*	*units/mg*	*ratio (L-selenocysteine/ L-cysteine)*
CsdB	37.9	5.5	0.019	290
CSD	63.4	6.2	0.90	6.9
IscS	57.3	3.1	0.38	8.2

[a] The amino acid sequence of the proteins can be accessed through NCBI Protein Database under NCBI Accession numbers 1742766 (CsdB), 1789175 (CSD), and 1788879 (IscS).

[b] Discrimination factor was calculated from the specific activity of the enzymes for L-selenocysteine divided by that for L-cysteine. Activity was measured in the reaction mixture containing 120 mM Tricine-NaOH (pH 7.5), 50 mM dithiothreitol, 0.2 mM PLP and 12 mM substrate.

Crystallization and Preliminary X-ray Characterization—CsdB was crystallized at 25 °C within two days by hanging drop vapor diffusion against a

100 mM cacodylate solution (pH 6.8) containing 1.4 M sodium acetate, which corresponds to the solution No.7 in the Crystal Screen™. The crystals were also obtained in 100 mM KPB (pH 6.8) containing 1.4 M sodium acetate and 10 μM PLP, and these conditions were further used for the crystallization of the enzyme. The yellow crystals ($0.5 \times 0.5 \times 0.4$ mm^3) had tetragonal-bipyramidal shapes (Fig. 19). They were grown in amorphous debris, which was removed from the crystals before they were sealed in thin-walled glass capillaries.

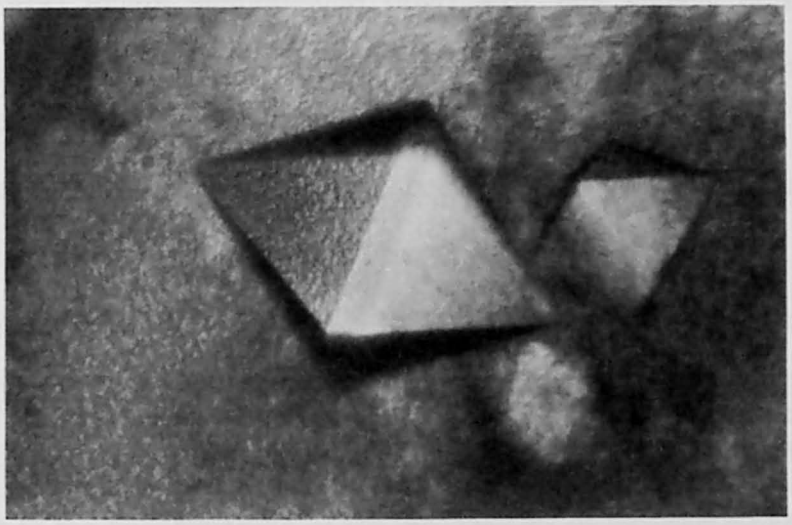

FIG. 19. **Photograph of crystals of CsdB grown by the hanging drop vapor diffusion method.**

The space group of the CsdB was $P4_32_12$ with the cell dimensions of a = b = 128.1 Å, and c = 137.0 Å. The assumption that a single dimer (89 kDa)

exists in the asymmetric unit of the crystal gives a V_m value of 3.19 Å^3/Da, which is equivalent to a solvent content of 62%. These values lie within the range of values commonly found for proteins (114). A set of native data was collected to 2.8 Å resolution on a Rigaku R-AXIS IIC using 1.5° oscillation over a range of 45° (94.2% complete with 23,770 independent reflections). The R_{merge} value for the intensity data was 7.22%. The data collection statistics obtained for the native CsdB crystals are given in Table XI. The X-ray crystal structure determination of the enzyme was carried out by the multiple isomorphous replacement method, and is described in Chapter V.

I also obtained crystals of CSD at 25 °C by hanging drop vapor diffusion against a 100 mM sodium acetate solution (pH 4.6) containing 200 mM ammonium acetate and 30% (w/v) polyethylene glycol (PEG) 4000. However, these crystals were small and not suitable for X-ray analysis. Further optimization of crystallization conditions by changing pH, PEG concentration and salt has resulted in little improvement.

TABLE XI
Data collection statistics

Unit cell dimensions (Å)	$a = b = 128.1$, $c = 137.0$
Space group	$P4_32_12$
Resolution limit (Å)	2.8
Number of reflections	73,138
Number of unique reflections	23,770
Percent completeness	94.2
R_{merge}[a] (%)	7.22

[a] $R_{merge} = \Sigma | I_i - \langle I \rangle | / \Sigma I_i$

DISCUSSION

Comparison with other PLP-dependent enzymes—Grishin *et al.* classified PLP enzymes into 7 distinct fold types on the basis of primary structure, secondary structure prediction and biochemical function (79). NifS proteins have been classified as 'aminotransferases class V' in the fold type I together with serine-pyruvate aminotransferase (EC 2.6.1.51), phosphoserine aminotransferase (PSAT) (EC 2.6.1.52), isopenicillin N epimerase, and the small subunit of the soluble hydrogenase. Recently, 3D structures of PSATs from *Bacillus circulans sbsp. alkalophilus* and *E. coli* (115) were solved and deposited in the PDB (http://www.pdb.bnl.gov/) with the ID code 1BT4 and 1BJN, respectively. Comparison of the structures of PSATs with that of CsdB will contribute to the understanding how the related proteins confer separate reaction specificities on the same coenzyme.

The reaction of CsdB shares some common features with that of other PLP-dependent enzymes such as aspartate β-decarboxylase (EC 4.1.1.12) (116), kynureninase (EC 3.7.1.3) (117), and SCL. These enzymes catalyze removal of β-substituent from the substrate to form alanine. None of their structures have been solved. The solution of the 3D structure of CsdB would contribute to the understanding of the mechanisms of these PLP-dependent enzymes.

A possible role of CsdB in vivo—Genome sequencing projects have revealed that homologs of *A. vinelandii nifS* are widespread throughout nature, and that some organisms contain more than one copy of a *nifS*

homolog (107, 113, Chapter II). Some of the 'NifS-like proteins' characterized so far prefer L-cysteine to L-selenocysteine, and some of them show the opposite preference. Further experiments will need to be done to determine whether putative NifS-like proteins can play a role in Fe-S cluster assembly.

Lacourciere and Stadtman (52) have pointed out that *in vivo* concentrations of sulfur-containing compounds are on the order of a thousand times greater than those of their selenium analogs (118). Thus enzymes showing higher activity toward L-cysteine, such as *A. vinelandii* NifS, will preferentially utilize L-cysteine over L-selenocysteine *in vivo* (52). Therefore, it may be reasonable to assume that enzymes which are specific toward L-selenocysteine probably function as a physiological selenide delivery system in *E. coli.* Although CsdB is not strictly specific to selenocysteine, its discrimination factor (290 times over the activity on cysteine) is much higher than those of other NifS homologs of *E. coli.* Accordingly, the enzyme can be regarded as an *E. coli* counterpart of mammalian selenocysteine lyase. It would be particularly intriguing to determine whether CsdB is more effective than CSD and IscS as a selenide delivery protein in the formation of selenophosphate catalyzed by *E. coli* selenophosphate synthetase.

SUMMARY

An open reading frame, named *csdB*, from *Escherichia coli* encodes a putative protein that is similar to selenocysteine lyase of pig liver and cysteine desulfurase (NifS) of *Azotobacter vinelandii*. In this study, the *csdB* gene was cloned and expressed in *E. coli* cells. The gene product was a homodimer with the subunit M_r of 44,439, contained 1 mol of PLP as a cofactor per mol of subunit, and catalyzed the release of Se, SO_2, and S from L-selenocysteine, L-cysteine sulfinic acid, and L-cysteine, respectively, to yield L-alanine; the reactivity of the substrates decreased in this order. Although the enzyme was not specific for L-selenocysteine, the high specific activity for L-selenocysteine (5.5 units/mg compared with 0.019 units/mg for L-cysteine) supports the view that the enzyme can be regarded as an *E. coli* counterpart of mammalian selenocysteine lyase. I crystallized CsdB, the *csdB* gene product, by the hanging drop vapor diffusion method. The crystals were of suitable quality for x-ray crystallography and belonged to the tetragonal space group $P4_32_12$ with unit cell dimensions of $a = b = 128.1$ Å and $c = 137.0$ Å. Consideration of the Matthews parameter V_m (3.19 $Å^3$/Da) accounts for the presence of a single dimer in the crystallographic asymmetric unit. A native diffraction dataset up to 2.8 Å resolution was collected. This is the first crystallographic analysis of a protein of NifS/selenocysteine lyase family.

CHAPTER IV

Kinetic and Mutational Studies of Three NifS Homologs from *Escherichia coli*: Mechanistic Difference between L-Cysteine Desulfurase and L-Selenocysteine Lyase Reactions

INTRODUCTION

Selenocysteine lyase (SCL) specifically catalyzes the elimination of selenium from L-selenocysteine to yield L-alanine (15, 20), whereas cysteine desulfurase acts on both L-selenocysteine and L-cysteine to produce selenium and sulfur, respectively, and L-alanine (73, 52). Cysteine desulfurase named NifS from *Azotobacter vinelandii* has been shown to supply inorganic sulfur for the formation of iron-sulfur clusters in nitrogenase. Several NifS homologs have been characterized: IscSs isolated from *A. vinelandii* (113) and *E. coli* (69) have cysteine desulfurase activity and are proposed to play a general role in the formation of iron-sulfur clusters of proteins other than nitrogenase. SCL is proposed to function as a selenium delivery protein in the selenoprotein synthesis (52). Since SCL shares sequence similarity with NifS, some of the NifS homologs are expected to function as SCL. Enzymatic discrimination between selenium compounds and corresponding sulfur compounds is important for the cells to control the metabolism of selenium and sulfur. However, the mechanism of enzymatic discrimination between selenocysteine and cysteine has not yet been elucidated.

In addition to *iscS* described above, *E. coli* has two more *nifS* homologs, *csdA* and *csdB*, whose physiological functions are unknown (107). The *csdA* gene product, CSD, was characterized, and shown to act on L-selenocysteine, L-cysteine, and L-cysteine sulfinate (Chapter II, 107). The *csdB* gene product, CsdB, shows much higher activity to L-selenocysteine than to L-cysteine (290 times), and is regarded as SCL (Chapter III, 119).

A reaction mechanism of desulfurization of L-cysteine catalyzed by *A. vinelandii* NifS has been proposed by Zheng *et al.* (73). In the proposed mechanism, the active-site residue, Cys325, first protonates the C4' atom of the cysteine-pyridoxal quinonoid intermediate and then attacks the sulfur atom of the substrate, L-cysteine, to yield the enzyme-bound persulfide intermediate. The mutant $NifS^{C325A}$, in which Cys325 is replaced with Ala, has no activity toward not only L-cysteine but also L-selenocysteine. Therefore, the mechanism of NifS for both substrates are thought to be the same (73, 52). Furthermore, this cysteine residue is conserved among all the NifS homologs so far analyzed. However, I found that no cysteinyl residue of CSD is essential for the activity with L-selenocysteine as described in Chapter II (107). It is worth examining the requirement of the conserved cysteine residues for the activity of CsdB and IscS to elucidate the reaction mechanisms of these NifS homologs.

In this Chapter, I describe kinetic characterization of CSD, CsdB, IscS, and their mutants with an alanine residue substituted for the conserved cysteine residue. I also report abortive transamination that occurs during the catalytic reactions and activating effects of pyruvate on the enzymes. The present study suggests that the cysteine desulfurase reaction and the SCL reaction proceed

through different mechanisms.

EXPERIMENTAL PROCEDURES

Construction of Expression Plasmids—The constructs for expression of *iscS* was made by PCR with the Kohara ordered clone No. 430 (110). *Nde*I and *Hind*III restriction sites were incorporated at the 3' and 5' ends of the gene, respectively. Oligonucleotide primers used for the PCR were 5'-GGAA TTCGGAGTTTATAGAGCACATATGAAATTACCGATT-3' (upstream), 5'-CCCAAGCTTAATGATGAGCCCATTCG-3' (downstream). The 1.2-kbp product was digested and subcloned into pET21a to form the pEF1. IscS was expressed about 16% of the crude extract.

Mutagenesis—The mutants were prepared by PCR from pCsdB for CsdB^{C364A} and pEF1 for IscS^{C328A}, respectively, according to the overlap extension method of Ito *et al.* (120). The following primers were used: 5'-GCATTGCGGCGTGATGTC-3', 5'-CATGATTACGAGTTCAGGAGGTG C-3' (for CsdB^{C364A}), 5'-GCTGACGTAGCCGCGGAACC-3', and 5'-TAA GAAGGAGATATACGTATGAAATTA-3' (for IscS^{C328A}). The insertions of only the desired mutations were verified by DNA sequencing.

Purification of IscS—Potassium phosphate buffer (KPB) (pH 7.4) was used as the buffer throughout the purification. *E. coli* BL21 (DE3) pLysS cells harboring pEF1 were grown in 0.8 liters of LB medium containing 100 μg/ml ampicillin at 37°C for 11.5 h. The culture was inoculated into a fresh 8 liters of the medium containing ampicillin and then permitted to grow for a further 1 h. At this point isopropyl-β-thiogalactoside (1 mM) was added.

After 3 h the cells were harvested by centrifugation, frozen-thawed in 30 mM KPB (pH 7.4) containing 5 mM DTT, and disrupted by sonication. The cell debris was centrifuged, and the supernatant was fractionated by ammonium sulfate (25-65% saturation). The enzyme was dissolved in 30 mM KPB and applied to a Phenyl-Toyopearl column (3 × 19 cm). IscS was eluted with a 2.6-liter linear gradient of 0.65-0 M ammonium sulfate in the buffer, pooled and concentrated by ammonium sulfate (70% saturation). The enzyme was dissolved and dialyzed with the 10 mM buffer, and applied to a DEAE-Toyopearl column (3 × 23 cm). IscS was eluted with a 1.6-liter linear gradient of 0-0.15 M NaCl in the buffer. The active fractions were pooled and concentrated by ultrafiltration. IscS was dialyzed against 10 mM buffer containing 0.9 M ammonium sulfate and applied to a Butyl-Toyopearl column (3 × 17 cm). The enzyme was eluted with a 1.2-liter linear gradient of 0.9-0 M ammonium sulfate in the buffer and concentrated by ultrafiltration. The enzyme was dialyzed against 5 mM buffer and applied to a Gigapite column (3 × 10 cm). The enzyme was eluted with a 0.75-liter linear gradient of 5-100 mM KPB, and concentrated by ultrafiltration. The enzyme was dialyzed with 10 mM buffer and applied to a Superose 12 FPLC column (1 × 10 cm) (Amersham Pharmacia Biotech, Uppsala, Sweden). Purified IscS was judged to be homogeneous by SDS-PAGE analysis. IscS did not have an associated protein whereas the enzyme originally isolated from the non-overproducing strain has been copurified together with acyl carrier protein, which is bound to IscS via a disulfide linkage (69). The N-terminal sequence of purified IscS was MKLPIYLDY, which matches that deduced from the nucleotide sequence

deposited in GenBank (accession number D90883). Recombinant IscS exhibited the specific activity of 0.38 units/mg at 12 mM of L-cysteine. The previously reported value for the native IscS was 0.078 units/mg (69). The difference in the specific activity is probably due to the differences in the conditions used for assay.

Purification of Other Proteins—The purified CSD and CsdB were obtained as described previously (107, 119). CSD^{C358A} and $IscS^{C328A}$ were purified as described for the purification of the wild-type enzymes except using ammonium sulfate fractionation and chromatographies with DEAE-Toyopearl and Phenyl-Toyopearl columns. $CsdB^{C364A}$ was purified by chromatographies with DEAE-Toyopearl, Phenyl-Toyopearl and Superose 12 columns. Buffers and elution conditions used for chromatographies were identical to those for the purification of the respective wild-type enzymes.

Assays—All enzymatic activities were assayed in the 0.12 M Tricine-NaOH buffer (pH 7.5), and the standard reaction mixture containing 50 mM DTT, 0.2 mM PLP, 0.12 M Tricine-NaOH buffer (pH 7.5), enzyme, and substrate amino acid. The enzymatic activities toward L-selenocysteine and L-cysteine were measured as described previously (107). DTT was omitted from the reaction mixture in the assay of desulfination of L-cysteine sulfinate, and sulfite produced was determined with fuchsin (55). Production of alanine from substrates was determined with a Beckman high performance amino acid analyzer 7300 (Beckman Coulter, Fullerton, CA). Specific activity was expressed as units/mg of protein, with one unit of enzyme defined as the amount that catalyzed the formation of 1 μmol of the product in one minute.

The concentration of the purified enzymes was determined spectrophotometrically (111) using $A_{280}^{1\%}$ = 11.3 (CSD), 11.2 (CsdB), and 9.15 (IscS).

Pyruvate Assays—The reaction mixture consisting of 92 nmol of enzyme, 20 μmol of KPB (pH 7.4) and 8 μmol of L-cysteine sulfinate in a total volume of 0.4 ml was incubated at 37°C for 24 h. The reaction mixture was loaded onto Microcon-10 and the products were separated from the enzyme by ultrafiltration. The 50-μl sample was added with 25 μl of 0.066% 2,4-dinitrophenylhydrazine in 2 M HCl and incubated for 5 min at ambient temperature. The solution was neutralized by adding 30 μl of 5 M NaOH, and absorbance at 520 nm was recorded and the pyruvate concentration was calculated based on a pyruvate standard curve.

Analytical Methods—N-terminal amino acid sequences were determined using a Shimazu PPSQ-10 protein sequencer (Shimadzu, Kyoto, Japan). The nucleotide sequences were confirmed with a Dye Terminator sequencing kit FS (Perkin-Elmer) and an Applied Biosystems 373A DNA sequencer.

RESULTS

CSD, CsdB and IscS Catalyze Abortive Transamination—Incubation of CSD with L-selenocysteine in the absence of PLP led to a time-dependent inactivation as shown in Fig. 20A (●). The presence of 0.1 mM PLP prevented the inactivation (Fig. 20A ○). When PLP (0.1 mM) was added to the inactivated enzyme, it regained the original catalytic activity (Fig. 20A △). This result indicates that CSD undergoes reversible inactivation. Similar result was obtained when L-cysteine sulfinate was used as a substrate (data not shown).

CsdB and IscS were also inactivated with time by incubation with L-selenocysteine in the absence of added PLP (Fig. 20B ●, 20C ●). The addition of PLP, again, restored their activity, showing that CsdB and IscS also undergo reversible inactivation.

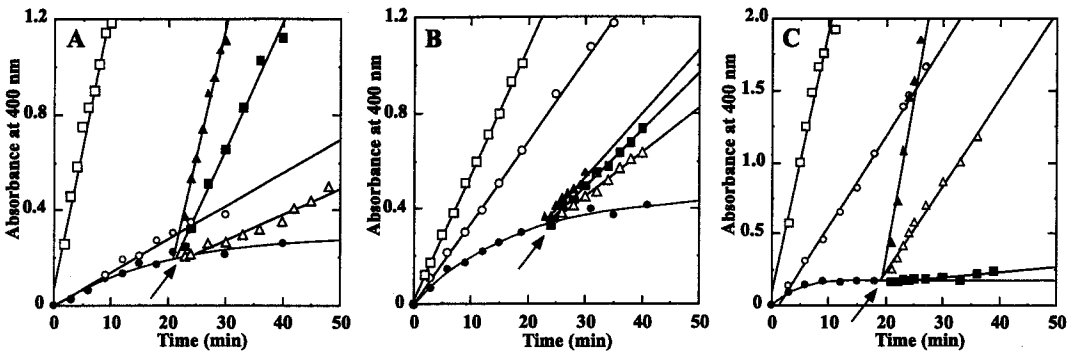

FIG. 20. **Effects of added PLP and pyruvate on the activities of CSD, CsdB and IscS.** Effects of the addition of PLP and pyruvate on the reactions catalyzed by CSD (*A*), CsdB (*B*) and IscS (*C*) are shown. The reaction mixture contained 5 mM L-selenocysteine, 50 mM DTT, and 0.12 M Tricine-NaOH (pH 7.5). The reactions were carried out under the following conditions: no additives (●), in the presence of 0.1 mM PLP (○), in the presence of 0.1 mM PLP plus 1 mM pyruvate (□). At the point indicated by the *arrow*, 0.1 mM PLP (△), 1 mM pyruvate (■), or 0.1 mM PLP plus 1 mM pyruvate (▲) was added.

Several pyridoxal enzymes other than transaminases are known to catalyze abortive transamination as a side reaction, where the substrates (amino acids) are converted into α-keto acids. This reaction results in the conversion of PLP into PMP, and the enzyme is inactivated without addition of PLP or addition of α-keto acids to convert PMP back to PLP. I examined whether abortive transamination occurs in the reactions catalyzed by CSD, CsdB, and IscS by determining the production of pyruvate as described in Experimental Procedures. During 24-h incubation in the presence of L-cysteine sulfinate

without added PLP, the following amounts of pyruvate were found to be produced: 0.3 mol/mol-CSD, 0.1 mol/mol-CsdB, and 0.4 mol/mol-IscS. The formation of PMP was indicated spectroscopically as follows. When 10 mM L-cysteine sulfinate was added to CSD in 10 mM KPB (pH 7.4), an absorption peak at 420 nm was greatly decreased, and a new peak at 325 nm was formed within 2 min (data not shown). The spectrum did not change significantly at least for 12 h thereafter (Fig. 21). CsdB and IscS exhibit an absorption maximum at 420 nm and 390 nm, respectively. A 325-nm peak was formed when CsdB or IscS was incubated with L-cysteine sulfinate with a concomitant decrease in the absorbance at 420 nm (CsdB) or 390 nm (IscS) (data not shown). The 325-nm peak is a characteristic of PMP-ketimine structure of the coenzyme (121). These results indicate that both PMP moiety and pyruvate are produced, supporting the view that the enzymes are inactivated through abortive transamination.

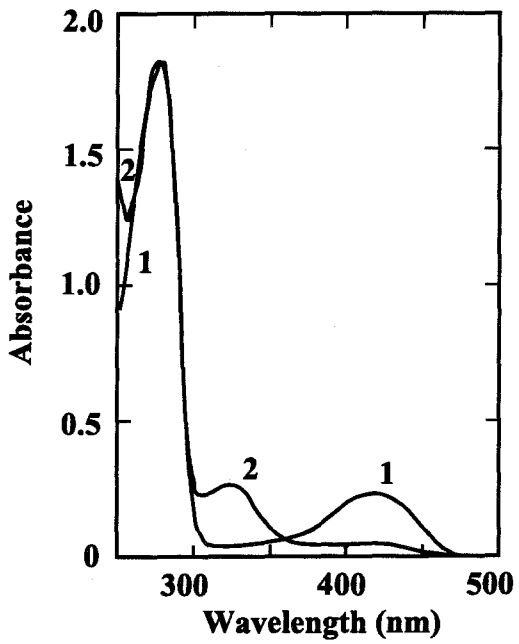

FIG. 21. **Spectral change of CSD during the catalytic reaction.** *Curve 1*, spectrum of the holoenzyme (1.6 mg/ml in 10 mM KPB, pH 7.4); *curve 2*, spectrum of the enzyme given in *curve 1* after 12 h-incubation with 10 mM L-cysteine sulfinate. Spectrum of *curve 2* was normalized by adjusting the peak absorbance at 280 nm to that in *curve 1*.

Pyruvate Activates the Reactions Catalyzed by CSD, CsdB and IscS— The fact that CSD, CsdB and IscS were inactivated through transamination suggests the possibility that the inactivation may be reversed or prevented by adding α-keto acid due to reverse transamination between added α-keto acid and PMP-enzyme to yield PLP-enzyme. Fig. 20A shows that addition of pyruvate (1 mM) to the inactivated CSD led to more activation than the addition of PLP (Fig. 20A ■). The reaction rate culminated by the addition of pyruvate plus PLP (Fig. 20A ▲). The highest rate was also achieved in the reaction mixture initially containing both pyruvate and PLP (Fig. 20A □). Effect of pyruvate on the CsdB and IscS reactions was also examined (Fig. 20B, 20C). In both enzyme reactions, pyruvate plus PLP initially added to the reaction mixture increased the rate of the reaction (Fig. 20B □, 20C □). The addition of pyruvate to the inactivated CsdB and IscS caused different responses in reversion of the activity: the activating effect of pyruvate on CsdB was more significant than that of PLP (Fig. 20B ■, △), whereas PLP lead to more drastic activation of IscS than pyruvate (Fig. 20C ■, △). It is probably because PMP is easily released from IscS due to low affinity, and pyruvate cannot reproduce PLP efficiently through transamination at the active site of IscS.

Fig. 22 describes the effect of added pyruvate on the initial rates of the enzymatic selenocysteine decomposition. The result clearly shows that the extents of activation of three enzymes by added pyruvate are significantly different from one another: the initial rate of the reaction increased 12-fold (CSD), 1.5-fold (CsdB), and 7-fold (IscS) by the addition of 1 mM pyruvate. The same concentration of pyruvate also accelerated enzymatic desulfination of

L-cysteine sulfinate (initial concentration: 12 mM): ~4-fold (CSD), ~2-fold (CsdB), and ~2-fold (IscS). However, the effect of pyruvate was much less significant on desulfurization of L-cysteine (60 mM) catalyzed by CSD, CsdB and IscS: only ~1.2-fold activation was observed for all three enzymes.

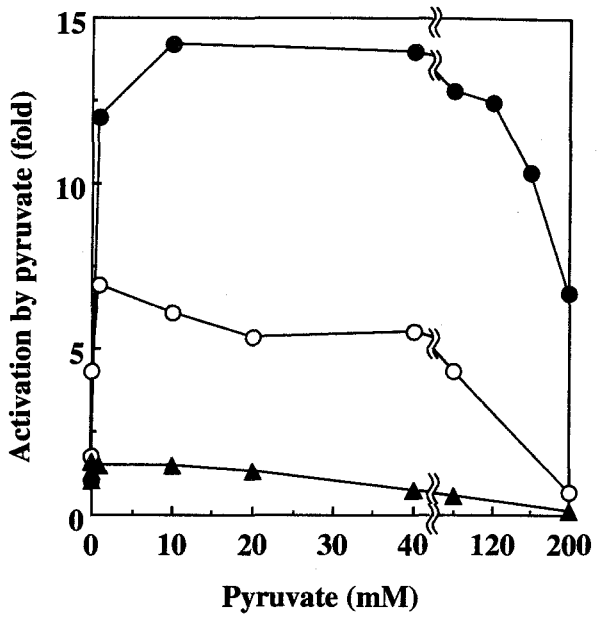

FIG. 22. **Effect of added pyruvate concentration on the initial rates of elimination of selenium from L-selenocysteine.** The reaction mixture contained 5 mM L-selenocysteine, 50 mM DTT, 0.2 M PLP, 0.12 M Tricine-NaOH buffer (pH 7.5), and pyruvate as indicated. Initial rates of the reaction by CSD (●), CsdB (▲), and IscS (○) are represented by relative activity, where specific activity of each enzyme in the absence of added pyruvate (CSD: 3.4 U/mg, CsdB: 2.6 U/mg, IscS: 1.7 U/mg) is set at 1.

In order to determine whether pyruvate endogenously formed from L-selenocysteine through the abortive transamination has an influence on the rate of the selenocysteine lyase reaction catalyzed by CSD, lactate dehydrogenase and NADH were added to the mixture to deplete endogenous pyruvate (122). The depletion markedly decreased the rate of the selenocysteine decomposition

(data not shown). Therefore, pyruvate formed via abortive transamination also plays a role in maintaining a high rate of the reaction.

Kinetic Analysis—The steady-state kinetic analyses of the reactions catalyzed by CSD, CsdB, and IscS were performed with L-selenocysteine, L-cysteine sulfinate, and L-cysteine as substrates in the absence and presence of added pyruvate. All data obtained are shown in Fig. 23 and analyzed by double reciprocal plotting shown in Fig. 24. This analysis revealed that CSD shows an anomalous behavior with L-selenocysteine in the absence of pyruvate (Fig. 24A ●). The plot of initial velocity in the absence of pyruvate vs. selenocysteine concentration for CSD is a hyperbolic curve at low substrate concentrations and an upward curve at higher substrate levels (Fig. 25). However, the addition of 1 mM pyruvate made the enzyme to show an apparent Michaelis-Menten behavior (Fig. 23A O, 5A O). CsdB and IscS also exhibit non-Michaelis-Menten behavior with L-selenocysteine in the absence of pyruvate, which is not seen in the presence of pyruvate (Fig. 24B, 24C). Taken together, pyruvate not only increases the activity of CSD, CsdB and IscS, but also changes the kinetic behavior of these enzymes with L-selenocysteine.

Unusual behavior of CSD was also observed using L-cysteine sulfinate as a substrate. A remarkable downward curvature was observed in the double reciprocal plot for CSD with L-cysteine sulfinate in the absence of pyruvate (Fig. 24D), indicating the presence of a negative cooperativity. Again, Michaelis-Menten kinetics was observed when pyruvate was added to the reaction mixture (Fig. 24D). In contrast, the double reciprocal plots for CsdB and IscS with L-cysteine sulfinate show only a slight, if any, deviation from the Michaelis-

Menten kinetics irrespective of the absence or presence of pyruvate (Fig. 24E, 24F).

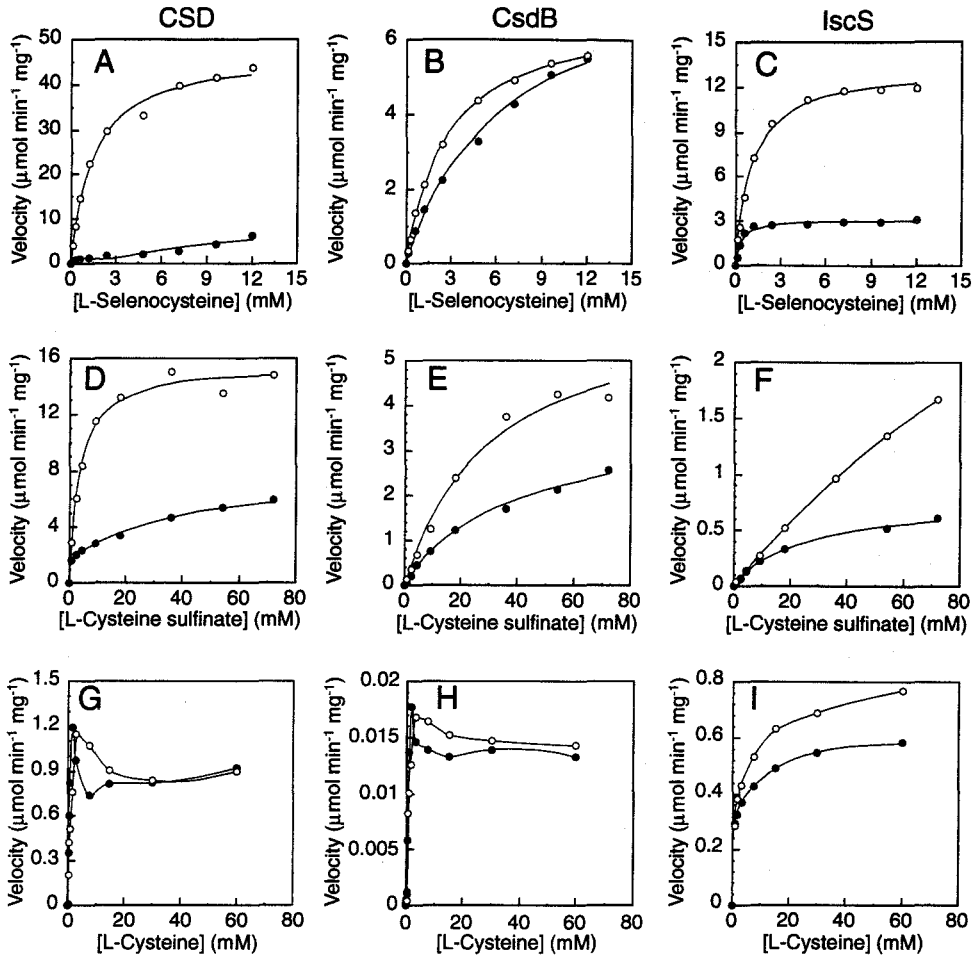

FIG. 23. **Dependence of the rates of the reactions catalyzed by CSD, CsdB and IscS on the substrate concentrations.** Assays were performed at 37 °C in 0.12 M Tricine-NaOH (pH 7.5), 50 mM DTT, and 0.2 mM PLP in the absence (●) or presence (○) of 1 mM pyruvate. L-Selenocysteine (*A*, *B*, *C*), L-cysteine sulfinate (*D*, *E*, *F*) and L-cysteine (*G*, *H*, *I*) were used as substrates, and production of selenide, sulfite and sulfide was determined, respectively, as described in "Experimental procedures". DTT was omitted in the assays with L-cysteine sulfinate. The plots for CSD (*A*, *D*, *G*), CsdB (*B*, *E*, *H*), and IscS (*C*, *F*, *I*) are shown. The lines represent the best fits generated with KaleidaGraph (Synergy software) based on the equation $V = V_{max}^{app}[S]/(K_m^{app} + [S])$ except that the lines in the panel *G-I* are added to guide the eye and have no theoretical significance.

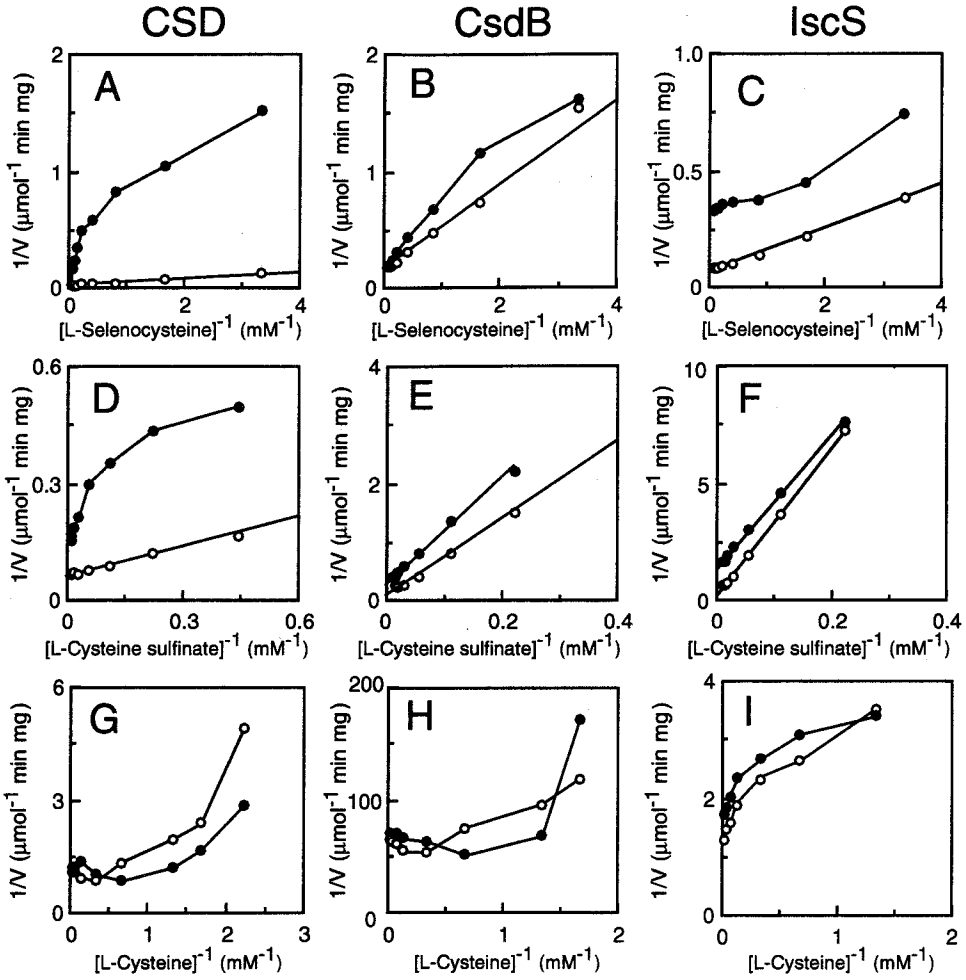

FIG. 24. **Double reciprocal plots of the data presented in Fig. 4 showing the dependence of the rates of the reactions catalyzed by CSD, CsdB, and IscS on the substrate concentrations.** L-Selenocysteine (*A*, *B*, *C*), L-cysteine sulfinate (*D*, *E*, *F*) and L-cysteine (*G*, *H*, *I*) were used as substrates. The plots for CSD (*A*, *D*, *G*), CsdB (*B*, *E*, *H*), and IscS (*C*, *F*, *I*) are shown. The linear lines are drawn only when a linearity is apparent with a correlation coefficient more than 0.99. Other lines are added to guide the eye and have no theoretical significance.

TABLE XII
Apparent kinetic constants

Substrate	CSD				CsdB				IscS			
	None		+ Pyruvate[a]		None		+ Pyruvate[a]		None		+ Pyruvate[a]	
	V_{max}^{app}	K_m^{app}	V_{max}^{app}	K_m^{app}	V_{max}^{app}	K_m^{app}	V_{max}^{app}	K_m^{app}	V_{max}^{app}	K_m^{app}	V_{max}^{app}	K_m^{app}
	units/mg	*mM*	*units/mg*	*mM*	*units/mg*	*mM*	*units/mg*	*mM*	*units/mg*	*mM*	*units/mg*	*mM*
L-Selenocysteine	(>6.2)[c]	—[b, c]	47	1.4	(8.3)[c]	(6.4)[c]	6.8	2.6	(3.1)[c]	(0.35)[c]	13	1.1
L-Cysteine sulfinate	(6.0)[c]	(7.6)[c]	16	3.5	3.8	39	6.4	30	0.80	26	6.2	194
L-Cysteine	(0.95)[c]	(0.40)[c]	(1.0)[c]	(0.68)[c]	(0.015)[c]	(0.63)[c]	(0.017)[c]	(0.77)[c]	(0.54)[c]	(0.93)[c]	(0.72)[c]	(1.6)[c]

[a]Assays were performed in the presence of 1 mM pyruvate.

[b]Not determined because of the anomalous kinetic behavior of CSD.

[c]An equation $V = V_{max}^{app}[S]/(K_m^{app} + [S])$ was used to determine the apparent kinetic constants, although hyperbolic curve was not apparent within the concentration range tested.

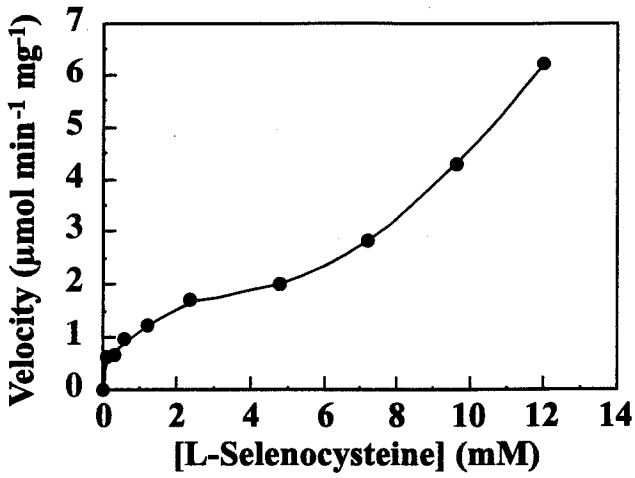

FIG. 25. **Non-Michaelis-Menten behavior of CSD.** The plot in Fig. 4*A* is magnified to show the anomalous kinetic behavior of CSD with L-selenocysteine in the absence of added pyruvate. The lines are added to guide the eye and have no theoretical significance.

The kinetic behaviors of CSD and CsdB with L-cysteine are similar to each other: the upward curvatures are seen in the double reciprocal plots (Fig. 24G, 24H). The plot of initial velocity vs. cysteine concentration for each enzyme (Fig. 23G, 23H) is similar to that for *A. vinelandii* NifS (52). These enzymes are probably inhibited by cysteine at high concentrations. In contrast, the double reciprocal plot for IscS with L-cysteine exhibits downward curvature (Fig 5I). It is notable that addition of pyruvate to the cysteine desulfurase reactions caused no significant changes in the kinetic behaviors of all these enzymes.

Apparent kinetic constants obtained in the present work are summarized in Table XII. Because of the anomalous relationships between the substrate concentration and velocity of the reaction described above, several values could not be determined. Difficulties in determining the accurate kinetic parameters of NifS and IscS from *A.vinelandii* were also noted by Lacourciere *et al.* (52) and

Zheng *et al.* (73, 113).

Role of Cys Residue—A cysteine residue conserved among NifS homologs (21, 107) has been suggested to play a crucial role in the catalysis (73). Zheng *et al.* (1994) proposed that the active site cysteinyl thiolate anion performs nucleophilic attack on the sulfur of a substrate-PLP adduct, resulting in formation of a cysteinyl persulfide and an enamine derivative of alanine. Because the conserved Cys325 of *A. vinelandii* NifS was reported to be essential for the activity toward both L-cysteine and L-selenocysteine (73), the degradation of these substrates was thought to proceed through the same mechanism (52). However, in Chapter II, I found that Cys358 of CSD corresponding to Cys325 of *A. vinelandii* NifS is not essential for the decomposition of L-selenocysteine (107).

In the present work, I substituted Ala for the conserved Cys of CSD, CsdB and IscS by site-directed mutagenesis. The mutant enzymes, C358A (CSD), C364A (CsdB), and C328A (IscS) were purified, and their activities were determined with L-selenocysteine, L-cysteine sulfinate and L-cysteine. The activities toward L-cysteine of all enzymes were almost completely lost by the mutation (Fig. 26). However, surprisingly, I found that the conserved cysteine residues are not essential for catalytic activity toward L-selenocysteine and L-cysteine sulfinate (Fig. 26). Thus, the conserved cysteine residue plays a crucial role only in the decomposition of L-cysteine. These results suggest that L-cysteine desulfurization and L-selenocysteine/L-cysteine sulfinate decomposition proceed through different mechanisms.

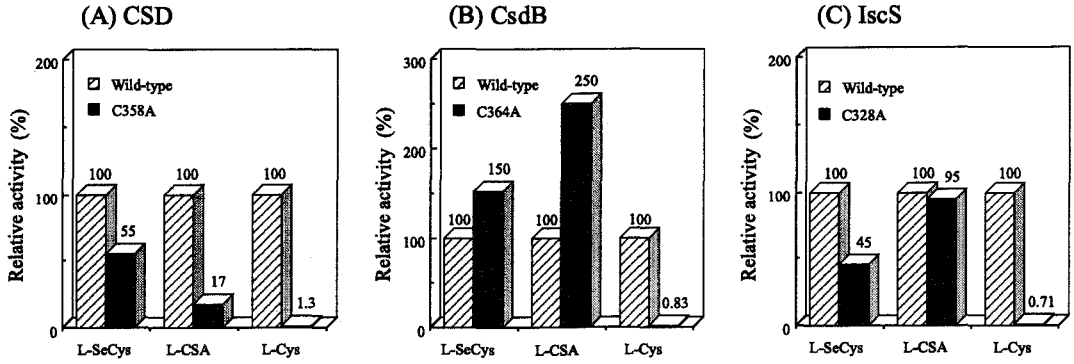

FIG. 26. **Activity of the wild-type and Cys → Ala mutant enzymes, CSD, CsdB and IscS.** The specific activities were determined in the reaction mixture containing L-selenocysteine (12 mM), L-cysteine sulfinate (90 mM) or L-cysteine (60 mM) as a substrate. The specific activity of wild-type enzyme with each substrate is set at 100%. The number on each column represents the relative activity.

DISCUSSION

Cysteine desulfurase, SCL, kynureninase (117), and aspartate β-decarboxylase (AspDC) (116) catalyze electrophilic displacement at C_β of α-amino acids to yield L-alanine, whereas other β-lyases and β-synthases catalyze elimination of a β-substituent to generate α,β-unsaturated aldimine (generally the aminoacrylate-PLP Schiff base). Recent studies on the catalytic mechanism of kynureninase from *Pseudomonas fluorescens* (123, 124) demonstrated the existence of both quinonoid and alanine-ketimine intermediates in the reaction. The evidence for the ketimine intermediate has also been presented for the catalytic mechanism of cystathionine γ-synthase (125). Thus the reactions catalyzed by PLP-dependent enzymes, including NifS homologs, whose reactions involve the formation of β-carbanionic intermediates are generally thought to proceed via a pyridoxamine-ketimine intermediate (125).

It is known that kynureninase and AspDC catalyze transamination as a side reaction besides their main reactions (126, 127). I have shown in the

present study that the NifS homologs, CSD, CsdB, and IscS, also catalyze abortive transamination. The activating effects of pyruvate and PLP on the decomposition of L-selenocysteine and L-cysteine sulfinate catalyzed by CSD, CsdB, and IscS (Fig. 23) are probably caused by repression of the abortive transamination (Scheme I). L-Alanine and pyruvate arise by partitioning of the alanine-ketimine intermediate (Scheme I, **III**) between deprotonation at C-4' and hydrolysis. The hydrolysis leads to the formation of PMP-enzyme (**VI**), which can release PMP to become apo-enzyme (**VII**). The presence of inactive species, **VI** and **VII**, decreases the reaction rate. The addition of pyruvate shifts the equilibrium between **III** and **VI** to the formation of **III**, resulting in an increase in the reaction rate. However, if the affinity between the enzyme and PMP is low, PMP-enzyme (**VI**) releases PMP to become apo-enzyme (**VII**), and pyruvate can no longer convert the enzyme to the active form (**III**). In the presence of added PLP, apo-enzyme (**VII**) can be directly converted into the active form of the enzyme (**V**), resulting in an increase in the concentration of a catalytically competent form of the enzyme.

The addition of pyruvate to the inactivated IscS had little activation effect (Fig. 20C). It is likely that affinity between IscS and PMP formed via transamination is low, and the enzyme releases PMP to become apo-form. The fact that apo-form of IscS is much more easily prepared by incubation with L-cysteine than that of CSD and CsdB supports this interpretation. The addition of PLP to the inactivated IscS regenerates holo-enzyme (**I**), and thus has more significant effect than the addition of pyruvate. In contrast, CSD and CsdB probably have much higher affinity for PMP, so that the added pyruvate can be utilized to convert PMP-enzyme (**VI**) to alanine-ketimine (**III**). On the other

hand, addition of lactate dehydrogenase and NADH lead to the formation of **VI** by shifting the equilibrium, resulting in significant decrease in reaction rate. Addition of PLP together with pyruvate converts **VII** to **V** and shifts the equilibrium between **III** and **VI** to the formation of **III**. Consequently, the concentration of the inactive forms of the enzyme, **VI** and **VII**, is greatly reduced, and the reaction proceeds at the maximum rate. The dissociation constant of apo-enzyme for PMP and the rate constant of the conversion between **III** and **VI** may vary in each enzyme, and thereby the effects of pyruvate on CSD, CsdB, and IscS are different from each other.

Kinetic characterization revealed that many of the reactions catalyzed by CSD, CsdB, and IscS in the absence of added pyruvate exhibit non-Michaelis-Menten features. One possible explanation for the unusual kinetic behaviours in the absence of pyruvate is the existence of cooperativity in the enzymes. The line curved to downward near the 1/V axis in the double reciprocal plot is also found in the studies of several enzymes regulated by negative cooperativity (128-130). Several mechanisms are known to explain negative cooperativity in a certain dimeric enzyme (131). One involves an induced allosteric response where high affinity binding of the first ligand to the dimer elicits a conformational transition in the free subunit which reduces the affinity for subsequent ligands. In another model, known as a hysteretic kinetic model (132), an anomalous behavior can be a consequence of the slow isomerization between two enzyme forms which differ from each other in their catalytic properties. It remains unclear which is the case for CSD, CsdB, and IscS, and how pyruvate affects such enzyme behaviors.

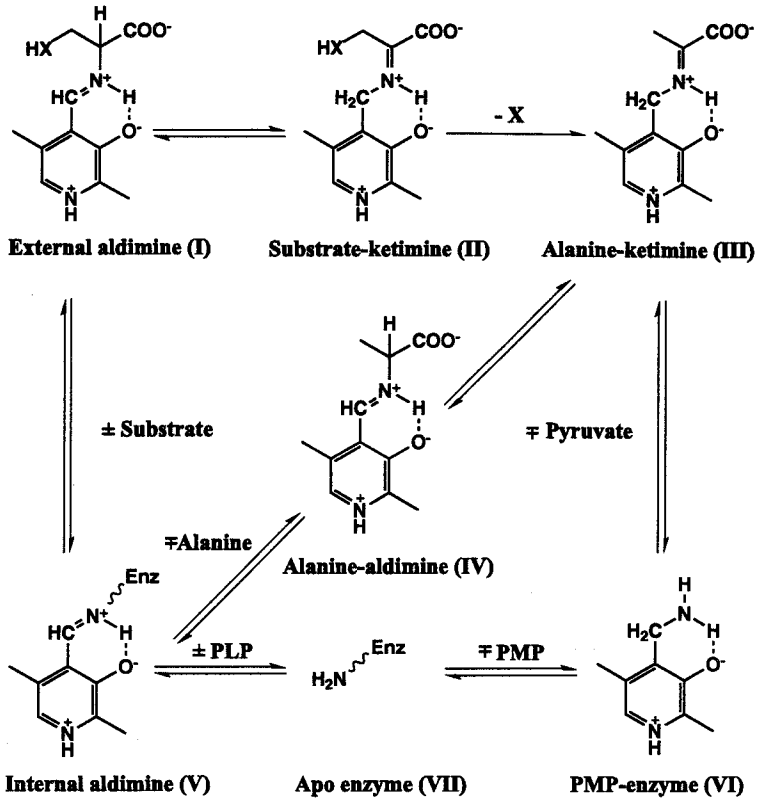

SCHEME I. A possible path of main reaction and side-transamination catalyzed by *E. coli* NifS homologs (*X* = Se , S, SO_2), aspartate β-decarboxylase (*X* = CO_2), and kynureninase (*HX* = 2-aminobenzoyl).

The anomalous kinetic characteristics of CSD with L-selenocysteine were not observed in the previous study (107). This is because the L-selenocysteine concentration was varied from 0.2 to 2.5 mM in that study, whereas the anomalous feature can be observed only above 2.5 mM (Fig. 25). Another finding about CSD in the present study is the activation of enzyme activity by pyruvate. In the previous study, the kinetic parameters for desulfination of L-cysteine sulfinate by CSD were determined by coupled-assay system using alanine dehydrogenase, where a significant amount of pyruvate is formed from

alanine, whereas the activities toward L-selenocysteine and L-cysteine were assayed by another method that does not produce pyruvate. Since the desulfination catalyzed by CSD is activated by pyruvate (Fig. 23), the desulfination activity was overestimated in the coupled-assay. The present study showed that CSD preferentially catalyzes the decomposition of L-selenocysteine as well as the desulfination of L-cysteine sulfinate in the range of ~7 mM of substrate (Fig. 24A, B), when coupled-assay is not employed for L-cysteine sulfinate.

Cys325 of NifS from *A. vinelandii* was reported to be essential for the activity toward both L-cysteine and L-selenocysteine by Zheng *et al.* (45). They proposed that the cysteinyl thiolate anion derived from Cys325 performs nucleophilic attack on the sulfur atom of a substrate-PLP adduct, resulting in formation of a cysteinyl persulfide as shown in Scheme II (A). In this reaction, Cys325 was believed to protonate C4'-atom of the PLP. L-Selenocysteine lyase reaction was also thought to proceed through a similar mechanism (52). However, Cys358 of CSD, Cys364 of CsdB, and Cys328 of IscS, corresponding to Cys325 of *A. vinelandii* NifS, were shown to be not required for the activity toward L-selenocysteine and L-cysteine sulfinate in the present study (Fig. 26). The finding that Cys328 of IscS is not essential was rather unexpected because IscS exhibits high sequence similarity with *A. vinelandii* NifS (44% identity).

One of the important consequences of this observation is that the cysteinyl residue is not involved in the protonation of the C4'-atom of the quinonoid intermediate at least in the mutant enzyme that has no active-site cysteine residue.

The protonation is probably carried out by the lysine residue bound to PLP as in the case for aspartate aminotransferase (133) (Scheme II (A), (B)).

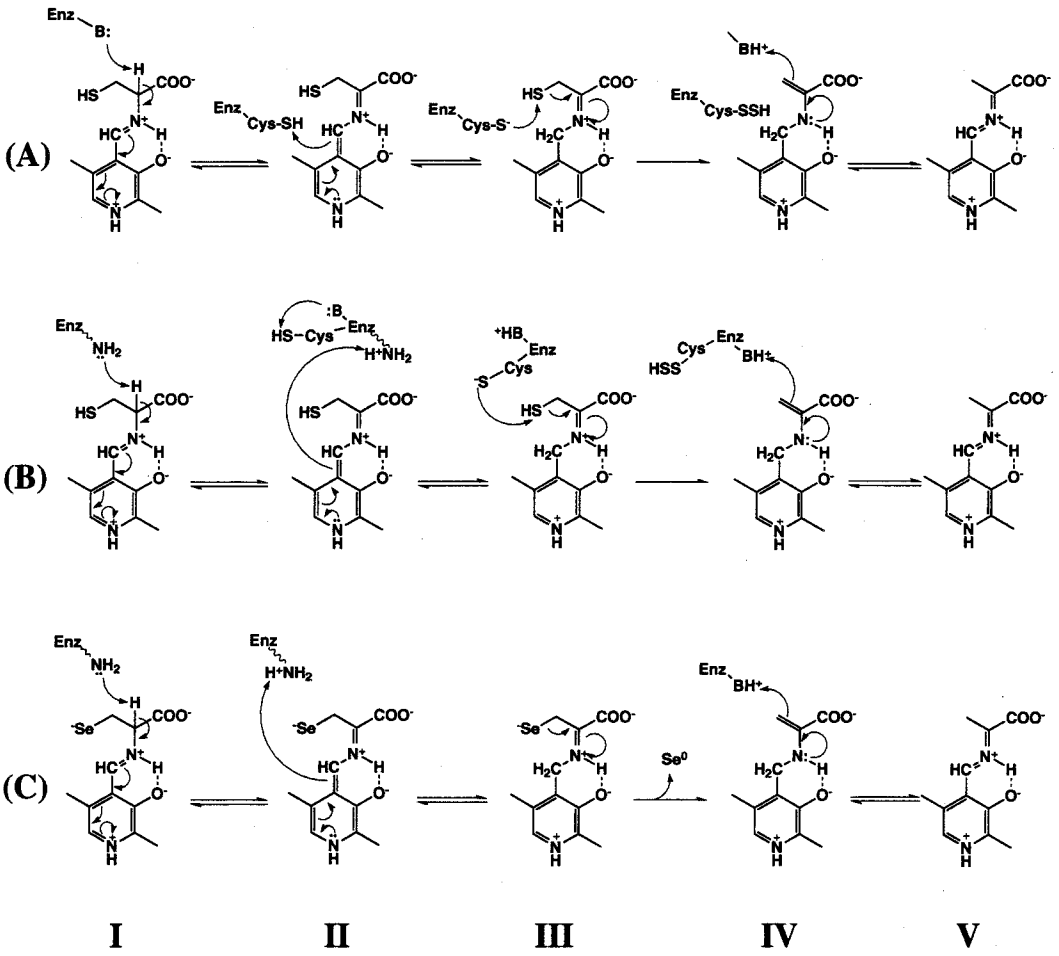

SCHEME II. Proposed reaction mechanism of desulfurization of L-cysteine catalyzed by *A. vinelandii* NifS adapted from Ref. 73 (A), and reaction mechanisms proposed in this study (B and C). Cysteine desulfurase reaction (B) and selenocysteine lyase reaction (C) catalyzed by CSD, CsdB, and IscS are shown.

The results obtained in this study clearly demonstrate that the conserved cysteine residue is important for cysteine desulfurase activity, but is not an

absolute requirement for the activities toward L-selenocysteine and L-cysteine sulfinate. Although it is possible that the decomposition of L-selenocysteine and L-cysteine sulfinate proceeds through a mechanism similar to that shown in Scheme II (B) in the wild-type enzyme, catalytic reaction not involving the cysteine residue must take place at least in the mutant enzyme that has no active-site cysteine residue. Scheme II (C) illustrates a possible mechanism for decomposition of L-selenocysteine that does not require any catalytic cysteine residue. The selenohydryl group of L-selenocysteine is probably deprotonated and present in an anionic form (Scheme II (C) **I**) because pK_a of the selenohydryl group is 5.2, which is much lower than the pH of the reaction mixture (pH7.4) (134, 135). Subsequently, selenium is released spontaneously from the intermediate III with one electron left on the β-carbon of the substrate (Scheme II (B)). Desulfination from L-cysteine sulfinate may also proceed through a mechanism similar to that in Scheme II (B) without aid of the active site cysteine residue as seen in the mechanism of desulfination of L-cysteine sulfinate catalyzed by AspDC (74).

One of the intriguing results obtained in this study is that addition of pyruvate to CSD greatly increases the rate of reaction with L-selenocysteine and L-cysteine sulfinate but not so much with L-cysteine. This result can be explained by assuming that the mechanism or rate-limiting step for the desulfurization of L-cysteine is different from those for the decomposition of L-selenocysteine and L-cysteine sulfinate. The decomposition of L-selenocysteine and L-cysteine sulfinate can proceed without the involvement of the active site cysteine residue as discussed above (Scheme II (C)), whereas the active site

cysteine residue plays an essential role in the reaction when L-cysteine is a substrate as shown in Scheme II (B). Flint suggested that the rate-limiting step for the desulfurization of L-cysteine catalyzed by IscS could be the restoration of the cysteine residue from the cysteine persulfide formed in the active site. If this is the case for CSD and pyruvate does not facilitate the restoration of the cysteine residue, the activating effect of pyruvate on cysteine desulfurization should not be observed. This is not the case for the degradation of L-selenocysteine and L-cysteine sulfinate, which does not require the cysteine residue at the active site. Accordingly, pyruvate could have a significant activating effect only on the decomposition of L-selenocysteine and L-cysteine sulfinate.

In conclusion, the present study suggests that the mechanisms employed by the NifS homologs for L-cysteine desulfurization and the degradation of L-selenocysteine and L-cysteine sulfinate are different from each other.

SUMMARY

I have isolated three NifS homologs from *Escherichia coli*, CSD, CsdB, and IscS. They catalyze eliminations of Se, S, and SO_2 from L-selenocysteine, L-cysteine, and L-cysteine sulfinate, respectively, to form L-alanine. These pyridoxal 5'-phosphate enzymes were inactivated during the catalysis through abortive transamination, yielding pyruvate and an inactive pyridoxamine 5'-phosphate-form enzyme. CSD showed non-Michaelis-Menten behavior. When pyruvate was added, CSD showed Michaelis-Menten behavior for L-selenocysteine and L-cysteine sulfinate. Pyruvate significantly enhanced the activity of CSD toward L-selenocysteine and L-cysteine sulfinate. Surprisingly, the enzyme activity toward L-cysteine was not so much increased by pyruvate, suggesting the presence of different rate limiting steps or reaction mechanisms for L-cysteine degradation and degradation of L-selenocysteine and L-cysteine sulfinate. I substituted Ala for each of Cys358 of CSD, Cys364 of CsdB, and Cys328 of IscS, which correspond to catalytically essential Cys325 of *Azotobacter vinelandii* NifS. The enzyme activity toward L-cysteine was extremely decreased by the mutations, whereas the activities toward L-selenocysteine and L-cysteine sulfinate were less affected. These indicate that the reaction mechanism of L-cysteine desulfurization is different from that of the decomposition of L-selenocysteine and L-cysteine sulfinate, and the conserved cysteine residues play a critical role only for L-cysteine desulfurization.

CHAPTER V

Structure of a NifS homolog: X-Ray Structure Analysis of CsdB, an *Escherichia coli* Counterpart of Mammalian Selenocysteine Lyase

INTRODUCTION

CsdB forms a homodimer, and each of the subunits consists of 406 amino acids (M_r 44,439) with one PLP molecule as a cofactor (Chapter III, 119). PLP-dependent enzymes have been classified into 7 distinct fold types on the basis of the similarity in primary structure, predicted secondary structure and biochemical function (79). NifS proteins have been grouped as "aminotransferases class V" in fold type I, together with serine-pyruvate aminotransferase, phosphoserine aminotransferase (PSAT), isopenicillin N epimerase, and the small subunit of cyanobacterial soluble hydrogenase. Aspartate β-decarboxylase (EC 4.1.1.12) (136) and kynureninase (EC 3.7.1.3) (137), which catalyze the same type of reaction as NifS, namely the removal of the β-substituent from the substrate to form alanine, also belong to this class. There has been no report on three-dimensional structure of this group of enzymes except for PSATs from *E. coli* and *Bacillus circulans sbsp. alkalophilus* (115). No three-dimensional structure of the enzyme catalyzing the removal of the β-substituent from the substrate to form alanine has been solved. Structural analysis of CsdB will contribute to understanding of the mechanisms of these PLP-dependent enzymes. It will also provide

useful information on the mechanism of enzymatic discrimination between selenium and sulfur in analogous substrates. Here I report the crystal structure of CsdB at 2.8 Å resolution. This is the first report on the three-dimensional structure of a NifS homolog. In this Chapter, I mainly describe the structural feature of the CsdB. The catalytic mechanism of the enzyme is discussed in the following Chapter VI based on the structure of CsdB complexed with substrates and analogs.

EXPERIMENTAL PROCEDURES

Crystallization and Preparation of Heavy-Atom Derivatives— Overexpression, purification, and crystallization of CsdB were performed as described in Chapter III (119). The tetragonal-bipyramidal crystals were grown by a hanging drop vapor diffusion method with a 20 mg/ml enzyme solution against 100 mM potassium phosphate buffer (pH 6.8) containing 1.4 M sodium acetate and 10 mM PLP at 25 °C. A typical size of the crystal was approximately 0.5 mm × 0.5 mm × 0.4 mm. They belonged to the tetragonal space group $P4_32_12$ with unit cell dimensions of $a = b = 128.1$ Å, and $c = 137.0$ Å. Assuming two subunits in the crystallographic asymmetric unit, the crystal volume per unit mass, V_m, and the solvent content are 3.19 $Å^3$/Da and 62%, respectively. These values fall within the ranges observed for general protein crystals (114). However, the self-rotation function calculated for native data with the program POLARRFN (138) was featureless. Moreover the electron density map calculated with experimentally determined phases showed only one lump of the CsdB subunit in an asymmetric unit, as

described later. These results revealed that the crystal of CsdB has one subunit in an asymmetric unit. Therefore, the present crystal of CsdB has an unusually high V_m value of 6.32 $Å^3$/Da, which corresponds to a solvent content of 81%. The crystals diffracted up to at least 2.8 Å resolution.

In order to solve the phase problem by the isomorphous replacement method, soaking conditions for preparing heavy-atom derivative crystals were searched by changing the kind and concentration of heavy-atom reagent, and the soaking time. Two kinds of isomorphous heavy-atom derivative crystals were prepared by soaking the native crystals in the mother liquors containing 0.1 mM phenyl mercury acetate (PMA) for 24 hours, and 30 mM $K_2Pt(CN)_4$ for 48 hours.

Data Collection and Processing—Diffraction data for the native and two derivative crystals were collected at 20 °C on a Rigaku R-AXIS IIc imaging plate detector system using Yale-type double-focusing-mirror monochromatized X-ray radiation produced by a Rigaku RU-300 rotating anode X-ray generator operated at 40 kV and 100 mA. All kinds of the crystals were mounted with the crystallographic c^* axes parallel to the crystal rotation axis to record Bijvoet-mates for the heavy-atom derivatives on the same frame. The crystal-to-detector distance was set to 130.0 mm. Each of the 1.5 ° oscillation patterns was recorded for 10 minutes. A total of 33 frames for each data set covered diffraction spots within a rotation range over 50 °. Data processing was accomplished at 2.8 Å resolution for the native and two derivative crystals with the R-AXIS IIc data processing software package. The diffraction intensities were merged and scaled with the program. Statistics of

data collection and processing are summarized in Table XIII.

TABLE XIII
Statistics of data collection and phase calculation

	Native	PMA	$K_2Pt(CN)_4$
Data collection			
Resolution limit (Å)	2.8	2.8	2.8
Observed reflections	73,138	58,403	69,180
Independent reflections	23,770	20,858	22,914
Completeness (%)	94.2	90.1	91.5
R_{merge}[a] (%)	7.22	8.22	7.04
MIR analysis (3.0 Å)			
Number of sites		2	4
R_{iso}[b]		0.160	0.112
R_{Cullis}[c] (acentric/centric)		0.93/0.83	0.92/0.81
Phasing power[d] (acentric/centric)		0.76/0.52	0.82/0.57
Mean FOM[e] (MIR+AS[f])	0.265		

[a] $R_{merge} = \Sigma_i|I_i - \langle I_i \rangle|/\Sigma_i I_i$, where $\langle I_i \rangle$ is the average of I_i over all symmetry equivalents.

[b] $R_{iso} = \Sigma||F_{PH}|-|F_P|| / \Sigma|F_P|$, where F_{PH} and F_P are the derivative and native structure factors, respectively.

[c] $R_{Cullis} = \Sigma||F_{PH}|\pm|F_P|-|F_H|| / \Sigma||F_{PH}|\pm|F_P||$ for all centric reflections, where F_{PH} and F_P are the observed derivative and native structure factors, respectively, and F_H is the calculated heavy atom structure factor.

[d] Phasing power = $\langle F_H \rangle / \langle E \rangle$, where $\langle F_H \rangle$ is the r.m.s. calculated heavy atom structure factor amplitude and $\langle E \rangle$ is the r.m.s. lack of closure error.

[e] FOM is the figure of merit.

[f] MIR+AS is the multiple isomorphous replacement method supplemented with anomalous scattering effects.

Structure Determination and Refinement—The structure was solved by the multiple isomorphous replacement (MIR) method supplemented with anomalous scattering effects from the mercury derivative crystal. The determination of heavy-atom positions and the calculation of MIR phases were carried out using the programs PHASES (139) and MLPHARE in the CCP4 program suit (140), respectively. The difference Patterson map for each

derivative was calculated at 5 Å resolution. One major site for mercury binding was found clearly on the Harker sections and the other site determined from an SIR difference Fourier map. The major and minor sites for platinum binding were obtained from an SIR cross-difference Fourier map and an MIR difference Fourier map, respectively. The PMA and $K_2Pt(CN)_4$ derivative crystals contained 2 and 4 binding sites per asymmetric unit, respectively. MIR phases were calculated up to 3.0 Å resolution, and relevant phase calculation statistics are summarized in Table XIII. The overall figure of merit was 0.265. The MIR map was significantly improved by the iterative procedures of density modification and phase extension to 2.8 Å which was performed gradually with the program SOLOMON (141). As described above, considering the crystallographic parameters of this crystal and the molecular weight of the enzyme, the solvent content of the crystal initially seemed to be 62%. In the procedures of density modification, therefore, the solvent mask was applied as the solvent content of 60%. However, the improved electron density map showed that there was no significant density other than that for one subunit of the dimer molecule in an asymmetric unit. This result corresponds to the solvent content of 81%, and indicates that the molecular two-fold axis of the dimer coincides with the crystallographic two-fold axis. Thus the lower solvent content was adopted throughout the improvement of the electron density map.

In the 2.8 Å resolution electron density map improved as above, the molecular boundary for one subunit was distinguishable from the solvent area. The phosphorous atom of PLP was identified in the map contoured at more

than 5 σ level, and was helpful to find the location of PLP. The electron densities were truncated to the bones with the program MAPMAN (142). The polypeptide chain was traced on the truncated map using the program O based on the bones (140). The side chains of the polypeptide were assigned by reference to the primary structure. The structural model was refined using simulated annealing protocol of the program X-PLOR (143). In the course of refinement, the model was carefully inspected with $2F_o - F_c$ and $F_o - F_c$ maps and manually rebuilt in unreasonable regions using the program Turbo-FRODO (144). The accuracy of the model was assessed by calculating omit maps. Four hundred and four residues (Phe3-Gly406) and one PLP were assigned in the electron density maps. The amino acid sequence assigned on the electron density map completely agreed with that deduced from the nucleotide sequence, except for two N-terminal residues (Met1-Ile2) which are disordered.

There were several lumps of extra densities observed in the electron density map. The most conspicuous one is the extra density elongated beyond the Sγ atom of Cys364 (Fig. 27). The size of the density is much larger than that of a typical Cys side-chain. The -SH group of Cys364 is assumed to be modified by insertion of a single atom. Since the species of the atom is difficult to be identified at the moment, the modification of Cys364 was not made in the present model, but this density feature is worthy of later discussion. A density peak other than those of the enzyme was located among PLP and the side chains of Arg379 and Asn175. The peak was interpreted as an acetate, which was a component of the precipitant for crystallization, because the ellipsoidal

peak was surrounded by positively charged substituents. Another peak having a spherical shape was found on the molecular two-fold axis and coordinated by the pairs of the Asp96 Oδ2 (2.35 Å) and Glu250 Oε1 (2.36 Å) atoms. Although the peak might be a cationic ion or an water molecule, it was not modeled in the present structure.

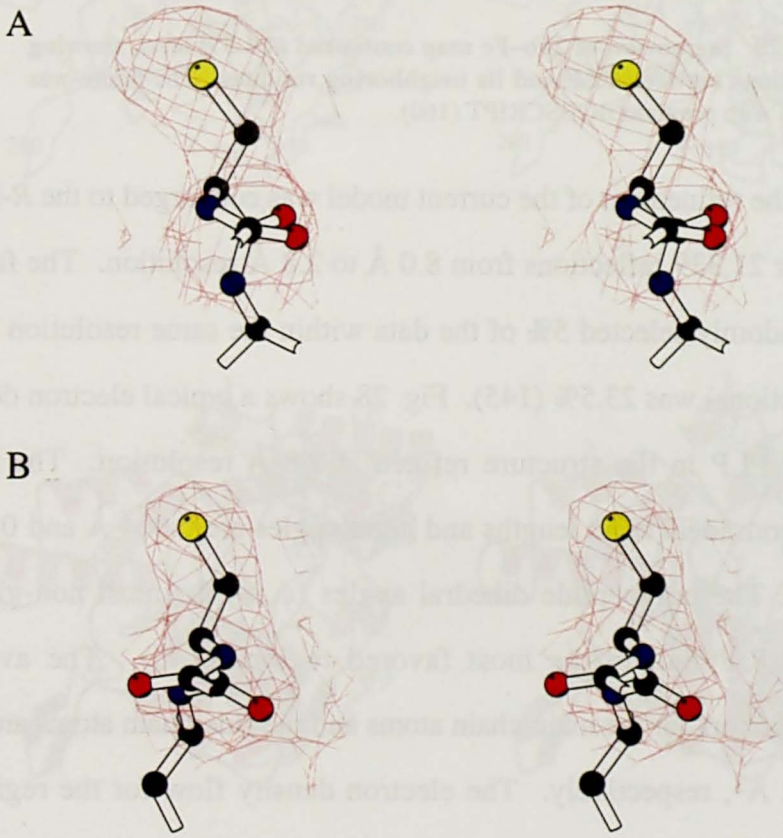

FIG. 27. **Stereoviews of the $2F_o$–F_c maps of Cys364 (A) and Cys378 (B) with their ball-and-stick models superimposed.** The maps are contoured at 1.0 σ level. The electron density peak of Cys364 is elongated beyond the tip of its side chain, compared with that of a typical cysteine Cys378. This elongation of the peak indicates that the side chain of Cys364 is apparently modified at the Sγ atom by a single atom. Both figures were produced with program BOBSCRIPT (160).

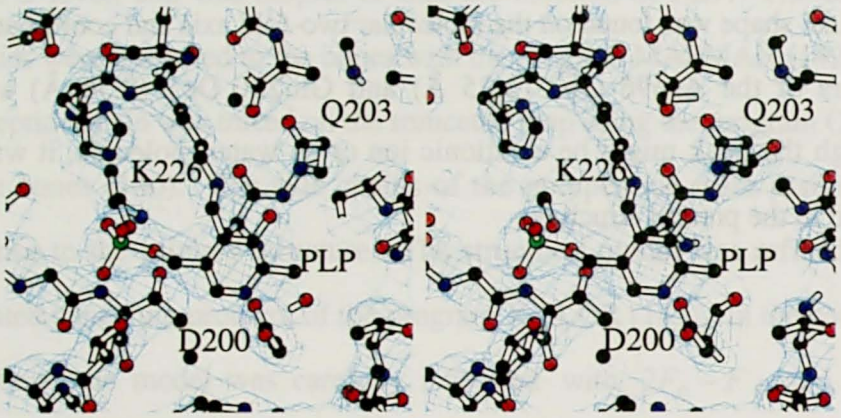

FIG. 28. **Stereoview of 2Fo–Fc map contoured at 1.5 σ level, showing interactions between PLP and its neighboring residues.** The figure was depicted with program BOBSCRIPT (160).

Finally, the refinement of the current model was converged to the *R*-factor of 18.6% for 21,339 reflections from 8.0 Å to 2.8 Å resolution. The free *R*-factor of randomly selected 5% of the data within the same resolution range (1,090 reflections) was 23.5% (145). Fig. 28 shows a typical electron density map around PLP in the structure refined at 2.8 Å resolution. The r.m.s. deviations from ideal bond lengths and bond angles are 0.004 Å and 0.876°, respectively. The polypeptide dihedral angles (ϕ, ψ) for most non-glycine residues (86.7%) fall in the most favored regions (146). The average temperature factors for the main-chain atoms and the side-chain atoms are 33.6 $Å^2$ and 38.2 $Å^2$, respectively. The electron density flow for the region of His55-Ile58 is relatively ambiguous; in particular, Arg56 and Ile58 were modeled as alanine. No water molecules that give significantly high electron density were found in the present analysis. The present structural model of the CsdB subunit is composed of a polypeptide chain of Phe3-Gly406, one PLP,

and one acetate.

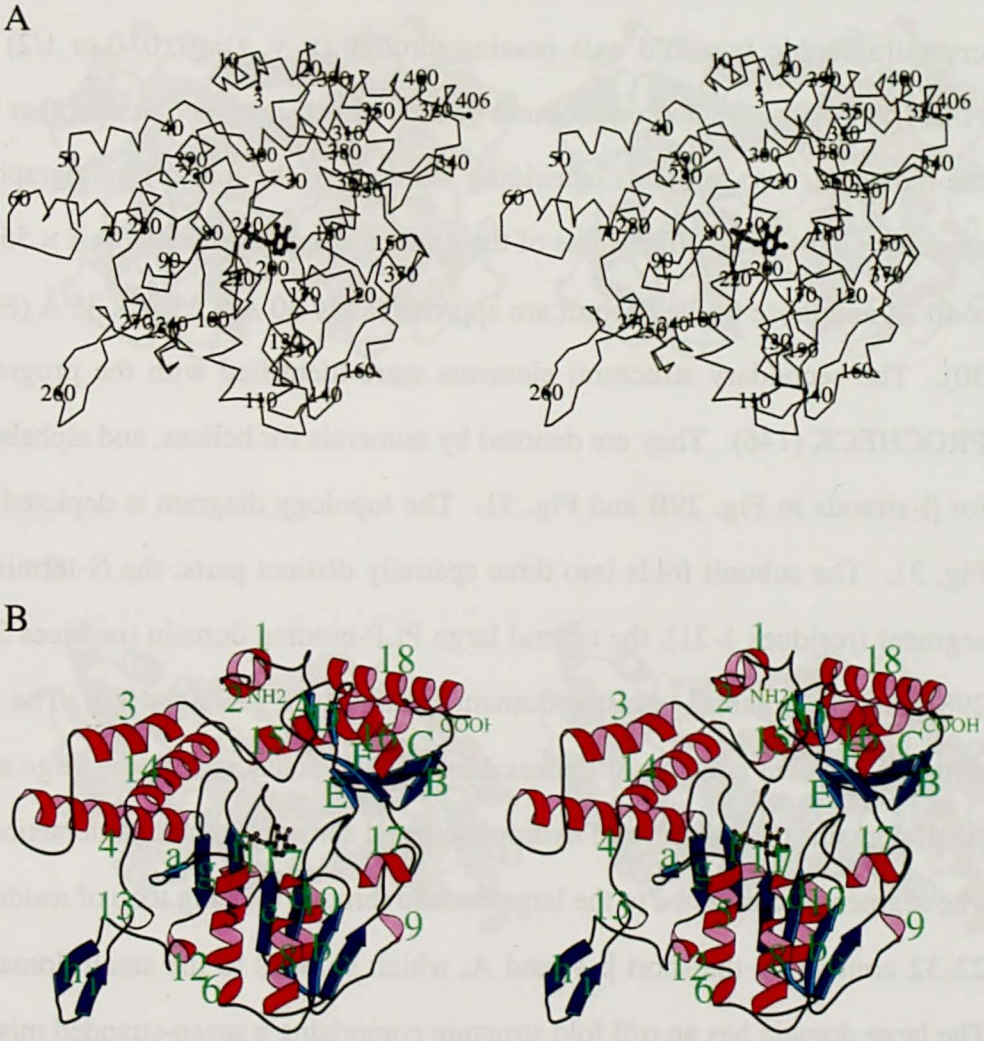

FIG. 29. **Stereoviews of α-carbon trace (A) and schematic drawing (B) of the CsdB subunit.** The current model comprises 404 residues of Phe3-Gly406 with omission of two N-terminal disordered residues. In Fig. (B), α- and 3_{10}-helices are represented by *spirals*, and β-strands by *arrows*. Both figures were drawn with program MOLSCRIPT (161).

RESULTS AND DISCUSSION

Overall Structure—The crystal structure of the CsdB subunit is represented in Fig. 29. The CsdB crystal contains four homodimer molecules in the unit cell. Each of the dimer molecules is positioned around the crystallographic two-fold axis passing through (x, y, z)=(0, 0, 0 or 1/2) or (1/2, 1/2, 1/4 or 3/4), and one subunit of each dimer is related to the other by the molecular two-fold axis coinciding with one of the four crystallographic symmetry axes. The dimensions of the dimer are approximately 80 Å × 55 Å × 40 Å, and those of the subunit are approximately 60 Å × 55 Å × 35 Å (Fig. 30). The secondary structural elements were identified with the program PROCHECK (146). They are denoted by numerals for helices, and alphabets for β-strands in Fig. 29B and Fig. 31. The topology diagram is depicted in Fig. 31. The subunit folds into three spatially distinct parts: the N-terminal segment (residues 1-21), the central large PLP-binding domain (residues 33-298), and the small C-terminal domain (residues 22-32, 299-406). The N-terminal segment consists of helices 1 and 2, and contacts with the large and small domains through several hydrophobic and some hydrophilic interactions. The segment is connected to the large domain through the long loop of residues 22-32 containing the short β-strand A, which belongs to the small domain. The large domain has an α/β fold structure comprising a seven-stranded mixed β-sheet (a, g, f, e, d, b, and c) flanked by seven α-helices (5-11), five additional α-helices (3, 4, and 12-14), and a small two-stranded antiparallel β-sheet (h and i). In the central β-sheet, the antiparallel β-sheet part (a, g, and f) and the parallel β-sheet part (f, e, d, b, and c) are mixed together, and each of

A

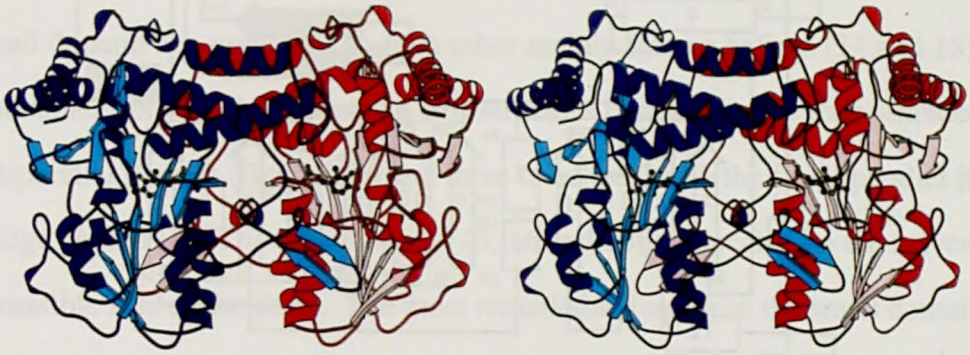

B

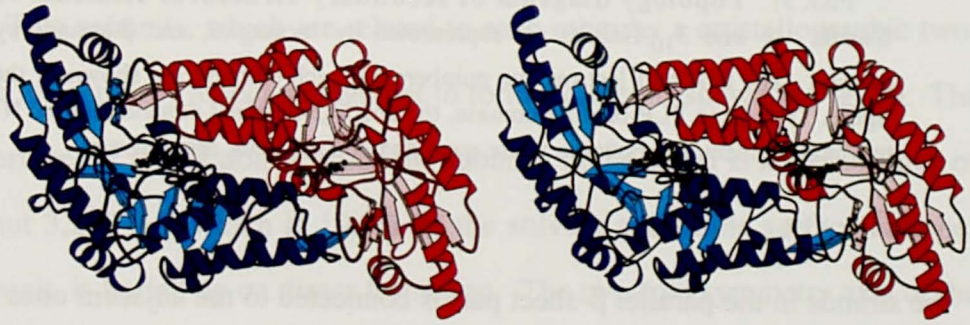

FIG. 30. **Stereoviews of the dimeric molecule of CsdB viewed perpendicular (A) and parallel (B) to the molecular two-fold axis.** The figures, showing a pair of subunits colored differently, were drawn with program MOLSCRIPT (161).

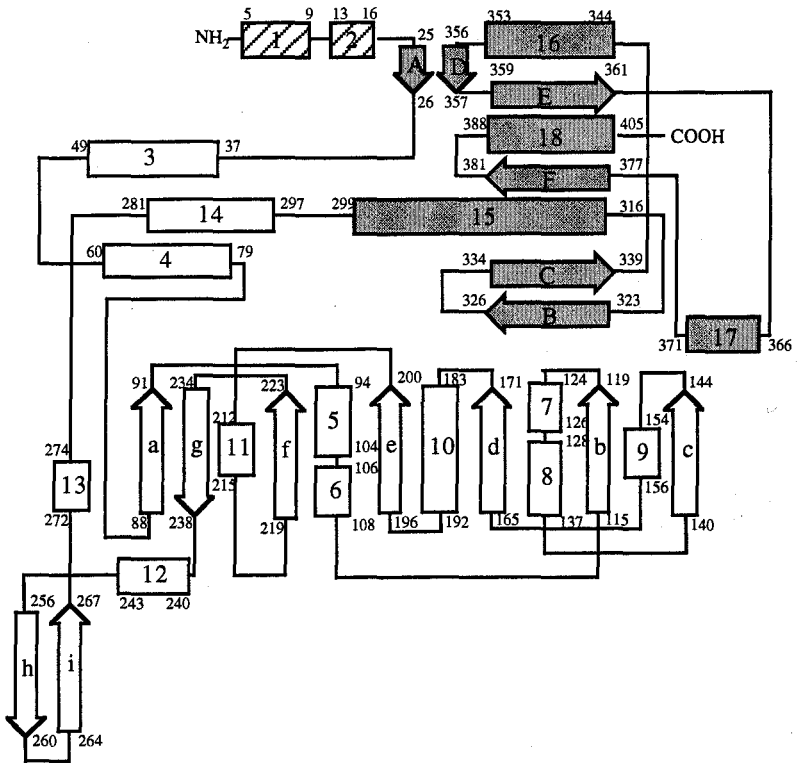

FIG. 31. **Topology diagram of secondary structural elements of CsdB.** α- and 3_{10}-Helices are represented by *rectangles*, and β-strands by *arrows*. The first and last residue numbers for each element are shown in the figure. The large PLP-binding domain, the small C-terminal domain and the N-terminal segment are shown in *white*, *gray* and *oblique* lines, respectively.

the strands in the parallel β-sheet part is connected to the adjacent ones by α-helices crossing the β-sheet in a right-handed manner. Helices 9, 10 and 11 are located on one side of the β-sheet to face the solvent area, and helices 5, 6, 7 and 8 lie in the interdomain interface on the opposite side. The short helices 7, 9 and 13 exhibit hydrogen bonding patterns typical of 3_{10}-helices. PLP is covalently attached to the side chain of Lys226 to make a Schiff base, and is settled near the N-terminus of helix 5 and the C-termini of strands e and f. The

most remarkable structural feature in the large domain lies in a protrusion of a β-hairpin loop containing the two-stranded antiparallel β-sheet (h and i). The loop plays an important role in formations of the dimer molecule and the intersubunit active site. The PLP-binding large domain and the C-terminal small domain are connected to each other mainly by two helices (14 and 15). The small domain also adopts an α/β structure containing the four-stranded antiparallel β-sheet (B, C, F, E) and three α-helices, with the small parallel β-bridge (A and D). The three helices (15, 16 and 18) are located on the solvent accessible side of the sheet. The most remarkable feature in the small domain lies in the extended lobe (residues 362-375) containing Cys364 and α-helix 17. The lobe extends from the small to large domains of the subunit, and plays an important role in forming the intersubunit active site by constituting one side of the entrance rim to the active site.

Two subunits, which are related to each other by a crystallographic two-fold axes, tightly associate together to form a dimer as shown in Fig. 30. The interface for interaction between the subunits in the dimer is large; the area of about 3,200 $Å^2$, which is 19.9% of the solvent accessible surface area per subunit, is buried up on dimer formation. The two-fold symmetry axis of the dimer molecule runs across the middle of helices 3 through the area surrounded by the N-termini of the helices 14 and PLP binding helices 5, and the C-termini of helices 8. Consequently, intimate association between two subunits in the dimer is established by intersubunit interactions in the active site through several hydrogen bonds and hydrophobic interactions. In the intersubunit interface, α-helix 17 in the lobe extending from the small to large domains of

one subunit interacts with the β-hairpin loop protruding from the large domain of the other subunit. These two portions, which are the extended lobe of one subunit and the protruded β-hairpin loop from the other subunit, form one side of a limb of the active site in the enzyme. Each of the active sites is formed by residues coming out from both subunits of the dimer. These intersubunit interactions to form the active sites in the dimeric molecule are remarkable structural features in CsdB.

Structural comparison with other PLP-dependent enzymes—PLP-dependent enzymes are grouped into seven fold types, and fold type I including NifS homologs is further divided into several subtypes, based on the homology of amino-acid sequence (79). NifS homologs including CsdB are classified into the so-called "aminotransferases class V of fold type I" family of PLP-dependent enzymes. The fold type I family of enzymes have two structural features as an identifiable signature within their sequences. First, the Schiff base lysine (Lys258 in aspartate aminotransferase (AAT) and Lys226 in CsdB) is closer to the C-terminus than the glycine-rich region (108-110 in AAT, 93-97 in CsdB), and directly follows a hydrophobic β-strand. Second, an invariant aspartic acid residue (Asp222 in AAT and Asp200 in CsdB), which binds the nitrogen atom of the pyridine ring, precedes the Schiff base lysine by 20-50 amino acid residues. The aminotransferases class V of fold type I includes NifS homologs, PSAT, serine-pyruvate aminotransferase, isopenicillin N epimerase and the small subunit of cyanobacterial soluble hydrogenase. A search for structural homologs of CsdB with the program DALI (147) identified three-dimensional structures of seven proteins belonging

to fold type I: PSAT (115), 2,2-dialkylglycine decarboxylase (148), tryptophanase (149), cystathionine β-lyase (CBL) (150), AAT (151) 1984; (152-154), glutamate semialdehyde aminotransferase (155), and ornithine decarboxylase (156), in the order of the score. Indeed, the Cα-trace of the subunit of CsdB is well superposed on those of AAT and PSAT (Fig. 32). The tertiary-structure comparison among seven structures identified above clearly shows that several helices flanking the central β-sheet of the large domain in PSAT and CsdB are shorter than those of the other enzymes. As observed in the structure of PSAT (115), two regular α-helices of the large domain in other PLP-dependent enzymes of fold type I are replaced with one-turn α- and 3_{10}-helices (11 and 9) in CsdB. Moreover, the small domain in both of the class V enzymes is compact in comparison with those of other enzymes in fold type I. These structural features are probably common to the class V family in fold type I of PLP-dependent enzymes. All of the secondary structural elements except those of helices 13 in CsdB are well superposed on the corresponding ones of PSAT.

The most remarkable structural feature in CsdB lies in the interaction mode between the extended lobe containing α-helix 17 in one subunit of the dimer and the β-hairpin loop, connecting strands h to i, which is protruded from the other subunit. The extended lobe exists between β-strands E and F in the small domain, and extends from the small to large domains in the same subunit. α-Helix 17 on the extended lobe in one subunit of the dimer interacts with the tip of the protruded hairpin loop from the other subunit through some hydrophobic interactions between Pro367 and Val259*. These structures

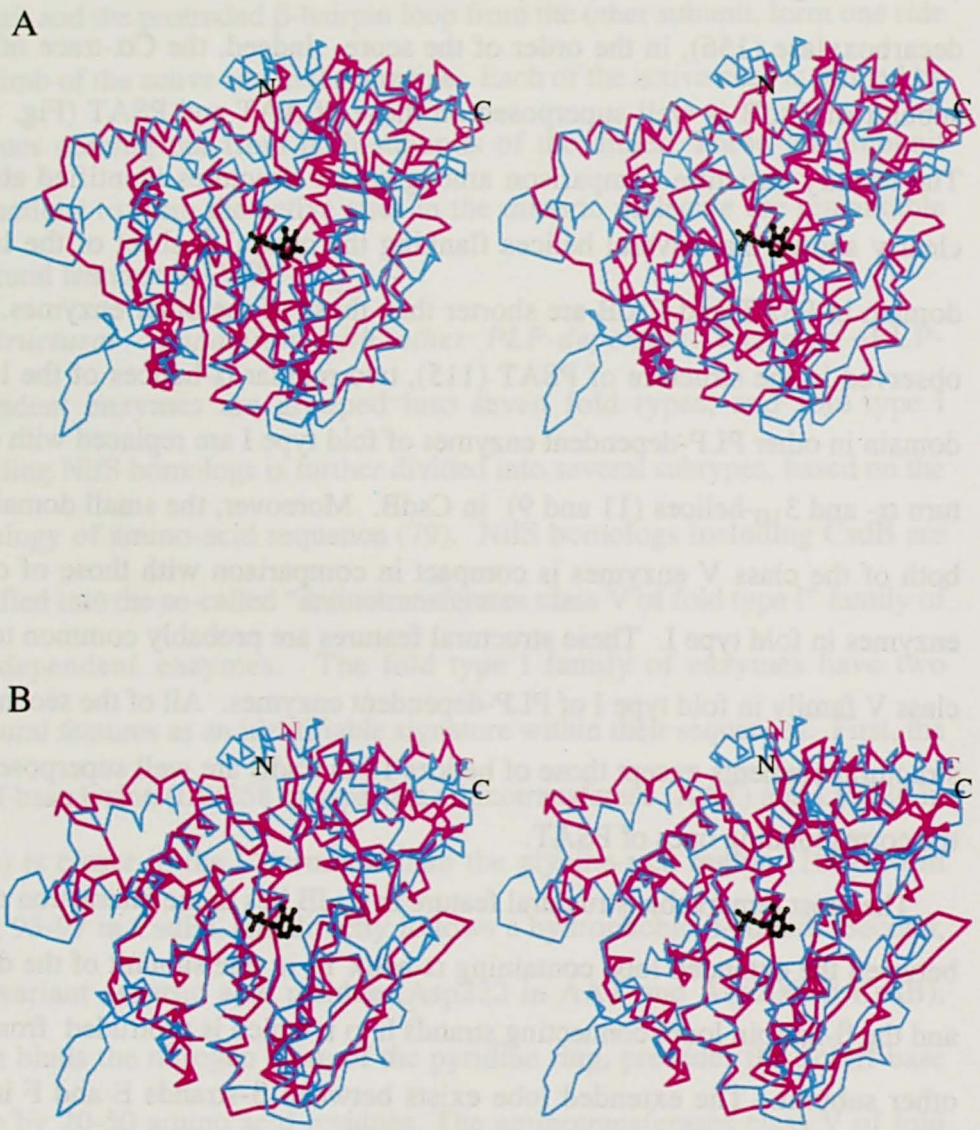

FIG. 32. **Stereoviews of superposition (A) between the Cα-traces of CsdB (cyan) and AAT (pink; PDB code 1ARS), and (B) between those of CsdB (cyan) and PSAT (pink; PDB code 1BJN).** The figures were generated using program MOLSCRIPT (161).

observed in CsdB, that is, the extension of a lobe containing α-helix from the small to large domains in the same subunit and the protrusion of a β-hairpin loop to the other subunit, are found neither in other PLP-dependent enzymes in fold type I nor in PSAT belonging to the same class. In PSAT, the β-hairpin loop in CsdB is replaced with an α-helix (residues 228-233) at the region corresponding to the bottom of the hairpin loop, and a short loop is protruded from β-strands E to F in the small domain. The short loop does not contain an α-helix and is shorter than the protrusion of CsdB by 13 residues. Thus the interaction mode observed in CsdB is not found in the other PLP-dependent enzymes.

Active-site Structure—The CsdB dimer has two active sites, which exist separately in two equivalent clefts formed at the interface of two subunits in the dimer. The PLP molecule settles at the bottom of the active site cleft, and the substrate must approach the PLP site through the cleft. Fig. 33 shows the active sites of CsdB, AAT, and PSAT. The circumstances of active site in these enzymes are similar to one another. As found in fold type I of PLP-dependent enzymes, PLP has the C4' atom connected with the Nζ atom of Lys226 making the Schiff base to form an internal aldimine. The O3' atom of PLP is hydrogen-bonded with the Nζ atom of Lys226, and probably with the Nε2 atom of Gln203. The pyridine nitrogen atom, N1, of PLP forms a hydrogen bond with Asp200. Asp200 in CsdB corresponds to Asp222 in AAT, which stabilizes the protonated N1 of PLP to strengthen the electron-withdrawing capacity of the coenzyme (157). Asp200, Gln203 and Lys226, which are supposed to affect the electron distribution on PLP, interact with

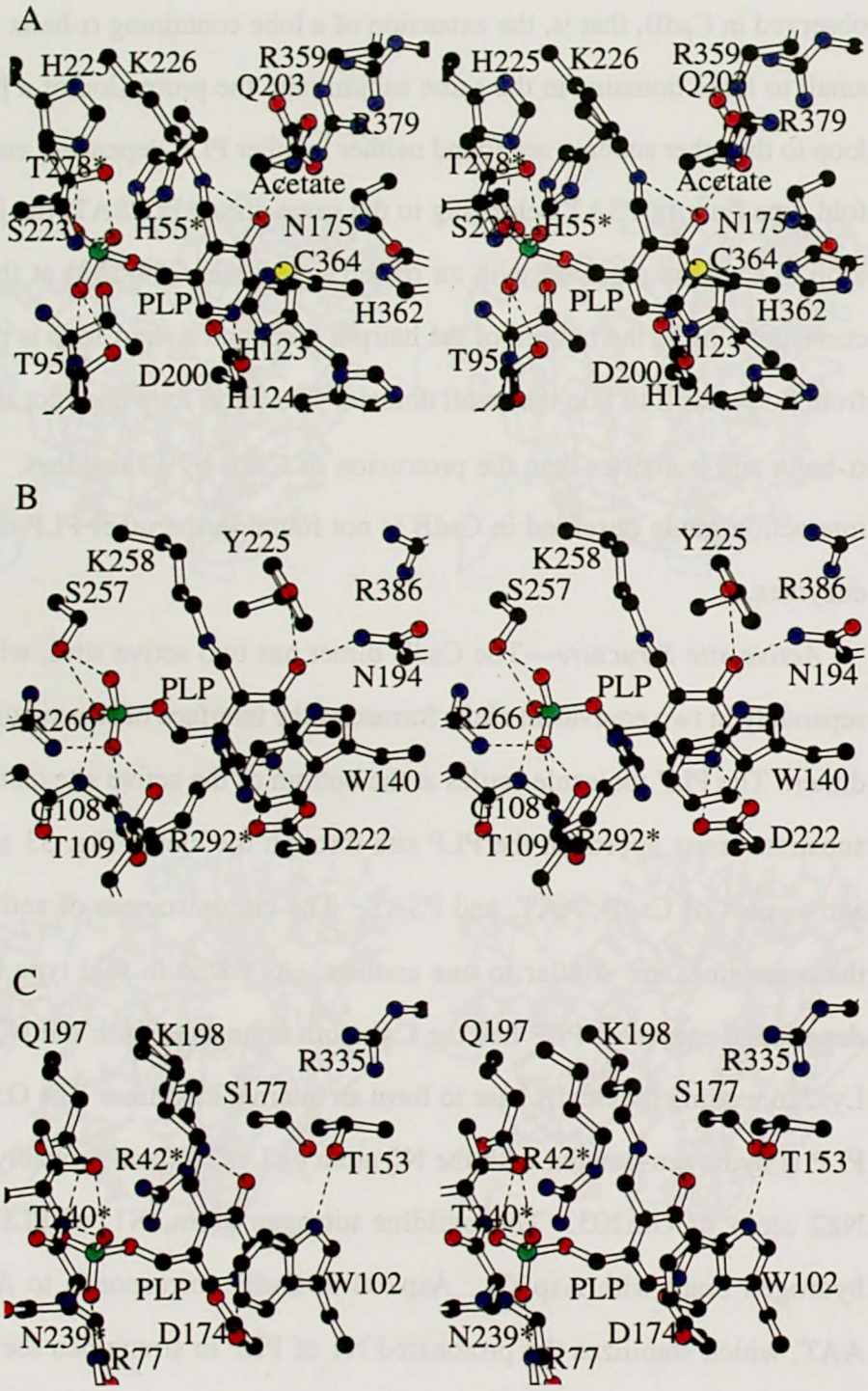

FIG. 33. **Active sites of CsdB (A), AAT (B) and PSAT (C).** The hydrogen-bond network is shown in *broken lines*. Water molecules in the active sites are not shown for clarity. The figures were generated using program MOLSCRIPT (161).

PLP in a manner similar to that observed in AAT. The OP2 and OP3 atoms of PLP are hydrogen-bonded with the side-chain Oγ and main-chain N atoms of Thr95 and the side-chain Oγ atom of Ser223 and the side-chain Nε2 atom of His225, while the OP1 atom of PLP makes a hydrogen-bond with the side-chain Oγ and main-chain N atoms of Thr278* from the other subunit. The residue recognizing the carboxylate group at Cα of the substrate is Arg386 in AAT. Arg379 in CsdB is spatially well superposed on Arg386 in AAT, and hydrogen-bonded with the carboxyl oxygen of the acetate ion found in the present crystal. The side chain of Asn175 is also hydrogen-bonded with the carboxyl group of the acetate ion. Thus, Asn175 and Arg379 in CsdB probably serve as the recognition residues for the α-carboxyl group of the substrate.

Although AAT, PSAT, and CsdB are similar to one another in the overall folding of protein and most of the interactions between protein residues and PLP, there are some significant differences observed among these enzymes. The most striking difference in the interactions between the protein and PLP lies in the stacking mode of the aromatic residue and the pyridine ring of PLP. In CsdB, the imidazole ring of His123 is stacked against the pyridine ring of PLP. The stacking residues in many PLP-dependent enzymes are aromatic residues such as Trp in AAT and PSAT, Tyr in cystathionine β-lyase from *E. coli* (150), and Phe in tyrosine phenol-lyase from *Citrobacter freundii* (158). Stacking of the histidine residue against the B-face of the pyridine ring in PLP, as observed in CsdB, has been reported only in the crystal structures of ornithine decarboxylase from *Lactobacillus* 30a (156) and serine

hydroxymethyltransferase from human cytosol (159).

Possible Modification of Cys364—A noticeable structural feature in the active site of CsdB is a possible modification of the side chain of Cys364, which is located near the pyridine ring of PLP and the His123 residue stacking against the ring (Fig. 33 A). This cysteine residue corresponds to Cys325 in NifS of *Azotobacter vinelandii*, which is necessary for the activity of the enzyme (73). Interestingly, the size of electron density for the side chain of Cys364 is larger than those of the other cysteine residues included in the CsdB molecule (Fig. 27). The size of the corresponding peak in electron density maps suggests the modification of the Cys364 side-chain by a single atom. Because the structure has been analyzed at a medium resolution of 2.8 Å, it is very difficult to determine the kind of atom for this modification. In addition, the occurrence may be an artifact in the purification and crystallization processes. However, there is a report on the formation of persulfide on the catalytic cysteine residue in NifS (73). Therefore, it is possible that Cys364 of CsdB was modified to -SSH or -SSeH after the catalytic reaction, although the size of the density peak at the modification site is smaller than those expected for ordered persulfide/selenosulfide with full occupancy. Cys364 may be modified to the -SSH or -SSeH form with high mobility and/or low occupancy.

Structural Comparison with Other NifS homologs—NifS homologs are classified into two groups, I and II, on the basis of their sequence similarity (Chapter II, 107). NifS from *A. vinelandii* and IscS are included in group I, and CSD and CsdB in group II. CsdB well resembles CSD in the amino-acid

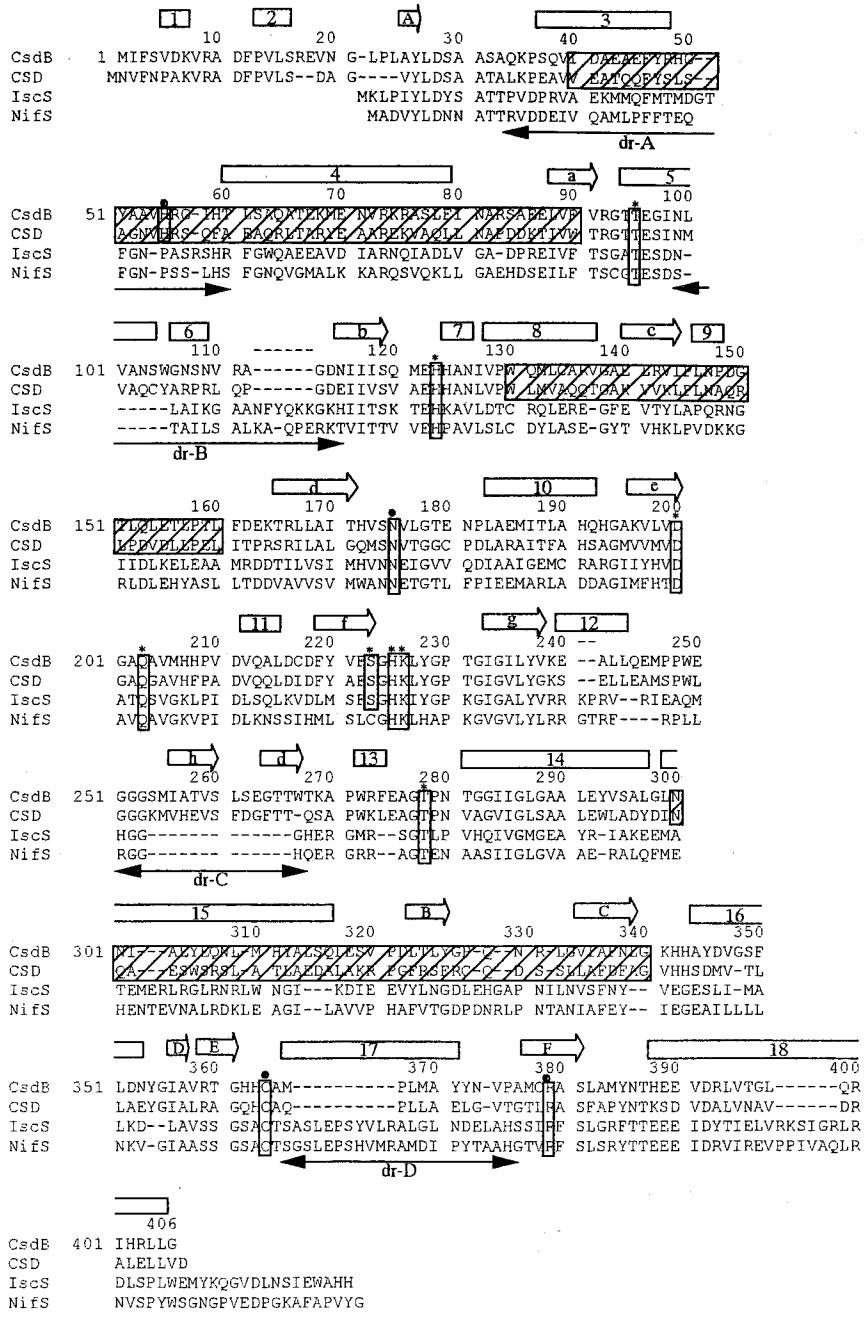

FIG. 34. **Sequence alignment of several NifS-family proteins.** *NifS* is the product of *nifS* gene of *A. vinelandii*. The numbering of the sequences is based on that of CsdB. The secondary structure elements of CsdB are denoted by *rectangles* with numerals for α- and 310-helices and *arrows* with alphabets for β-strands. The amino acids in squares capped with * or $ interact with PLP or possibly with the substrate, respectively. The *lines with arrows* denote the regions (*dr-A*, *dr-B*, *dr-C* and *dr-D*) whose sequences are different between groups I and II. The regions where the marked differences between CsdB and CSD exist are indicated by *boxes with oblique lines*.

sequence (44% identical). The important residues in CsdB for interacting with PLP and participating in the catalytic reaction are completely conserved in CSD (Fig. 34). The marked differences between the sequences of CsdB and CSD lie in the regions of residues 40-90, 130-160, and 300-340 of CsdB, which are expected to have different conformations between the two enzymes. His55 of CsdB and His51 of CSD located in the region of residues 40-90 may cause differences in catalytic specificity between CsdB and CSD.

The CsdB structure in Fig. 35 shows the regions (A-D) markedly different in sequence between group I (NifS and IscS) and group II (CSD and CsdB) of NifS homologs. It should be noted that most of the regions (regions A, C, and D in Fig. 34 and 9) are distributed in or around the active site. It is plausible that differences in substrate specificity among these enzymes are attributed to structural differences in these regions. The β-hairpin loop of residues 256-268 (region C), which contains strands h and i and makes up one side of the active site in CsdB, is deleted in IscS and NifS, and 10 residues are inserted in IscS and NifS between the residues corresponding to Met366 and Pro367 of CsdB on α-helix 17 (residues 366-371) (region D). The latter region just follows the putative catalytic residue, Cys364. Therefore, the extended lobe anchoring the catalytic cysteine residue seems to be much larger in IscS and NifS than in CsdB, and the catalytic cysteine residue of CsdB is probably located differently from those of IscS and NifS. The low activity of CsdB against L-cysteine may be caused by longer distance between the γ-atom of the substrate and the possible catalytic residue, Cys364, than that in CSD and IscS. The lobe extending from the small to large domains of the subunit and containing the

putative catalytic cysteine residue is the most remarkable structural feature common to the NifS homologs. This structure is not found in other "fold type I" PLP-dependent enzymes. It is probably a prerequisite for the proteins to function as SCL and cysteine desulfurase. Structural analysis of other NifS homologs including IscS and CSD will clarify the relationship between the molecular structure and the catalytic properties of NifS homologs.

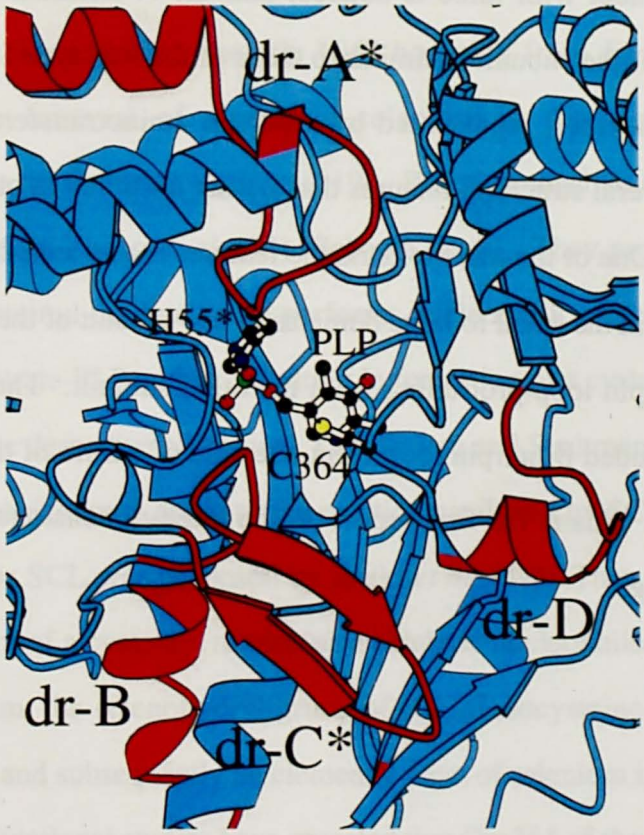

FIG. 35. **Schematic representation of CsdB showing sequence differences between CsdB and NifS.** The regions showing differences between CsdB and NifS denoted in Fig. 34, are colored *red* and labeled "*dr-B*" for residues 99-115 and "*dr-D*" for residues 366-376 in one subunit, and "*dr-A**" for residues 34-60 and "*dr-C**" for residues 251-268 from the other subunit. PLP, Cys364 and His55* are depicted as ball-and-stick models. Helices and β-strands are represented by *spirals* and *arrows*, respectively. The figure was drawn with program MOLSCRIPT (161).

SUMMARY

The crystal structure of *Escherichia coli* CsdB, a NifS homolog with a high specificity for L-selenocysteine, has been determined by X-ray crystallographic method of multiple isomorphous replacement. The structure was refined to an *R*-factor of 18.6% at 2.8 Å resolution. The subunit structure consists of three parts: the large domain of an α/β fold containing a seven-stranded β-sheet flanked by helices, the small domain containing a four-stranded β-sheet with three α-helices, and the N-terminal segment. The overall fold of the subunit is similar to those of the fold type I family of PLP-dependent enzymes, represented by aspartate aminotransferase. However, CsdB has several structural features that are not observed in other enzymes of this family. One of the most remarkable features is that an α-helix in the lobe extending from the small to large domains in one subunit of the dimer interacts with a β-hairpin loop protruding from the other subunit. The extended lobe and the protruded β-hairpin loop form one side of a limb of the active site in the enzyme. This is the first report on the three-dimensional structure of a NifS homolog.

CHAPTER VI

X-Ray Structure of CsdB, Selenocysteine Lyase from *Escherichia coli*, Complexed with Aspartate and Substrate Analogs and Implications for the Roles of the Active-Site His55 and Cys364

INTRODUCTION

CsdB, a selenocysteine specific NifS homolog from *Escherichia coli*, catalyzes the removal of elemental selenium at the γ position of L-selenocysteine to produce L-alanine (119). Reaction mechanism of NifS has been proposed by Zheng *et al.* (73) (Scheme III A). They proposed that the active site cysteinyl thiolate anion performs nucleophilic attack on the sulfur atom of a substrate-PLP adduct, resulting in formation of a cysteinyl persulfide and an enamine derivative of alanine. Lacourciere and Stadtman (52) described that this mechanism may apply to the reaction catalyzed by SCL. Alternative mechanism for SCL was proposed by Esaki *et al.* (42). They do not assume an involvement of a cysteinyl residue as a catalytic nucleophile. According to this mechanism, the selenohydryl group of the selenocysteine-PLP adduct is deprotonated, and subsequently an elemental form of selenium is released from the adduct. Mutational studies have revealed that Cys364 of the enzyme acts as a catalytically essential residue for the desulfurization of L-cysteine, which is consistent with the former mechanism, but it is not necessary for L-selenocysteine decomposition, which is consistent with the latter mechanism

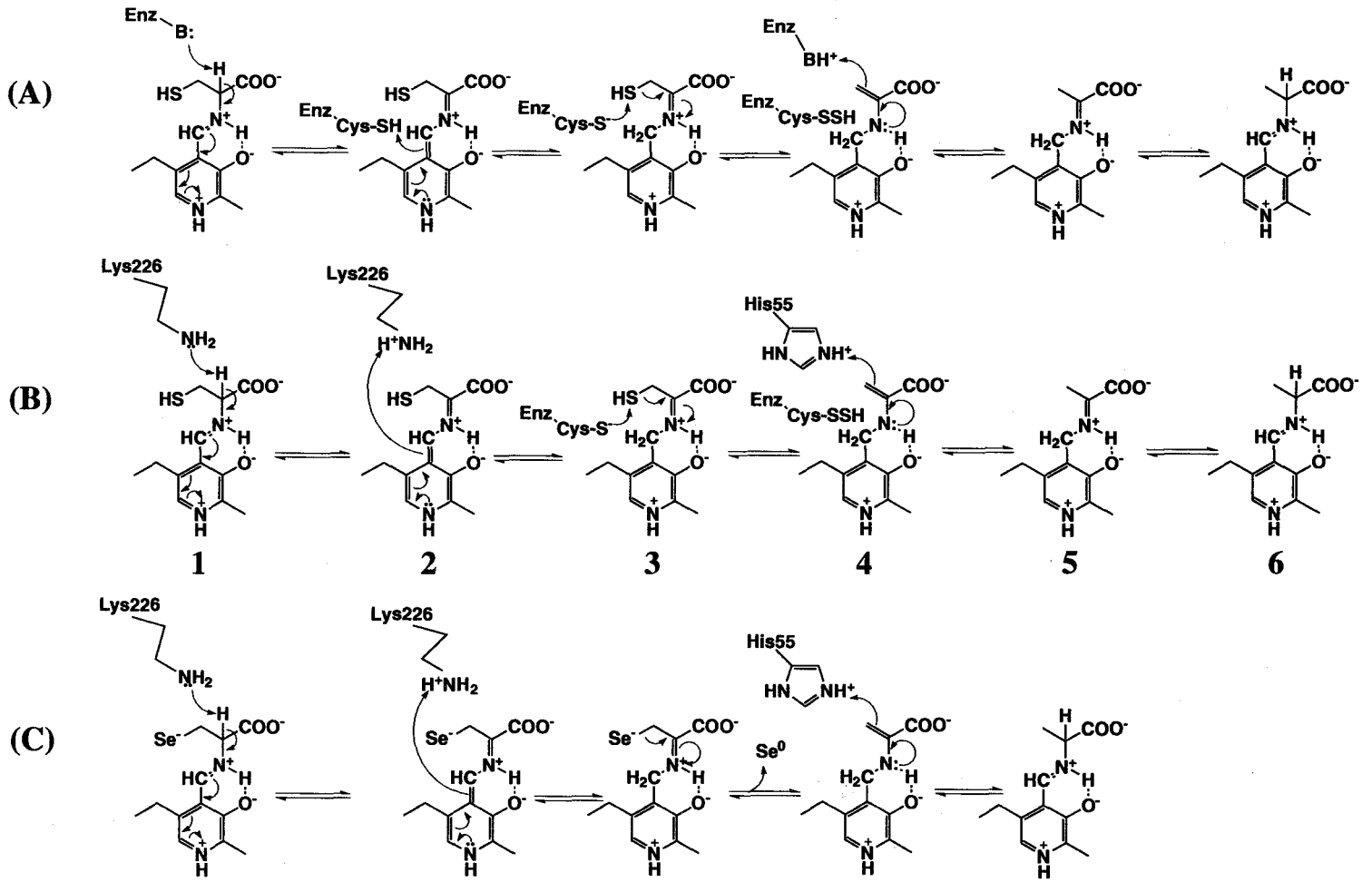

SCHEME III. (A), Proposed reaction mechanism of *A. vinelandii* NifS adapted from Ref. 73; (B), Proposed mechanism of the cysteine desulfurase reaction catalyzed by CsdB; (C), Proposed mechanism of the selenocysteine lyase reaction catalyzed by CsdB.

(Chapter IV).

In order to clarify the reaction mechanism of CsdB at the atomic level, I have prepared crystals of CsdB complexed with L-aspartate (ASP), L-cysteine sulfinate (CSA), L-propargylglycine (PG), and L-β-chloroalanine (CA). The crystal structures of these complexes were determined by X-ray crystallographic method. This is the first experimentally determined structure of CsdB with PLP-substrate external aldimine complex. The role of residues around the active site of CsdB is discussed on the basis of the external aldimine structure and of the mutagenesis study presented in Chapter IV.

EXPERIMENTAL PROCEDURES

Preparation of CsdB—CsdB was overproduced in recombinant *E. coli* JM109 cells and purified as described in Chapter III.

Crystal Preparation and Soaking Conditions —Crystals of CsdB were grown at 25 °C by the hanging drop vapor diffusion method. Each droplet was prepared by mixing 5 μl of 20 mg/ml enzyme in 10 mM KPB (pH 7.4) with an equal volume of 100 mM KPB (pH 6.8) containing 1.4 M sodium acetate.

The crystals were soaked at 25 °C in reservoir solutions containing one of the substrates or substrate analogs: the composition of the reservoir solutions are listed in Table XIV. The unit cell dimensions of all the complexed crystals are shown in Table XV.

Data collection and Processing—Diffraction data for the complex crystals were collected at 20 °C with a Rigaku R-AXIS IIc imaging plate detector

system using graphite-monochromated CuK_α radiation produced by a Rigaku RU-300 rotating anode X-ray generator operated at 40 kV and 100 mA. The data collection for each of the four kinds of crystals was performed with one crystal sealed in a glass capillary. The crystal-to-detector distance was set to 130.0 mm. Each frame of 1.5° crystal oscillation was collected for 15 min.

TABLE XIV
Composition of reservoir solution for soaking experiment

Ligand	Composition
L-Aspartate (ASP)	2.0 M L-aspartate, 2.0 M pyruvate, 0.1 M KPB (pH 6.8)
L-Cysteine sulfinate (CSA)	0.5 M L-cysteine sulfinate, 2.0 M pyruvate, 0.1 M KPB (pH 6.8)
L-Propargylglycine (PG)	0.8 M L-propargylglycine, 2.0 M pyruvate, 0.1 M KPB (pH 6.8)
L-β-Chloroalanine (CA)	0.4 M L-β-chloroalanine, 0.56 M sodium acetate, 0.1 M KPB (pH 6.8)

Data processing was accomplished at 2.8 Å resolution with the R-AXIS IIc data processing software package. All the frames of diffraction data were merged for every data set and scaled together. Data collection and processing are summarized in Table XV.

Structure Determination and Refinement—The subunit structure of each ligand-complexed CsdB was analyzed using the structure of the subunit of native CsdB containing Phe3-Gly406 out of 406 residues, which has been previously reported at 2.8 Å resolution to a *R*-factor of 18.6% (Chapter V). Each subunit of the Asp-CsdB, CSA-CsdB, PG-CsdB, and CA-CsdB complex molecules was positioned by means of a rigid-body refinement using

the structure of native CsdB as a starting model. The further refinement of the models was carried out with the simulated annealing protocol of X-PLOR, followed by the positional and individual temperature factor refinements. The regions where conformational changes occur were checked on the basis of the 2Fo-Fc and Fo–Fc difference electron density maps and rebuilt manually with the program Turbo-FRODO. In the initial stage of refinement, the structures of the protein regions were refined in all of the complexes. Then the model of PLP was added to the protein structure. In the final stage of refinement, the model of ligand moiety was added to the protein-PLP structure of the complexes based on the 2Fo-Fc omit map. In the map, the electron density corresponding to a substrate or its analog moiety was connected to that of PLP in each complex. Each of the complexed structures was further refined to the convergence. The refinement statistics are summarized in Table XVI.

TABLE XV
Summary of data collection statistics

	ASP-CsdB	CSA-CsdB	PG-CsdB	CA-CsdB
Soaking time (days)	2	5	1	1
Cell parameters				
a (Å)	128.3	128.1	128.5	128.4
b (Å)	128.3	128.1	128.5	128.4
c (Å)	136.6	137.1	136.8	137.0
Data statistics				
Resolution (Å)	2.8	2.8	2.8	2.8
Number of reflections				
observed	61964	89337	65095	62359
unique	25800	26842	25650	26631
Completeness (%)	90.0	93.3	89.0	92.2
R_{merge} (%)[a]	12.75	9.91	9.63	9.47

[a] $R_{merge} = \Sigma_i|I_i - <I_i>|/\Sigma_i I_i$, where $<I_i>$ is the average of I_i over all symmetry equivalents.

RESULTS AND DISCUSSION

Structural Features of the CsdB-Ligand Complexes—Using the high concentration of L-aspartate, L-cysteine sulfinate, L-propargylglycine, and L-β-chloroalanine, the ligand-CsdB complex structures were obtained. The structure of each complex is composed of a polypeptide chain of Phe3-Gly406 and one ligand-PLP moiety. The N-terminal two residues are invisible on the density maps as is the case with that of the native CsdB (Chapter V).

The structures around the active site in the ASP-, CSA-, CA-, and PG-CsdB complexes are shown in Fig. 36. The appropriate omit-maps of all the complex structures show that a substrate moiety is connected to C4' atom of the PLP moiety most probably through the Schiff base linkage to form an external aldimine (Fig. 36). In the case of Asp-, CSA- and CA-CsdB complexes, the electron density of Lys226 is also weakly connected to that of the ligand-PLP complexes. These situations suggest the possibilities that a part of Lys226 remains connected with PLP via Schiff base, or the complex structure presents a diamine intermediate in the transaldimination step of the reaction. I made a model of the ligand-PLP complexes as in a form of PLP-amino acid aldimine since the diamine intermediate is generally very unstable and difficult to be trapped. On the other hand, the electron density of Lys226 is completely separated from that of PG-PLP in the PG-CsdB complex structure. In CA-CsdB complex structure, the electron density of the β-chloride group of the β-chloroalanine moiety is relatively ambiguous and only the alanine moiety was clearly observed in the electron density map.

The most striking structural feature of the ligand-CsdB complexes lies in

the location of a putative catalytic residue; the side chain of Cys364 existing on the extended lobe of one subunit is located close enough to interact with the γ-atom of the substrates and the analogs in the active site. His55 from the other subunit is positioned so as to interact with the γ- or β-atom of the substrates/analogs, implying that it may play a role in the catalytic reaction.

Fig. 37 shows the interactions around the external aldimines in the active site of CsdB in the four structures. The binding modes of PLP are almost identical to one another, but there are some differences in the binding modes of the side chains of the substrate and analog moieties. In CsdB-ASP and CsdB-CSA complexes, the α-carboxyl group is hydrogen-bonded with only Nη2 atom of Arg379. On the other hand, the α-carboxyl group is hydrogen-bonded with Nη2 atom of Arg379 and Nδ atom of Asn175 in the structure of PG-CsdB and CA-CsdB. There are also differences in the interaction between the enzyme and the side chain of the substrates and analogs. In ASP-CsdB structure, the distances from Nδ1 and Nε2 atoms of His55* to the oxygen atoms of the distal carboxyl group of ASP are 3-5 Å, but their geometry is not favorable for hydrogen bonding. The sulfinate group in the CSA-CsdB complex is hydrogen-bonded with the δ-guanido group of Arg359 and the hydroxyl group of Thr278 with a distance of 2.6 Å and 2.7 Å, respectively. The conformations of the Arg359 residues are remarkably different from one another among the four structures.

Comparison of the Native and Complex Structures—Conformational differences between the four ligand-CsdB complexes and the native structure were assessed by comparing each complex structure with the 2.8 Å-refined

(A)

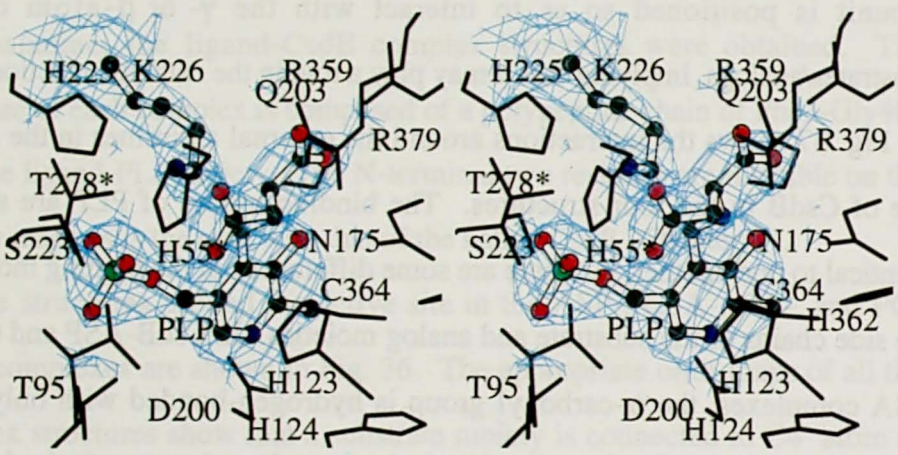
H225
K226
R359
Q203
R379
T278*
S223
H55*
N175
C364
PLP
T95
H123
D200
H124
H225
K226
R359
Q203
R379
T278*
S223
H55*
N175
C364
H362
PLP
T95
H123
D200
H124

(B)

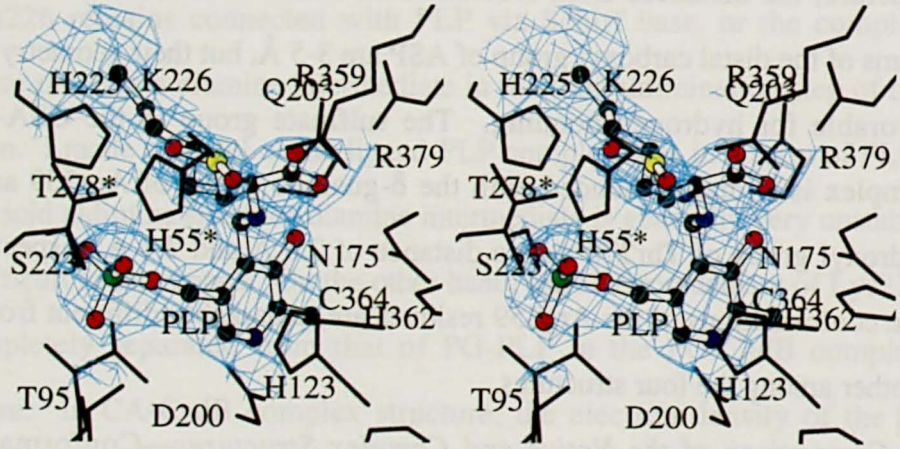
H225
K226
R359
Q203
R379
T278*
H55*
S223
N175
C364
H362
PLP
T95
H123
D200
H225
K226
R359
Q203
R379
T278*
H55*
S223
N175
C364
H362
PLP
T95
H123
D200

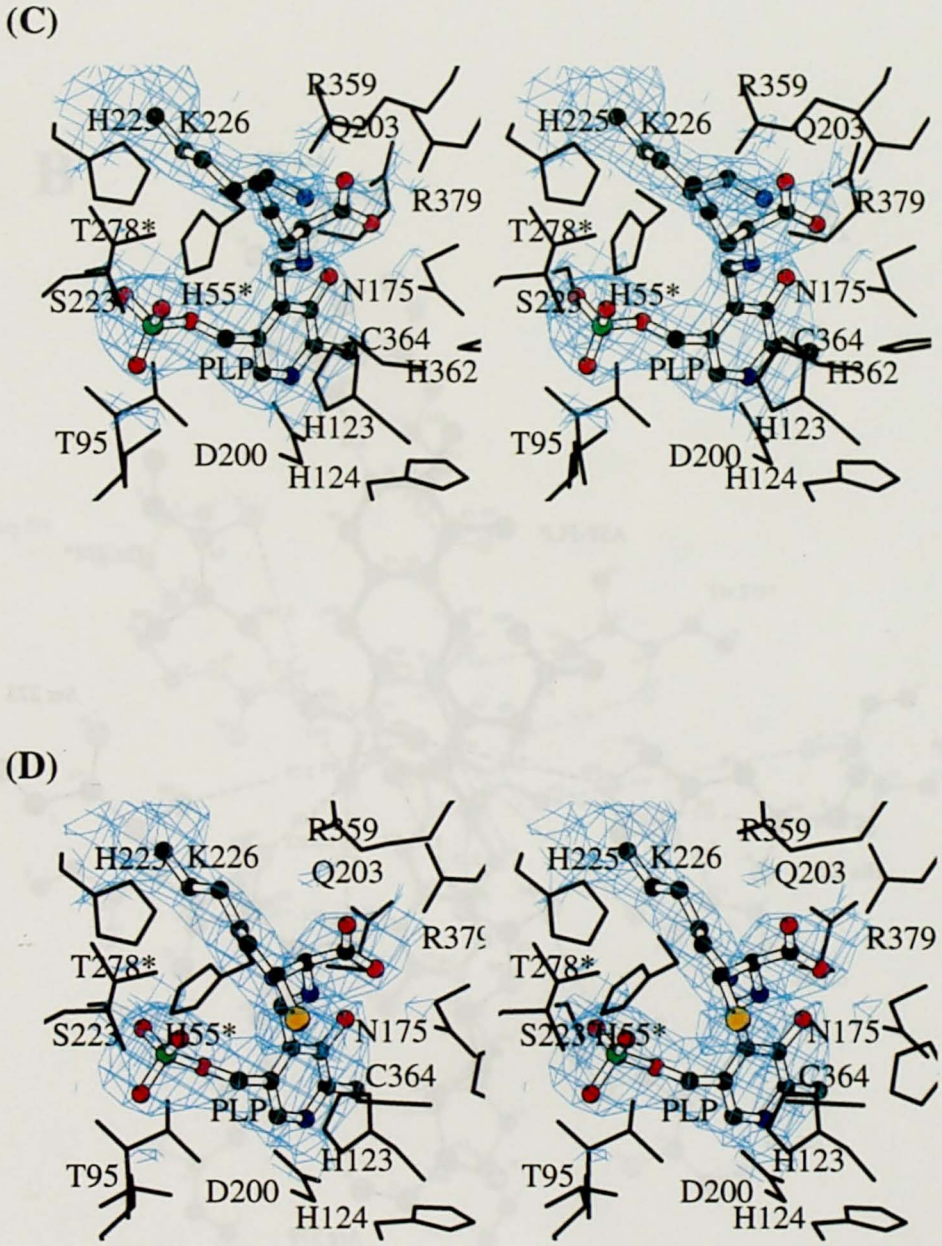

FIG. 36. **Stereoviews of the 2Fo–Fc maps overlaid on the final models of the active sites in the structures of the ASP-CsdB (A), CSA-CsdB (B), PG-CsdB (C), and CA-CsdB (D) complexes.** The electron density peaks of only Lys226 and the amino acid-PLP external aldimine are shown. The maps are contoured at 1.0 s level. The figures were produced with program BOBSCRIPT (160).

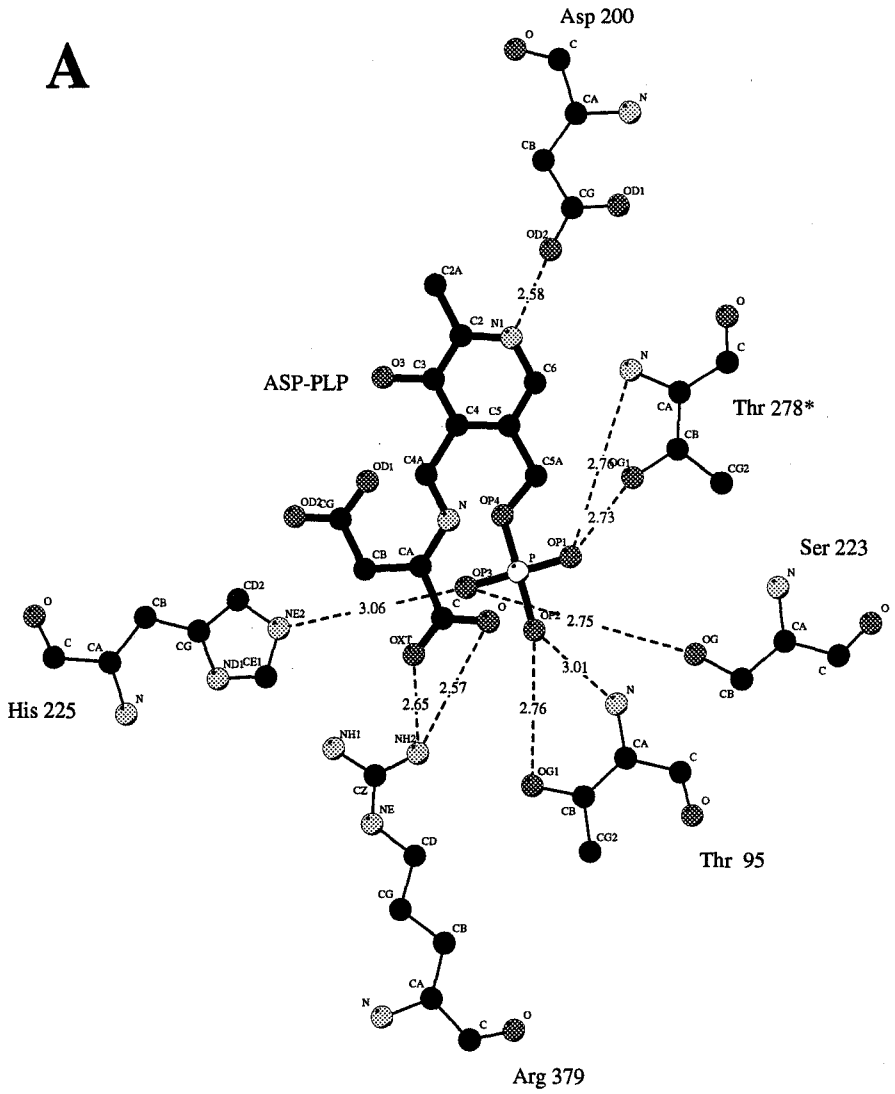
A
Asp 200
ASP-PLP
Thr 278*
Ser 223
His 225
Thr 95
Arg 379
2.58
2.76
2.73
3.06
2.75
3.01
2.65
2.57
2.76

B

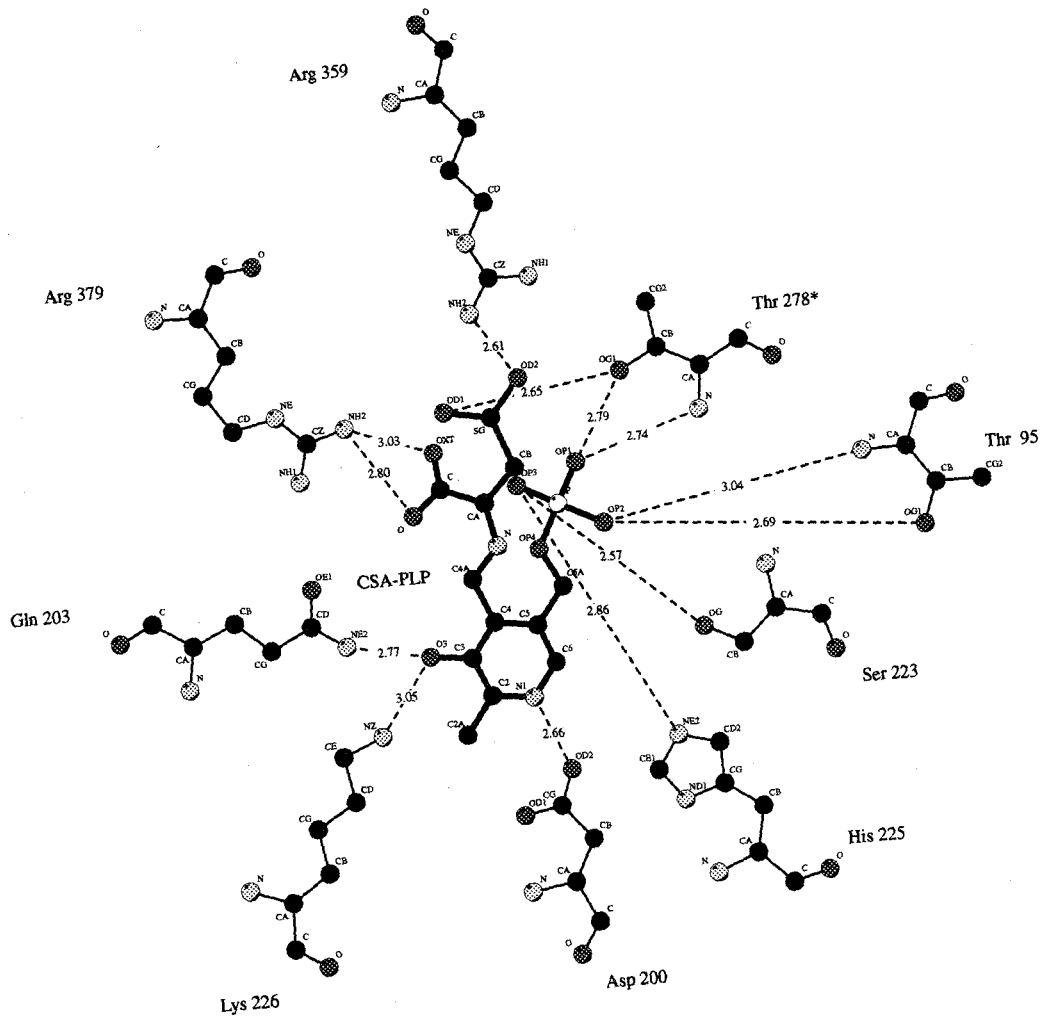
Arg 359
Arg 379
Thr 278*
Thr 95
CSA-PLP
Gln 203
Ser 223
His 225
Asp 200
Lys 226
2.61
2.65
2.79
2.74
3.03
2.80
3.04
2.69
2.57
2.86
2.77
3.05
2.66

C

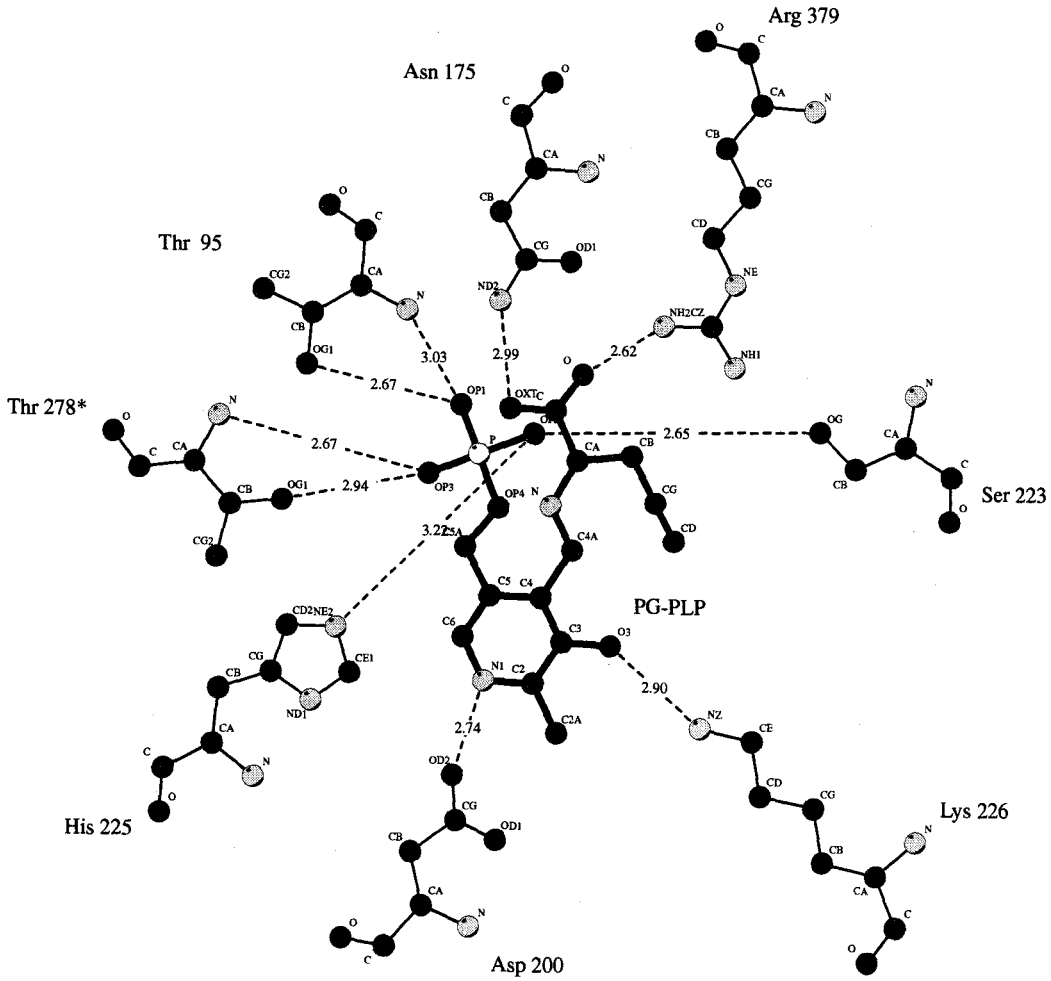
Arg 379
Asn 175
Thr 95
Thr 278*
Ser 223
PG-PLP
His 225
Lys 226
Asp 200
2.67
3.03
2.99
2.62
2.65
2.94
3.22
2.90
2.74

D

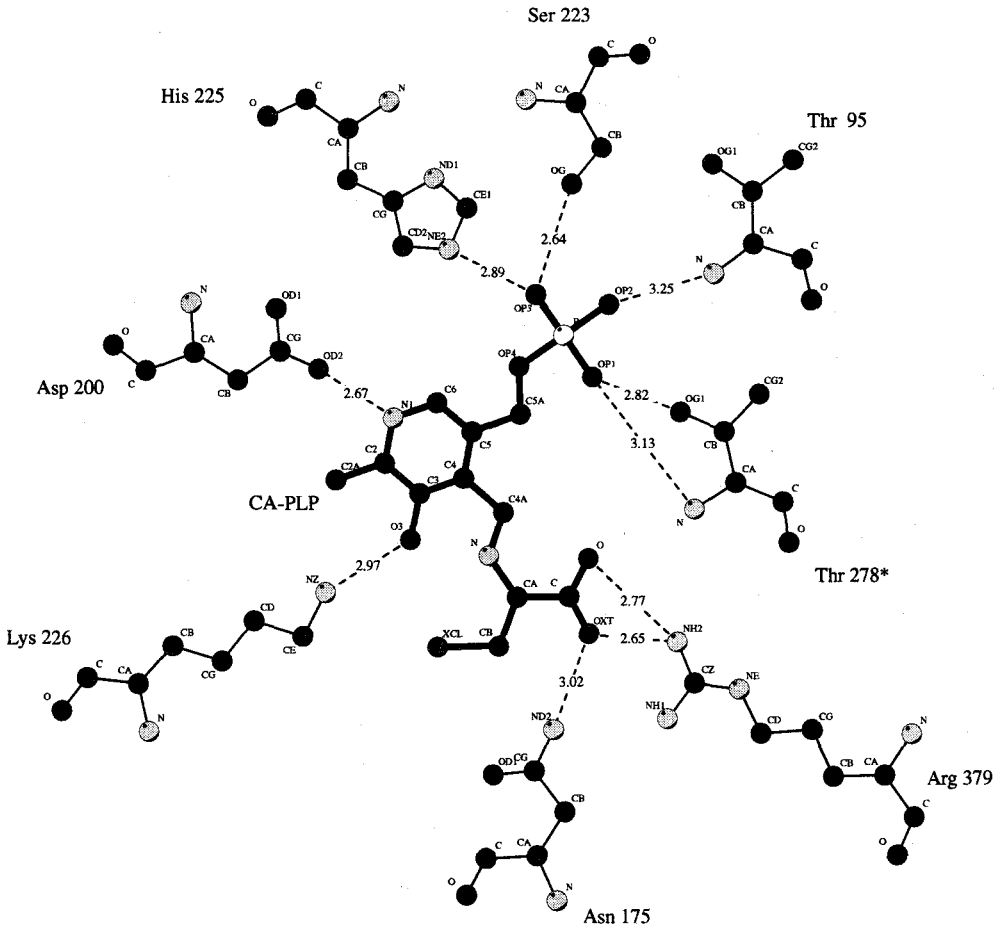

FIG. 37. **Schematic diagrams of hydrogen-bonding interactions around the amino acid-PLP external aldimines in the active sites of the ASP-CsdB (A), CSA-CsdB (B), PG-CsdB (C), and CA-CsdB (D) complexes.** Hydrogen bonds are depicted by dotted lines with interatomic distance (Å). The figures were drawn with program LIGPLOT (163).

native structure. The polypeptide chains of 3-406 in the complex structures were superposed on that of the native enzyme. The average rms deviations in the Cα atoms between the ASP-, CSA-, CA-, and PG-CsdB complexes and the native structure were 0.265, 0.205, 0.235, and 0.232 Å, respectively. This indicates that the overall structure of the polypeptide chain in each complex is similar to that of the native CsdB. The plots of rms deviation against residue number are shown in Fig. 38. In the complex structures, large deviations are observed in three regions of Val19-Asn20, His55-Ile58, and Gly251-Ser254. Small deviations are also seen around Arg136 and Leu339. Val19-Asn20, Arg136 and Leu339 are located on the surface of the molecule and are exposed to the solvent. Gly251-Ser254 contains a Gly-Gly-Gly triplet motif and is situated near the active site, possibly providing a flexibility for the enzyme. The most remarkable region where the deviations are seen is the loop containing His55-Ile58. This region is extruded to the β-substituent of the ligands. His55* projecting from the other subunit in the dimer is a putative recognition residue for the side chain of the substrate in CsdB. This deviation seems to be caused by high flexibility in the region His55-Ile58 because the electron density of the region is also ambiguous in native CsdB (Chapter V).

Fig. 39 shows the external aldimines between PLP and ASP, CSA, PG, and CA in the four ligand-CsdB complex structures and the internal aldimine between PLP and Lys226 in the native CsdB structure. The phosphates are located at similar positions in all the structures (Fig. 39 E). The conversion of the internal aldimine to the external aldimine in the ASP-, CSA-, PG-, and CA-CsdB complexes results in tilting of the planar coenzyme ring by about 12°, 8°,

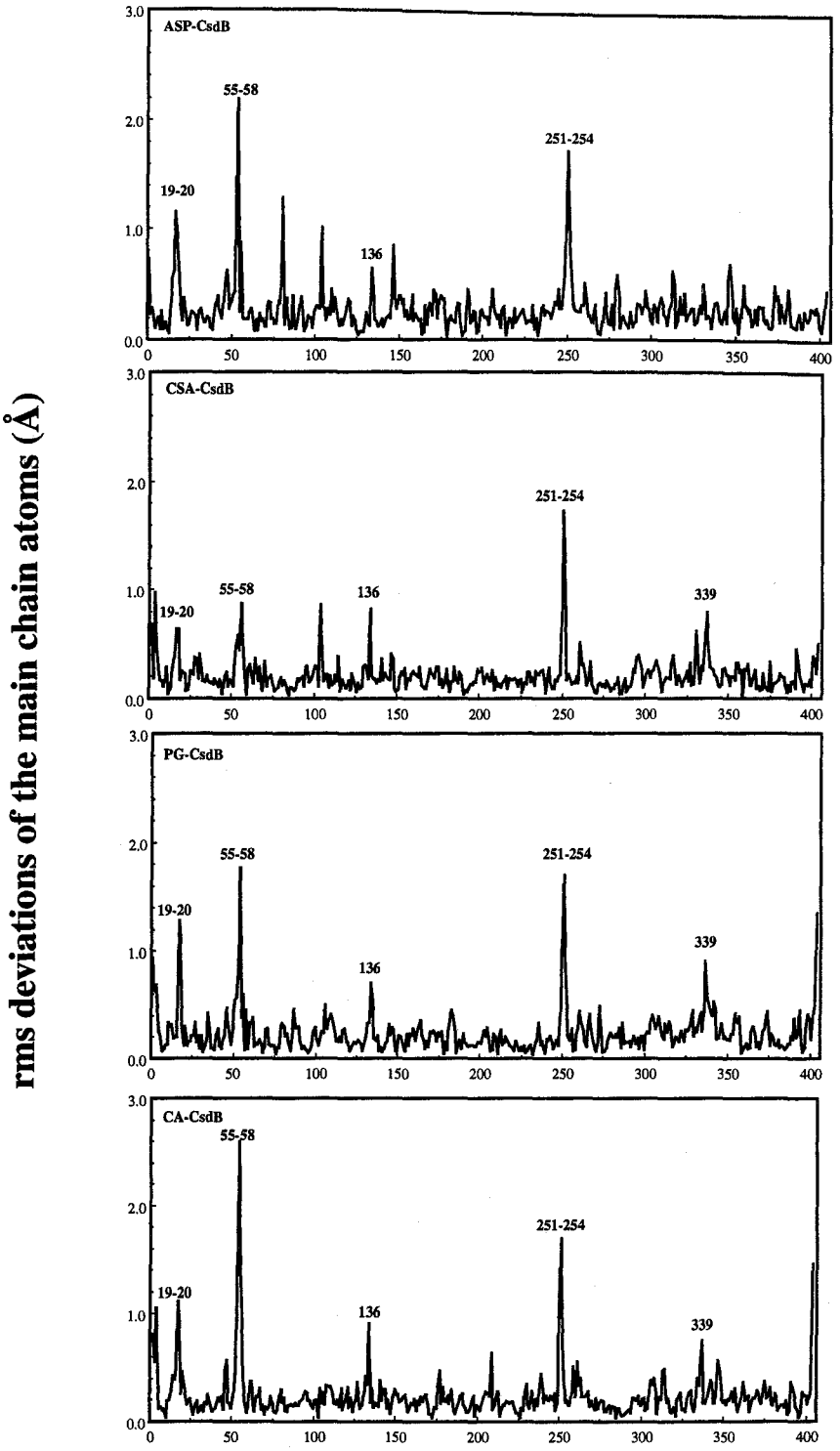

FIG. 38. **Plots of rms Cα deviation of the complexes from the native CsdB against residue number.** Plots were drawn with the CCP4 program (138). Regions with large rms deviation are marked with residue numbers.

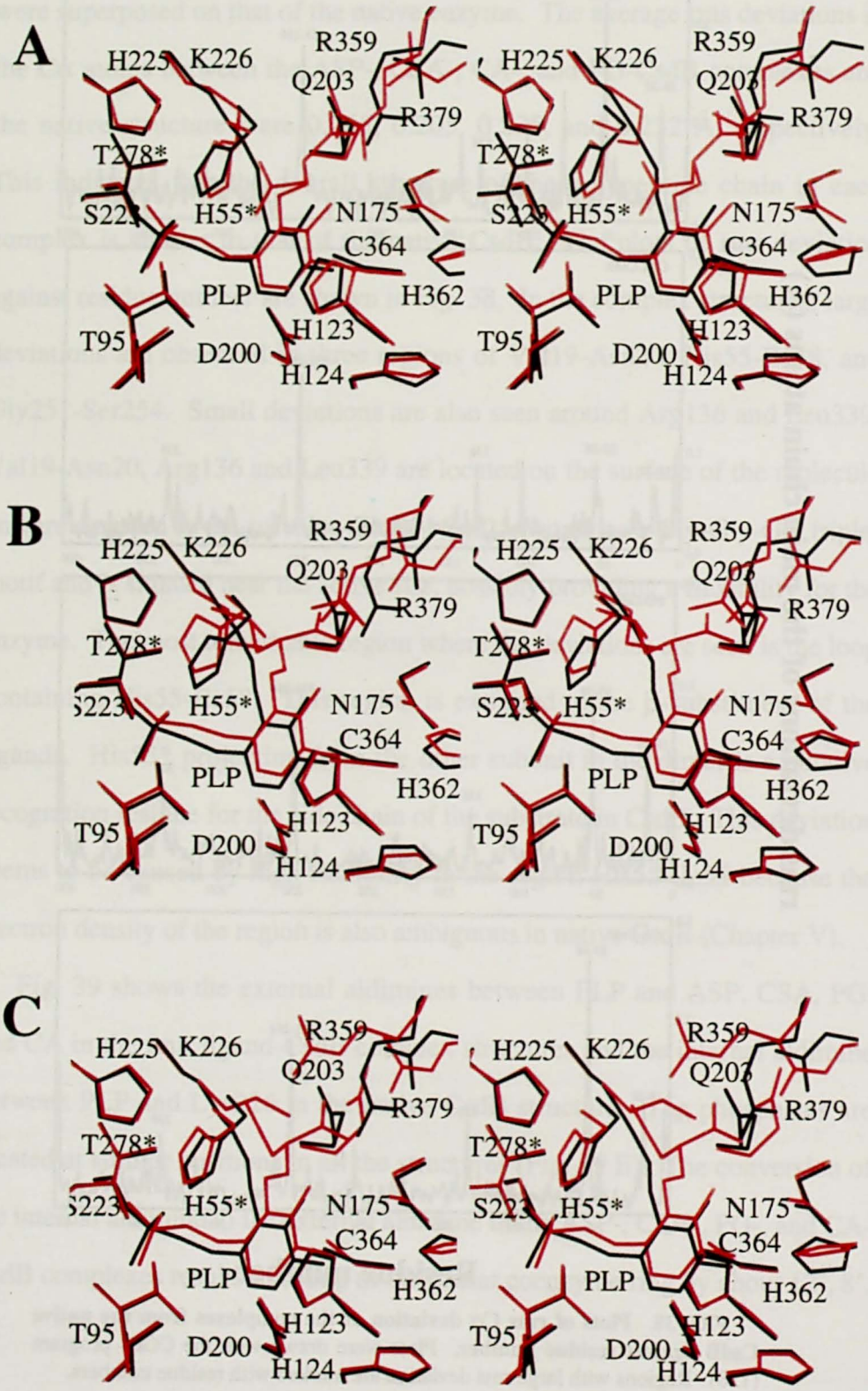
A
H225
K226
R359
Q203
R379
T278*
S223
H55*
N175
C364
PLP
H362
T95
D200
H123
H124
B
C

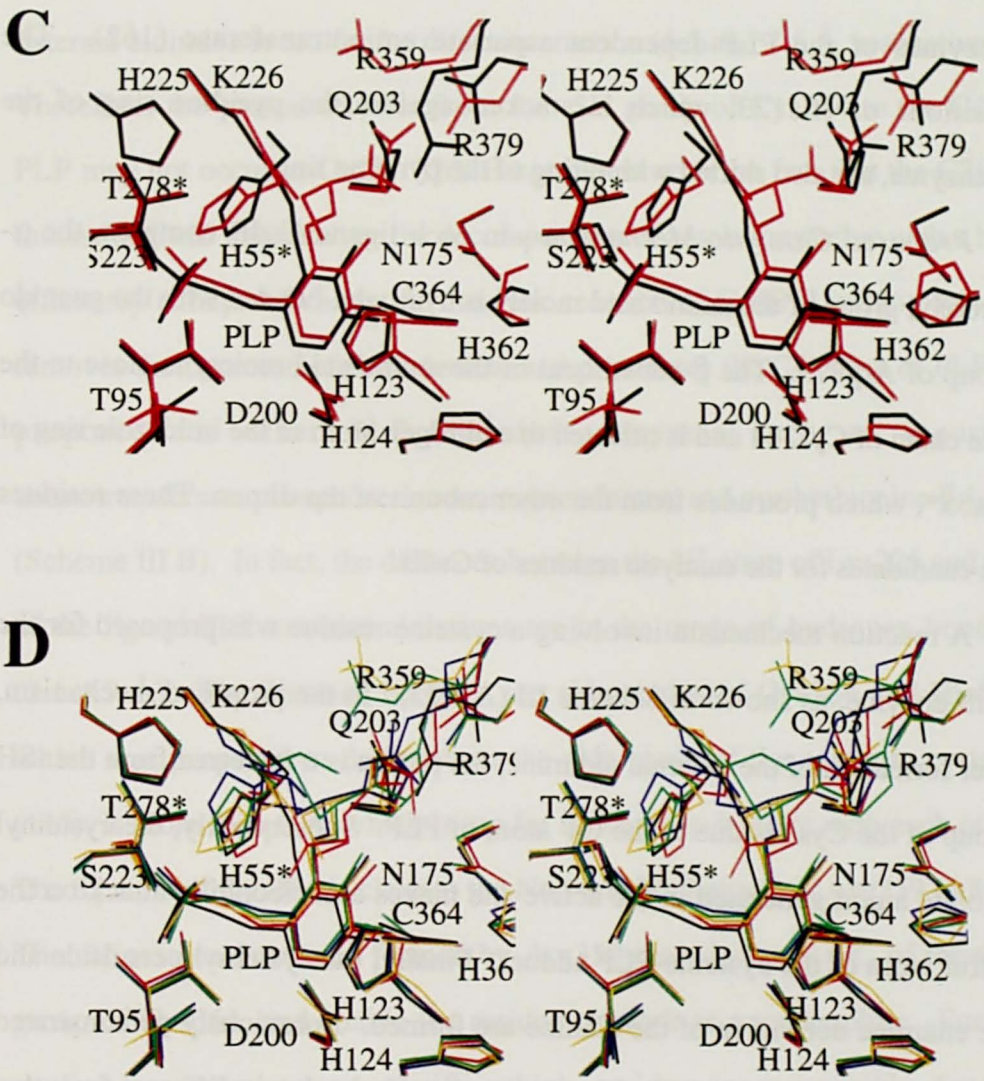

FIG. 39. **Stereoscopic superpositions of the external aldimine structures on the internal aldimine structure.** The external aldimine of the ASP-CsdB (A), CSA-CsdB (B), PG-CsdB (C), and CA-CsdB (D) complexes (shown in *red*) is superposed on the internal aldimine of native CsdB (shown in *black*). In panel E, the active site structure of native CsdB and the four complexes are superposed. The internal aldimine in the native structure is in *black*, and the external aldimines in ASP-CsdB, CSA-CsdB, PG-CsdB, and CA-CsdB are in *red*, *blue*, *green*, and *yellow*, respectively. The figures were drawn with program MOLSCRIPT (161).

19°, and 7°, respectively. A tilt of about 27° has been observed in various isozymes of the PLP-dependent aspartate aminotransferase (162). The positions of His123, which is stacked against the pyridine ring of the coenzyme, are also shifted with tilting of the pyridine ring.

Proposed Catalytic Mechanism—In each ligand-CsdB complex, the α-carboxyl group of the amino acid moiety is hydrogen-bonded with the guanido group of Arg379. The β-substituent of the amino acid moiety is close to the side chain of Cys364 and is oriented to a nitrogen atom of the imidazole ring of His55*, which protrudes from the other subunit of the dimer. These residues are candidates for the catalytic residues of CsdB.

A reaction mechanism involving a cysteine residue was proposed for the NifS enzyme, as shown in Scheme III (A) (73). In the proposed mechanism, after formation of the external aldimine, the proton is transferred from the -SH group of the Cys residue to the C4' atom of PLP. Subsequently, the cysteinyl thiolate anion generated in the active site makes a nucleophilic attack on the sulfur atom of the cysteine-PLP adduct. Finally, the cysteinyl persulfide and the enamine derivative of the alanine are formed. I previously demonstrated that the reaction mechanism of L-cysteine desulfurization is different from that of the decomposition of L-selenocysteine and L-cysteine sulfinate, and Cys364 plays a critical role only for L-cysteine desulfurization (Chapter IV). The present study showed that Cys364 exists on the extending lobe from the small domain. The sulfur atom of Cys364 is located in the close proximity of the γ-position of the substrates/analogs, indicating that they can interact with each other, which is consistent with the proposed mechanism (73). However, the

distance from the Sγ atom of Cys364 to the C4' and Cα atoms of a ligand-PLP external aldimine is too far for direct interaction (6.5 and 7.5 Å, respectively). Therefore, the proton transfer from the -SH group of Cys364 to the C4' of PLP may not occur in CsdB. This is consistent with the fact that the C364A mutant of CsdB can catalyze the decomposition of L-selenocysteine with a high efficiency (Chapter IV). In the catalytic reaction of CsdB, Lys226 probably removes the α-proton of the substrate and protonates the C4' atom of PLP, as proposed for other PLP-dependent enzymes such as aspartate aminotransferase, phosphoserine aminotransferase, and cysthathionine β-lyase (Scheme III B). In fact, the distances between the Nζ atom of Lys226 and C4' of the ligand-PLP external aldimines are in the range of hydrogen bonding (3.1-4.9 Å). The distance between the side chains of Cys364 and His55*, which was proposed to deprotonate the side chain of the catalytic cysteine (115), is more than 6 Å, which is too far for them to interact with each other. The Sγ atom of Cys364 is close to the Nη1 and Nη2 atoms of Arg359 (4.8 Å). The cationic environment formed by Arg359 may decrease pK_a of the thiol group of Cys364, and enable the residue to work as a nucleophile. Further studies are required to clarify which residue is responsible for the deprotonation of Cys364. His55* is located in the vicinity of the Cβ atom of the substrate/analog moiety of the complex, and possibly participates in the protonation at the Cβ atom in β-carbanionic intermediate (Scheme III B **4**).

I proposed a mechanism that does not involve an active-site cysteine residue for the decomposition of L-selenocysteine by CsdB in Chapter IV (Scheme III C). According to this mechanism, the selenohydryl group of the

selenocysteine-PLP adduct is deprotonated because of its low pK_a (pK_a = 5.2), and subsequently an elemental form of selenium is released from the adduct. Active-site His55* may facilitate the deprotonation of the selenohydryl group of the substrate.

In conclusion, the present data suggest that CsdB catalyzes the cysteine desulfurase reaction through the nucleophilic attack on Sγ atom of L-cysteine by Cys364 (Scheme III B), and that the enzyme decomposes L-selenocysteine without Cys364 (Scheme III C). Similar mechanism may be applied to the reactions catalyzed by CSD and IscS.

SUMMARY

Three-dimensional structures are reported for a CsdB complex with either the poor substrates L-aspartate and L-cysteine sulfinate or the analogs L-propargylglycine and L-β-chloroalanine at the active site of the enzyme. In the obtained structures, amino acids form external aldimines with the coenzyme, pyridoxal phosphate. The results further identify the substrate binding sites in the active site of the enzyme and provide insight into conformational changes that occur upon formation of these complexes. The four structures having ligands at the active sites reveal that the formation of external aldimine between amino acids and the coenzyme is associated with a small tilting (7-19°) of the plane of pyridine ring of the coenzyme. The Cys364 residue, which is necessary for the cysteine desulfurase reaction of CsdB, is located near the γ position of the ligand, suggesting that they would interact each other. His55 extruding from the other subunits of the dimer into the active site is proposed to play a role in the catalysis by protonate at Cβ atom of β-carbanionic intermediate.

CONCLUSION

The present study was carried out to elucidate the enzymological properties and the reaction mechanism of cysteine desulfurase and selenocysteine lyase.

The mouse liver cDNA termed m-*Scl* was cloned and sequenced. m-*Scl* is comprised of 2,172 bp, containing an open reading frame encoding a polypeptide chain of 432 amino acids. The gene product m-SCL was overproduced in *E. coli*, purified to homogeneity, and characterized. m-SCL is a PLP-dependent homodimer and catalyzes the removal of elemental selenium from L-selenocysteine to form L-alanine. I concluded that the enzyme is selenocysteine lyase, because it has high specificity for L-selenocysteine. The deduced amino acid sequence shows that selenocysteine lyase establishes a distinct class of enzymes with weak sequence similarity with NifS proteins. m-SCL mainly exists in the cytosol of the liver, kidney, and testis, where mouse selenophosphate synthetase is also abundant, consistent with the proposal that m-SCL functions in cooperation with selenophosphate synthetase in the selenoprotein synthesis.

E. coli contains three genes, *csdA*, *csdB*, and *iscS*, all of which show sequence similarity with both *nifS* and m-*Scl*. The *csdA* gene was cloned, and its product was characterized. The product (CSD) is a PLP-dependent homodimer and catalyzes the same reaction as cysteine desulfurase and selenocysteine lyase. The enzyme acts on L-cysteine, L-selenocysteine, and L-cysteine sulfinate. Cys358 of CSD corresponding to Cys325 of *A. vinelandii* NifS, which is catalytically essential, is not required for selenocysteine

decomposition.

The *csdB* gene product (CsdB), which shows significant sequence identity with CSD (45%), was also characterized. CsdB also catalyzes the selenocysteine lyase and cysteine desulfurase reactions. However, since the enzyme shows high specificity toward L-selenocysteine, it is regarded as *E. coli* selenocysteine lyase. CsdB was crystallized by the hanging drop vapor diffusion method. The crystals were of suitable quality for x-ray crystallography and belonged to the tetragonal space group $P4_32_12$ with unit cell dimensions of $a = b = 128.1$ Å and $c = 137.0$ Å.

Kinetic and mutational analyses were carried out with the three NifS homologs, CSD, CsdB, and IscS. These enzymes were inactivated during the catalysis through abortive transamination, yielding pyruvate and an inactive pyridoxamine 5'-phosphate-form enzyme. Pyruvate significantly enhanced the activities of CSD toward L-selenocysteine and L-cysteine sulfinate. However, the enzyme activity toward L-cysteine was not so much increased by pyruvate, suggesting the presence of different rate limiting steps or reaction mechanisms for L-cysteine degradation and degradation of L-selenocysteine and L-cysteine sulfinate. The mutational analysis in which I substituted Ala for each of Cys358 of CSD, Cys364 of CsdB, and Cys328 of IscS, indicated that the reaction mechanism of L-cysteine desulfurization is different from that of the decomposition of L-selenocysteine and L-cysteine sulfinate, and the conserved cysteine residues play a critical role only for L-cysteine desulfurization.

The crystal structure of CsdB was determined by X-ray crystallographic method of multiple isomorphous replacement. The overall fold of the subunit

is similar to those of the fold type I family of PLP-dependent enzymes, represented by aspartate aminotransferase.

Three-dimensional structures of CsdB complexes with L-aspartate, L-cysteine sulfinate, L-propargylglycine, or L-β-chloroalanine were determined by X-ray crystallographic method. These amino acids formed external aldimines with PLP. The Cys364 residue, which is necessary for the cysteine desulfurase reaction of CsdB, is located near the γ position of the ligand, suggesting that they interact with each other. His55 extruding from the other subunits of the dimer into the active site probably plays a role in the catalysis by protonating the Cβ atom of the β-carbanionic intermediate.

Taken together, the present study suggests that in CsdB, Lys226 first removes the α proton from the substrate-PLP external aldimine, and then protonates at C4' of the intermediate to form the ketimine intermediate. In the following step, the thiolate anion of Cys364 performs nucleophilic attack on the sulfur atom of the sulfuhydryl group of a cysteine-PLP ketimine intermediate, resulting in formation of a cysteinyl persulfide and an enamine derivative of alanine. In contrast, when L-selenocysteine is the substrate, selenium is released spontaneously from the intermediate with one electron left on the β-carbon of the substrate, since the selenohydryl group of L-selenocysteine is in an anionic form due to its low pK_a value. The protonation of the selenohydryl group may be facilitated by His55. Desulfination of L-cysteine sulfinate may also proceed through a mechanism similar to that of the degradation of L-selenocysteine without aid of the active site cysteine residue.

ACKNOWLEDGEMENTS

I wishes to express my sincere gratitude to Dr. Nobuyoshi Esaki, Professor of the Laboratory of Microbial Biochemistry, Institute for Chemical Research, Kyoto University, for his kind guidance and generous encouragement throughout the course of this study.

I am grateful to thank Dr. Tohru Yoshimura, Associate Professor of the Laboratory of Microbial Biochemistry, Institute for Chemical Research, Kyoto University, for his kindness and helpful suggestions.

I would like to express my gratitude to Dr. Tatsuo Kurihara, Assistant Professor of the Laboratory of Microbial Biochemistry, Institute for Chemical Research, Kyoto University, for his precise advice, valuable discussion, and warm encouragement through the course of this study.

I am greatly indebted to Dr. Kenji Soda, Professor Emeritus of Kyoto University, for his kind support and warm encouragement in carrying out this study.

I am greatly indebted to Dr. Yasuo Hata, Associate Professor of the Laboratory of Biopolymer Structure, Institute for Chemical Research, Kyoto University, for his kind suggestions and warm encouragement.

I am also indebted to Dr. Tomomi Fujii, Assistant Professor of the Laboratory of Biopolymer Structure, Institute for Chemical Research, Kyoto University, for his kind help and valuable discussion.

I acknowledge the helpful comments and suggestions of my colleagues, especially Dr. Ji-Quan Liu, Dr. Marek Tchórzewski, Dr. Andrey

Galkin, Dr. Kwang-Hwan Jhee, and Dr. Young-Fu Li.

I am also deeply indebted to Mr. Masaki Maeda, Mr. Shin-ichiro Kato, and Ms. Tasuku Watanabe. They shared their valuable time with me and helped me during the course of this study.

I am also expressing my sincere thanks to Dr. Shigeki Ito, Dr. Takashi Tamura, Mr. Hiroyuki Ashida, Dr. Hirohide Toyama, Dr. Mamoru Wakayama, Dr. Makoto Ashiuchi, Dr. Young-Hee Lim, Dr. Vincenzo Nardi-Dei, Dr. Sundraraju Bakthavatsalam, Dr. Hiromoto Koshikawa, Dr. Sergey Gorlatov, Dr. Natasha Gorlatova, Dr. Yoichi Kurokawa, Mr. Akira Shimotoyodome, Mr. Hauke Smidt, Mr. Tomas Schnibbe, Mr. Shin-ichi katsura, Mr. Hitoshi Nakazato, Ms. Tae Uesaka, Ms. Tomoko Aoki, Mr. Jongrak Kittiworakarn, Mr. Yousuke Doi, Mr. Takeshi Kurono, Mr. Hitoki Miyake, Mr. Kenji Endo, Mr. Mitsuhiro Nishihara, Dr. Chung Park, Dr. Dong-Won Choo, Dr. Li-Dong Liu, Dr. Gutierrez Aldo, Dr. Kazuhisa Kishimoto, Mr. Yoshihiro Fuchikami, Mr. Akira Watanabe, Mr. Takuma Uo, Mr. Susumu Ichiyama, Ms. Luda Kulakova, Mr. Song-Chul Bahk, Mr. Kazuo Shiomi, Ms. Yuriko Hirano, Mr. Kazuaki Yoshimune, Ms. Momoko Ueda, Mr. Sou Takeda, Mr. Tozo Nishiyama, Mr. Takeshi Suzuki, Mr. Seung-Pyo Hong, Dong-Ho Seong, Mr. Yun-lin Wei, Mr. Takahiro Yamauchi, Mr. Daisuke Nakayama, Ms. Ayako Isui, Ms. Mami Saito, Ms. Fumiko Todo, Ms. Megumi Saito, Mr. Muneyuki Takahata, Ms. Michiko Nakano, Mr. Kensuke Mori, Mr. Robert Alexander John Douglas Kennedy, Ms. Geok-Yong Yow, Mr. Miroliaei Mehran, and all the other members of the Laboratory of Microbial Biochemistry, at both past and present, for sharing their valuable time and

encouraging me.

I am grateful to Ms. Mio Seki, Ms. Toshiko Hirasawa, Ms. Tomoko Kurihara, Ms. Kyoko Yokoyama, Ms. Kumiko Nishikawa, and Ms. Machiko Utsunomiya for their kind help and warm encouragement.

I would like to express my gratitude to Dr. Kunihiko Watanabe, Associate Professor of Kyoto Prefectural University, for his kind suggestions and warm encouragement.

I am also grateful to the Japan Society for the Promotion of Scienece for the financial support during my PhD. course in Kyoto University.

Finally, I would like to express my hearty gratitude to my parents and sister for their immense understanding and encouragement.

REFERENCES

1. Stadtman, T. C. (1990) *Ann. Rev. Biochem.* **59,** 111-127
2. Virupaksha, T. K., and Shrift, A. (1965) *Biochem. Biophys. Acta* **107,** 69-80
3. Martin, J. L. (1973) in *Organic Selenium Compounds: Their Chemistry and Biology* (Klayman, D. L., and Günther Wolfgang, H. H., eds), pp. 663-691, John Wiley & Sons, New York
4. Klung, H. L., Petersen, D. F., and Moxon, A. L. (1949) *Dakota Acad. Sci.* **28,** 117
5. Moxon, A. L., DuBois, K. P., and Potter, R. L. (1941) *J. Pharmacol. Therap.* **72,** 184
6. Schwarz, K., and Foltz, C. M. (1957) *J. Am. Chem. Soc.* **79,** 3292
7. Stadtman, T. C. (1996) *Ann. Rev. Biochem.* **65,** 83-100
8. Stadtman, T. (1974) *Science* **183,** 915-922
9. Dilworth, G. L., and Bandurski, R. S. (1977) *Biochem. J.* **163,** 521-529
10. Young, P. A., and Kaiser, I. I. (1975) *Arch. Biochem. Biophys.* **171,** 483-489
11. Hoffman, J. L., and McConnell, K. P. (1974) *Biochim. Biophys. Acta* **366,** 109-113
12. Coch, E. H., and Greene, R. C. (1971) *Biochim. Biophys. Acta* **230,** 223-236
13. Mudd, S., and Gantoni, G. L. (1957) *Nature* **180,** 1052

14. Esaki, N., Nakamura, T., Tanaka, H., Suzuki, T., Morino, Y., and Soda, K. (1981) *Biochemistry* **20,** 4492-4496

15. Esaki, N., Nakamura, T., Tanaka, H., and Soda, K. (1982) *J. Biol. Chem.* **257,** 4386-4391

16. Veres, Z., Kim, I. Y., Scholz, T. D., and Stadtman, T. C. (1994) *J. Biol. Chem.* **269,** 10597-10603

17. Forchhammer, K., and Böck, A. (1991) *J. Biol. Chem.* **266,** 6324-6328

18. Neuhierl, B., and Böck, A. (1996) *Eur. J. Biochem.* **239,** 235-238

19. Chocat, P., Esaki, N., Nakamura, T., Tanaka, H., and Soda, K. (1983) *J. Bacteriol.* **156,** 455-457

20. Chocat, P., Esaki, N., Tanizawa, K., Nakamura, K., Tanaka, H., and Soda, K. (1985) *J. Bacteriol.* **163,** 669-676

21. Zheng, L., White, R. H., Cash, V. L., Jack, R. F., and Dean, D. R. (1993) *Proc. Natl. Acad. Sci. U. S. A.* **90,** 2754-2758

22. Zinoni, F., Birkmann, A., Stadtman, T. C., and Böck, A. (1986) *Proc. Natl. Acad. Sci. U. S. A.* **83,** 4650-4654

23. Böck, A., Forchhammer, K., Heider, J., Leinfelder, W., Sewers, G., Veprek, B., and Zinoni, F. (1991) *Mol. Microbiol.* **5,** 515-520

24. Liu, Z., Reches, M., Groisman, I., and Engelberg-Kulka, H. (1998) *Nucleic Acids. Res.* **26,** 896-902

25. Leinfelder, W., Forchhammer, K., Zinoni, F., Sawers, G., Mandrand-Berthelot, M. A., and Böck, A. (1988) *J. Bacteriol.* **170,** 540-546

26. Böck, A., and Stadtman, T. (1988) *Biofactors* **1,** 245-250

27. Leinfelder, W., Forchhammer, K., Veprek, B., Zehelein, E., and Böck, A. (1990) *Proc. Natl. Acad. Sci. U. S. A.* **87,** 543-547

28. Stadtman, T. (1991) *J. Biol. Chem.* **266,** 16257-16260

29. Leinfelder, W., Stadtman, T. C., and Böck, A. (1989) *J. Biol. Chem.* **264,** 9720-9723

30. Leinfelder, W., Zehelein, E., Mandrand-Berthelot, M. A., and Böck, A. (1988) *Nature* **331,** 723-725

31. Forchhammer, K., Leinfelder, W., Boesmiller, K., Veprek, B., and Böck, A. (1991) *J. Biol. Chem.* **266,** 6318-6323

32. Glass, R. S., Singh, W. P., Jung, W., Veres, Z., Scholz, T. D., and Stadtman, T. C. (1993) *Biochemistry* **32,** 12555-12559

33. Forchhammer, K., Leinfelder, W., and Böck, A. (1989) *Nature* **342,** 453-456

34. Forchhammer, K., Rucknagel, K. P., and Böck, A. (1990) *J. Biol. Chem.* **265,** 9346-9350

35. Baron, C., Heider, J., Böck, A. (1993) *Proc. Natl. Acad. Sci. U. S. A.* **90,** 4181-4185

36. Chambers, I., Frampton, J., Goldfarb, P., Affara, N., McBain, W., and Harrison, P. R. (1986) *Embo J.* **5,** 1221-1227

37. Hill, K. E., Lloyd, R. S., Yang, J. G., Read, R., and Burk, R. F. (1991) *J. Biol. Chem.* **266,** 10050-10053

38. Hill, K. E., Lloyd, R. S., and Burk, R. F. (1993) *Proc. Natl. Acad. Sci. U. S. A.* **90,** 537-541

39. Berry, M. J., Banu, L., and Larsen, P. R. (1991) *Nature* **349,** 438-440

40. Tamura, T., and Stadtman, T. (1996) *Proc. Natl. Acad. Sci. U.S.A.* **93,** 1006-1011

41. Berry, M. J., Banu, L., Chen, Y. Y., Mandel, S. J., Kieffer, J. D., Harney, J. W., and Larsen, P. R. (1991) *Nature* **353,** 273-276

42. Esaki, N., Karai, N., Nakamura, T., Tanaka, H., and Soda, K. (1985) *Arch. Biochem. Biophys.* **238,** 418-423

43. Chocat, P., Esaki, N., Tanizawa, K., Nakamura, K., Tanaka, H., and Soda, K. (1987) *Methods Enzymol.* **143,** 493

44. Jacobson, M. R., Cash, V. L., Weiss, M. C., Laird, N. F., Newton, W. E., and Dean, D. R. (1989) *Mol. Gen. Genet.* **219,** 49-57

45. Zheng, L., and Dean, D. R. (1994) *J. Biol. Chem.* **269,** 18723-18726

46. Green, J., Bennett, B., Jordan, P., Ralph, E. T., Thomson, A. J., and Guest, J. R. (1996) *Biochem. J.* **316,** 887-892

47. Hidalgo, E., and Demple, B. (1996) *J. Biol. Chem.* **271,** 7269-7272

48. Sun, D., and Setlow, P. (1993) *J. Bacteriol.* **175,** 1423-1432

49. Kolman, C., and Söll, D. (1993) *J. Bacteriol.* **175,** 1433-1442

50. Stadtman, T. C. (1979) *Adv. Enzymol. Relat. Areas. Mol. Biol.* **48,** 1-28

51. Heider, J., and Böck, A. (1993) *Adv. Microb. Physiol.* **35,** 71-109

52. Lacourciere, G. M., and Stadtman, T. C. (1998) *J. Biol. Chem.* **273,** 30921-30926

53. Tanaka, H., and Soda, K. (1987) *Methods Enzymol.* **143,** 240-243

54. Blobel, G., and Potter, V. R. (1966) *Proc. Natl. Acad. Sci. U. S. A.* **55,** 1283-1288

55. Leinweber, F. J., and Monty, K. J. (1987) *Methods Enzymol.* **143,** 15-17

56. Bradford, M. M. (1976) *Anal. Biochem.* **72,** 248-254

57. Gill, S. C., and von Hippel, P. H. (1989) *Anal. Biochem.* **182,** 319-326

58. Laemmli, U. K. (1970) *Nature* **227,** 680-685

59. Guimaraes, M. J., Peterson, D., Vicari, A., Cocks, B. G., Copeland, N. G., Gilbert, D. J., Jenkins, N. A., Ferrick, D. A., Kastelein, R. A., Bazan, J. F., and Zlotnik, A. (1996) *Proc. Natl. Acad. Sci. U. S. A.* **93,** 15086-15091

60. Land, T., and Rouault, T. A. (1998) *Mol. Cell* **2,** 807-815

61. Nakai, Y., Yoshihara, Y., Hayashi, H., and Kagamiyama, H. (1998) *FEBS lett.* **433,** 143-148

62. Strain, J., Lorenz, C. R., Bode, J., Garland, S., Smolen, G. A., Ta, D. T., Vickery, L. E., and Culotta, V. C. (1998) *J. Biol. Chem.* **273,** 31138-31144

63. Combs, G. F., Jr., and Combs, S. B. (1984) *Annu. Rev. Nutr.* **4,** 257-280

64. Shapiro, J. R. (1973) in *Organic Selenium Compounds: Their Chemistry and Biology* (Klayman, D. L., and Günther Wolfgang, H. H., eds), pp. 693-726, John Wiley & Sons, New York

65. Scott, M. L. (1973) in *Organic Selenium Compounds: Their*

Chemistry and Biology (Klayman, D. L., and Günther Wolfgang, H. H., eds), pp. 629-661, John Wiley & Sons, New York

66. Blattner, F. R., Plunkett, G. r., Bloch, C. A., Perna, N. T., Burland, V., Riley, M., Collado-Vides, J., Glasner, J. D., Rode, C. K., Mayhew, G. F., Gregor, J., Davis, N. W., Kirkpatrick, H. A., Goeden, M. A., Rose, D. J., Mau, B., and Shao, Y. (1997) *Science* **277,** 1453-1474

67. Yamamoto, Y., Aiba, H., Baba, T., Hayashi, K., Inada, T., Isono, K., Itoh, T., Kimura, S., Kitagawa, M., Makino, K., Miki, T., Mitsuhashi, N., Mizobuchi, K., Mori, H., Nakade, S., Nakamura, Y., Nashimoto, H., Oshima, T., Oyama, S., Saito, N., Sampei, G., Satoh, Y., Sivasundaram, S., Tagami, H., Horiuchi, T., and et al. (1997) *DNA Res.* **4,** 91-113

68. Aiba, H., Baba, T., Hayashi, K., Inada, T., Isono, K., T., I., Kasai, H., Kashimoto, K., Kimura, S., Kitakawa, M., Kitagawa, M., Makino, K., Miki, T., Mizobuchi, K., Mori, H., Mori, T., Motomura, K., Nakade, S., Nakamura, Y., Nashimoto, H., Nishio, Y., Oshima, T., Saito, N., Sampei, G., Seki, Y., Sivasundaram, S., Tagami, H., Takeda, J., Takemoto, K., Takeuchi, Y., Wada, C., Yamamoto, Y., and Horiuchi, T. (1996) *DNA Res.* **3,** 363-377

69. Flint, D. H. (1996) *J. Biol. Chem.* **271,** 16068-16074

70. Sambrook, J., Fritsch, E. F., and Maniatis, T. (1989) *Molecular Cloning: A Laboratory Manual*, 2nd Ed., Cold Spring Harbor Laboratory, Cold Spring Harbor, NY

71. Braunstein, A. E., Goryachenkova, E. V., and LAC, N. D. (1969) *Biochem. Biophys. Acta* **171,** 366-368

72. Kunkel, T. A. (1985) *Proc. Natl. Acad. Sci. U. S. A.* **82,** 488-492

73. Zheng, L., White, R. H., Cash, V. L., and Dean, D. R. (1994) *Biochemistry* **33,** 4714-4720

74. Soda, K., Novogrodsky, A., and Meister, A. (1964) *Biochemistry* **3,** 1450-1454

75. Walsh, C. T. (1986) in *Vitamin B6 pyridoxal phosphate: partB* (Dolphin, D., Poulson, R., and Avramovic, O., eds), pp. 43-70, Wiley, New York

76. Mulligan, M. E., and Haselkorn, R. (1989) *J. Biol. Chem.* **264,** 19200-19207

77. Jackman, D. M., and Mulligan, M. E. (1995) *Microbiology* **141,** 2235-2244

78. Lyons, E. M., and Thiel, T. (1995) *J. Bacteriol.* **177,** 1570-1575

79. Grishin, N. V., Phillips, M. A., and Goldsmith, E. J. (1995) *Protein Sci.* **4,** 1291-1304

80. Mehta, P. K., and Christen, P. (1993) *Eur. J. Biochem.* **211,** 373-376

81. Flint, D. H., Tuminello, J. F., and Miller, T. J. (1996) *J. Biol. Chem.* **271,** 16053-16067

82. Badet, B., Roise, D., and Walsh, C. T. (1984) *Biochemistry* **23,** 5188-5194

83. Roise, D., Soda, K., Yagi, T., and Walsh, C. T. (1984) *Biochemistry*

23, 5195-5201

84. Ueno, H., Likos, J. J., and Metzler, D. E. (1982) *Biochemistry* **21,** 4387-4393

85. Tate, S. S., Relyea, N. M., and Meister, A. (1969) *Biochemistry* **8,** 5016-5021

86. Kishore, G. M. (1984) *J. Biol. Chem.* **259,** 10669-10674

87. Hosokawa, Y., Matsumoto, A., Oka, J., Itakura, H., and Yamaguchi, K. (1990) *Biochem. Biophys. Res. Commun.* **168,** 473-478

88. Reymond, I., Sergeant, A., and Tappaz, M. (1996) *Biochim. Biophys. Acta, Gene Struct. Expr.* **1307,** 152-156

89. Recasens, M., Benezra, R., Basset, P., and Mandel, P. (1980) *Biochemistry* **19,** 4583-4589

90. Beynon, J., Ally, A., Cannon, M., Cannon, F., Jacobson, M., Cash, V., and Dean, D. (1987) *J. Bacteriol.* **169,** 4024-4029

91. Evans, D. J., Jones, R., Woodley, P. R., Wilborn, J. R., and Robson, R. L. (1991) *J. Bacteriol.* **173,** 5457-5469

92. Singh, M., Tripathi, A. K., and Klingmuller, W. (1989) *Mol. Gen. Genet.* **219,** 235-240

93. Steibl, R., Steibl, H. D., Siddavattam, D., and Klingmeuller, W. (1993) in *NEW HORIZONS IN NITROGEN FIXATION* (Palacios, R., Mora, J., and Newton, W. E., eds), pp. 496-496, Kluwer Academic Publishers, Dortrecht

94. Meijer, W. G., and Tabita, F. R. (1992) *J. Bacteriol.* **174,** 3855-3866

95. Masepohl, B., Angermuller, S., Hennecke, S., Hubner, P., Moreno-

Vivian, C., and Klipp, W. (1993) *Mol. Gen. Genet.* **238,** 369-382

96. Thiel, T., Lyons, E. M., Erker, J. C., and Ernst, A. (1995) *Proc. Natl. Acad. Sci. U. S. A.* **92,** 9358-9362

97. Kaneko, T., Tanaka, A., Sato, S., Kotani, H., Sazuka, T., Miyajima, N., Sugiura, M., and Tabata, S. (1995) *DNA Res.* **2,** 153-166

98. Kaneko, T., Sato, S., Kotani, H., Tanaka, A., Asamizu, E., Nakamura, Y., Miyajima, N., Hirosawa, M., Sugiura, M., Sasamoto, S., Kimura, T., Hosouchi, T., Matsuno, A., Muraki, A., Nakazaki, N., Naruo, K., Okumura, S., Shimpo, S., Takeuchi, C., Wada, T., Watanabe, A., Yamada, M., Yasuda, M., and Tabata, S. (1996) *DNA Res.* **3,** 109-136

99. Fleischmann, R. D., Adams, M. D., White, O., Clayton, R. A., Kirkness, E. F., Kerlavage, A. R., Bult, C. J., Tomb, J. F., Dougherty, B. A., Merrick, J. M., McKenney, K., Sutton, G., FitzHugh, W., Fields, C., Gocayne, J. D., Scott, J., Shirley, R., Liu, L. I., Glodek, A., Kelley, J. M., Weidman, J. F., Phillips, C. A., Spriggs, T., Hedblom, E., Cotton, M. D., Utterback, T. R., Hanna, M. C., Nguyen, D. T., Saudek, D. M., Brandon, R. C., Fine, L. D., Fritchman, J. L., Fuhrmann, J. L., Geoghagen, N. S. M., Gnehm, C. L., McDonald, L. A., Small, K. V., Fraser, C. M., Smith, H. O., and Venter, J. C. (1995) *Science* **269,** 496-512

100. Leong-Morgenthaler, P., Oliver, S. G., Hottinger, H., and Soll, D. (1994) *Biochimie* **76,** 45-49

101. Wilson, R., Ainscough, R., Anderson, K., Baynes, C., Berks, M.,

Bonfield, J., Burton, J., Connell, M., Copsey, T., Cooper, J., Coulson, A., Craxton, M., Dear, S., Du, Z., Durbin, R., Favello, A., Fraser, A., Fulton, L., Gardner, A., Green, P., Hawkins, T., Hillier, L., Jier, M., Johnston, L., Jones, M., Kershaw, J., Kirsten, J., Laister, N., Latreille, P., Lightning, J., Lloyd, C., Mortimore, B., O'Callaghan, M., Parsons, J., Percy, C., Rifken, L., Roopra, A., Saunders, D., Shownkeen, R., Sims, M., Smaldon, N., Smith, A., Smith, M., Sonnhammer, E., Staden, R., Sulston, J., Thierry-Mieg, J., Thomas, K., Vaudin, M., Vaughan, K., Waterston, R., Watson, A., Weinstock, L., Wilkinson-Sproat, J., and Wohldman, P. (1994) *Nature* **368,** 32-38

102. Smith, D. R., Richterich, P., Rubenfield, M., Rice, P. W., Butler, C., Lee, H. M., Kirst, S., Gundersen, K., Abendschan, K., Xu, Q., Chung, M., Deloughery, C., Aldredge, T., Maher, J., Lundstrom, R., Tulig, C., Falls, K., Imrich, J., Torrey, D., Engelstein, M., Breton, G., Madan, D., Nietupski, R., Seitz, B., Mao, J. I., and et al. (1997) *Genome Res* **7,** 802-819

103. Himmelreich, R., Hilbert, H., Plagens, H., Pirkl, E., Li, B.-C., and Herrmann, R. (1996) *Nucleic Acids Research* **24,** 4420-4449

104. Fraser, C. M., Gocayne, J. D., White, O., Adams, M. D., Clayton, R. A., Fleischmann, R. D., Bult, C. J., Kerlavage, A. R., Sutton, G., Kelley, J. M., Fritchman, J. L., Weidman, J. F., Small, K. V., Sandusky, M., Fuhrmann, J., Nguyen, D., Utterback, T. R., Saudek, D. M., Phillips, C. A., Merrick, J. M., Tomb, J. F., Dougherty, B.

A., Bott, K. F., Hu, P. C., Lucier, T. S., Peterson, S. N., Smith, H. O., Hutchison III, C. A., and Venter, J. C. (1995) *Science* **270,** 397-403

105. Altschul, S. F., Gish, W., Miller, W., Myers, E. W., and Lipman, D. J. (1990) *J. Mol. Biol.* **215,** 403-410
106. Pearson, W. R., and Lipman, D. J. (1988) *Proc. Natl. Acad. Sci. U. S. A.* **85,** 2444-2448
107. Mihara, H., Kurihara, T., Yoshimura, T., Soda, K., and Esaki, N. (1997) *J. Biol. Chem.* **272,** 22417-22424
108. Rudd, K. E. (1998) *Microbiol. Mol. Biol. Rev.* **62,** 985-1019
109. Tanaka, H., and Soda, K. (1987) *Methods Enzymol.* **143,** 240-243
110. Kohara, Y., Akiyama, K., and Isono, K. (1987) *Cell* **50,** 495-508
111. Perkins, S. J. (1986) *Eur. J. Biochem.* **157,** 169-180
112. Adams, E. (1979) *Methods Enzymol.* **62,** 407-410
113. Zheng, L., Cash, V. L., Flint, D. H., and Dean, D. R. (1998) *J. Biol. Chem.* **273,** 13264-13272
114. Matthews, B. W. (1968) *J. Mol. Biol.* **33,** 491-497
115. Hester, G., Stark, W., Moser, M., Kallen, J., Markovi, cacute, Housley, Z., and Jansonius, J. N. (1999) *J. Mol. Biol.* **286,** 829-850
116. Tate, S. S., Meister, A. (1971) *Advances in Enzymology and Related Areas in Molecular Biology* **35,** 503-543
117. Soda, K., and Tanizawa, K. (1979) *Advances in Enzymology and Related Areas in Molecular Biology* **49,** 1-40
118. Sliwkowski, M. X., and Stadtman, T. C. (1985) *J. Biol. Chem.* **260,**

3140-3144

119. Mihara, H., Maeda, M., Fujii, T., Kurihara, T., Hata, Y., and Esaki, N. (1999) *J. Biol. Chem.* **274,** 14768-71472

120. Ito, W., Ishiguro, H., and Kurosawa, Y. (1991) *Gene* **102,** 67-70

121. Peterson, E. A., and Sober, H. A. (1954) *J. Am. Chem. Soc.* **76,** 169-175

122. Tate, S. S., and Meister, A. (1969) *Biochemistry* **8,** 1660-1668

123. Phillips, R. S., Sundararaju, B., and Koushik, S. V. (1998) *Biochemistry* **37,** 8783-8789

124. Koushik, S. V., Moore JA, r., Sundararaju, B., and Phillips, R. S. (1998) *Biochemistry* **37,** 1376-1382

125. Brzovic, P., Holbrook, E., Greene, R., and Dunn, M. (1990) *Biochemistry* **29,** 442-451

126. Moriguchi, M., and Soda, K. (1973) *Biochemistry* **12,** 2974-2979

127. Novogrodsky, A. M., A. (1964) *J. Biol. Chem.* **239,** 879-888

128. Onuffer, J. J., and Kirsch, J. F. (1994) *Protein Eng.* **7,** 413-424

129. Bloom, C. R., Kaarsholm, N. C., Ha, J., and Dunn, M. F. (1997) *Biochemistry* **36,** 12759-12765

130. Koshland, D. E., Jr. (1996) *Curr Opin Struct Biol* **6,** 757-761

131. Neet, K. E. (1980) *Methods Enzymol.* **64,** 139-192

132. Neet, K. E., and Ainslie, G. R., Jr. (1980) *Methods Enzymol.* **64,** 192-226

133. John, R. A. (1995) *Biochim. Biophys. Acta* **1248,** 81-96

134. Gladyshev, V. N., Khangulov, S. V., Axley, M. J., and Stadtman, T. C. (1994) *Proc. Natl. Acad. Sci. U. S. A.* **91,** 7708-7711

135. Axley, M., Böck, A., and Stadtman, T. (1991) *Proc. Natl. Acad. Sci. U. S. A.* **88,** 8450-8454

136. Rozzell, J. D. (1991) in *United State Patent* Vol. 5019509, Genetics Institute, Inc., Cambridge, Mass., U.S.A.

137. Koushik, S. V., Sundararaju, B., McGraw, R. A., and Phillips, R. S. (1997) *Arch. Biochem. Biophys.* **344,** 301-308

138. Collaborative Computational Project, Number 4 (1994) *Acta Crystallogr. D* **50,** 760-763

139. Furey, W., and Swaminathan, S. (1990) *American Crystallographic Association Meeting Abstracts* **18,** 73

140. Jones, T. A., Zou, J.-Y., and Cowan, S. W. (1991) *Acta Crystallogr. A* **47,** 110-119

141. Abrahams, J. P., and Leslie, A. G. W. (1996) *Acta Crystallogr. D* **52,** 30-42

142. Kleywegt, G. J., and Jones, T. A. (1996) *Acta Crystallogr. D* **52,** 826-828

143. Brünger, A. T. (1992) *X-PLOR, Version 3.1: A system for Crystallography and NMR*, Yale Univ. Press, NewHaven, CT

144. Cambillau, C. (1992) *Turbo-FRODO, Version 5.02*, Bio-Graphics, Marseille, Marseille, France

145. Brünger, A. T. (1992) *Nature* **335,** 472-474

146. Laskowski, R. A. (1993) *J. Appl. Crystallogr.* **26,** 283-291

147. Holm, L., and Sander, C. (1993) *J. Mol. Biol.* **233,** 123-138

148. Toney, M. D., Hohenester, E., Cowan, S. W., and Jansonius, J. N.

(1993) *Science* **261,** 756-759

149. Isupov, M. N., Antson, A. A., Dodson, E. J., Dodson, G. G., Dementieva, I. S., Zakomirdina, L. N., Wilson, K. S., Dauter, Z., Lebedev, A. A., and Harutyunyan, E. H. (1998) *J. Mol. Biol.* **276,** 603-623

150. Clausen, T., Huber, R., Laber, B., Pohlenz, H.-D., and Messerschmidt, A. (1996) *J. Mol. Biol.* **262,** 202-224

151. Kirsch, J. F., Eichele, G., Ford, G. C., Vincent, M. G., Jansonius, J. N., Gehring, H., and Christen, P. (1984) *J. Mol. Biol.* **174,** 497-525

152. Jager, J., Moser, M., Sauder, U., and Jansonius, J. (1994) *J. Mol. Biol.* **239,** 285-305

153. Okamoto, A., Higuchi, T., Hirotsu, K., Kuramitsu, S., and Kagamiyama, H. (1994) *J. Biochem.* **116,** 95-107

154. Rhee, S., Parris, K., Hyde, C., Ahmed, S., Miles, E., and Davies, D. (1997) *Biochemistry* **36,** 7664-7680

155. Hennig, M., Grimm, B., Contestabile, R., John, R. A., and Jansonius, J. N. (1997) *Proc. Natl. Acad. Sci. U. S. A.* **94,** 4866-4871

156. Momany, C., Ernst, S., Ghosh, R., Chang, N. L., and Hackert, M. L. (1995) *J. Mol. Biol.* **252,** 643-655

157. Yano, T., Kuramitsu, S., Tanase, S., Morino, Y., and Kagamiyama, H. (1992) *Biochemistry* **31,** 5878-5887

158. Antson, A., Demidkina, T., Gollnick, P., Dauter, Z., von Tersch, R., Long, J., Berezhnoy, S., Phillips, R., Harutyunyan, E., and Wilson,

K. (1993) *Biochemistry* **32,** 4195-4206

159. Renwick, S. B., Snell, K., and Baumann, U. (1998) *Structure* **6,** 1105-1116

160. Esnouf, R. M. (1997) *J. Mol. Graph. Mod.* **15,** 132-134

161. Kraulis, P. J. (1991) *J. Appl. Cryst.* **24,** 946-950

162. Jansonius, J. N., and Vincent, M. G. (1987) in *Biological Macromolecules & Assemblies* (Jurnak, F. A., and McPherson, A., eds), pp. 187-288, Wiley & Sons, New York

163. Wallace, A. C., Laskowski, R. A., and Thornton, J. M. (1995) *Protein Eng.* **8,** 127-134